TÉCNICO LISBOA

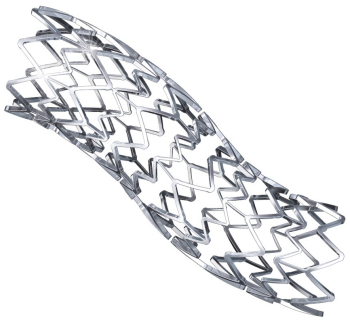

ENHANCEMENT OF NITI ALLOYS BIOCOMPATIBILITY AND CORROSION RESISTANCE BY THERMAL TREATMENTS

Gonçalo Nuno Vieira da Silva Mealha

Thesis to obtain the Master of Science Degree in

Chemical Engineering

Supervisor(s): Prof. Doctor João Carlos Salvador Santos Fernandes
Prof. Doctor Maria Teresa Oliveira de Moura e Silva

Examination Committee

Chairperson: Prof. Doctor Benilde de Jesus Vieira Saramago
Supervisor: Prof. Doctor João Carlos Salvador Santos Fernandes
Member of the Committee: Prof. Doctor Maria João Pedroso Carmezim

December 2016

Acknowledgments

I would like to address special thanks to professor João Salvador Fernandes, supervisor of this scientific work, for giving me the opportunity to develop this project, for his patience, guidance, support and given knowledge through the all time.

I would like to thank Dr. Teresa Moura e Silva for her co-supervision, concern, advice, support and encouragement.

To Dr. Maria João Carmezim, I would like to thank for the performed thermal treatments on the samples, and for her concern and sympathy.

I also would like to express my gratitude to all the professors and colleagues of Centro de Quimica Estrutural (CQE) for having received me so kindly and for their availability to help me whenever I needed. I must express a special thank to Miguel, due to his constant support, availability and friendship.

Finally, I am very grateful to all my friends, Maria and family, for their support and affection through the entire time. I would like to thank to Patanisca, SL Benfica and GD Vialonga, for the joys they gave me and for being an escape from this work.

Resumo

O Nitinol é uma liga composta por níquel e titânio, em proporções atómicas praticamente iguais, e que apresenta como propriedades mecânicas efeito de memória de forma e uma alta deformação elástica (superelasticidade). Para além destas propriedades, caracteriza-se por ter uma elevada resistência à fadiga e resistência à corrosão e por ser um material biocompatível, o que leva à sua utilização em aplicações biomédicas.
Porém, a elevada presença de níquel e a sua possível libertação dos dispositivos de Nitinol é um problema habitual destas ligas, o que pode levar a processos inflamatórios e alérgicos por parte do paciente.

Neste trabalho procedeu-se à modificação da superfície do Nitinol através de tratamentos térmicos em dois tipos de atmosfera (ar e azoto) e duas diferentes temperaturas (250 ℃ e 350 ℃). A resistência à corrosão das amostras modificadas foi investigada através de técnicas electroquímicas numa solução que simula o meio fisiológico (solução de Hank) a 37 ℃ e comparada com Nitinol sem tratamento. Para a caracterização das superfícies resultantes foram usadas espectroscopia de fotoelectrões de raio-X e espectroscopia de electrões Auger.

Verificou-se que os tratamentos efectuados têm infuência no comportamento electroquímico do Nitinol. Através de ensaios de EIS, e por ajuste a um circuito equivalente, considerou-se uma estrutura ”duplex” para o filme de óxido, constituído por uma densa camada interna e uma camada externa porosa. As técnicas de análises de superfície permitem concluir que o teor de níquel é substancialmente reduzido nos filmes superficiais após tratamento a 350 ℃, especialmente em atmosfera de azoto.

Palavras-chave: Nitinol, biomateriais, corrosão, tratamentos térmicos, filme de óxido

Abstract

Nitinol is a nickel-titanium alloy, nearly in the same atomic proportion, which combines unique mechanical properties, like shape-memory effect and high elastic deformation (superelasticity). In addition to these properties, the material presents high fatigue strength, corrosion resistance and superior biocompatibility, which turns it suitable for biomedical applications.
Due to the high nickel presence, inflammatory and allergic processes may be initiated as result of the release of nickel ions from Nitinol devices, being a great problem to its use.

In the present work, thermal treatments were performed in the surface of Nitinol in two types of environment (air and nitrogen) and at two different temperatures (250 ℃ and 350 ℃). Corrosion resistance of the treated alloys was analyzed through electrochemical techniques in simulated physiological conditions (Hank's solution at 37 ℃) and the results were compared with untreated Nitinol. The modified surfaces were characterized by X-ray photoelectron spectroscopy and Auger electron spectroscopy.

The performed surface treatments proved to influence the electrochemical behaviour of Nitinol. From EIS spectra, and by fitting the data to an equivalent circuit, a "duplex" structure was proposed to the alloy's oxide film, composed by an inner compact layer and an outer porous layer. Results from the surface analysis concluded that the nickel content was substantially decreased in the outermost surface layers, especially when treated at 350 ℃ in N_2-controlled environment.

Keywords: Nitinol, biomaterials, corrosion, thermal treatments, oxide film

Contents

List of Tables

List of Figures

Nomenclature

$\|Z\|$	Impedance modulus
ΔG	Gibbs Free Energy
ω	Radial frequency
ϕ	Phase-shift or phase angle
σ	Stress or surface rougness factor
θ	Phase angle (in Bode diagrams)
ε	Strain
A	Parent Phase (Austenite)
A_f	Austenite finish temperature
A_s	Austenite start temperature
AES	Auger Electron Spectroscopy
BCC	Body Centered Cubic
C	Capacitance
C_b	Barrier layer capacitance
C_{dl}	Double layer capacitance
C_f	Capacitance of film thcikness outside the pores
CFC	Corrosion Fatigue Cracking
CPE	Constant Phase Element
E	Potential
E	Young's or elastic modulus
E_b	Breakdown potential
E_{corr}	Corrosion potential

E_{pp}	Passivation potential
EIC	Environmentally Induced Cracking
EIS	Electrochemical Impedance Spectroscopy
ESCA	Electron Spectroscopy for Chemical Analysis
f	Frequency
HA	Hydroxyapatite
HIC	Hydrogen Induced Cracking
I	Current
i_{crit}	Critical current density
i_{pass}	Passive region current density
j	Imaginary number
L	Self-inductance
M	Product Phase (Martensite)
M_f	Martensite finish temperature
M_s	Martensite start temperature
Ni-Ti	Nickel and Titanium alloy
NiTi	Nitinol
OCP	Open-Circuit Potential
PBS	Phosphate-Buffered Saline
PEO	Plasma Electrolytic Oxidation
PIII	Plasma Immersion Ion Implantation
R	Resistance
R_b	Barrier layer resistance
R_{ct}	Charge Transfer resistance
R_{pore}	Electrolyte resistance inside the pores
R_s	Solution resistance
SBF	Simulated Body Fluid
SCC	Stress Corrosion Cracking

SCE	Saturated Calomel Electrode
SEM	Scanning Electron Microscopy
SHE	Standard Hydrogen Electrode
SMA	Shape Memory Alloy
SME	Shape Memory Effect
T	Temperature
t	time
TEM	Transmission Electron Microscopy
UTS	Ultimate Tensile Stress
W	Warburg impedance
XPS	X-ray Photoelectron Spectroscopy
Z	Impedance
Z_0	Impedance's magnitude or modulus

Chapter 1

Introduction

1.1 Topic Overview

The use of metallic materials in the biomedical field can be traced back to the 19^{th} century, having started with demands for the development of metallic implants in bone repair, commonly internal fracture fixation of long bones. Since then, these materials have predominated in orthopedic surgery, being used either as temporary devices (in form of bone plates or screws) or as permanent implants (for total joint replacements), but also found application in orthodontic practice, for example.

The important role of some metals in the human body, in molecular scale functions, is well known, with Mg ensuring the strength and stiffness of the bones and Fe being present in hemoglobin; besides these, many other metals exist in the human tissue as trace elements.
Recently, increasing research effort in metallic biomaterials has been invested in application of the non-conventional reconstructive surgery of hard tissues/organs and even in non-osseous tissues, such as blood vessels [1].

Nowadays, there is a wide variety of metals and alloys able to be produced in industry, although not all being biocompatible and capable of being successfully implanted into the human body.
Shape-Memory Alloys (SMA) is a group of materials that have been largely applied in the production of biomedical devices in the last years, in particular for minimal invasive techniques [2], due to their capability to recovering the original shape and dimensions after large deformations. The most used SMA is Nitinol (NiTi), characterized by its superelasticity, relatively stable cyclic performance, good workability and good resistance to corrosion and fatigue [1].

1.2 Objectives

The aim of this master thesis is to understand the effect of thermal treatments in the corrosion resistance of Nitinol, and the consequences of those treatments in the composition of the outermost layers of the material.

1.3 Thesis Outline

The present work is divided in 5 main chapters.

In the first chapter, a brief overview of metallic biomaterials is given , with the objectives of this master thesis being presented, along with the contents of each chapter.

Chapter 2 starts to give a short overview of Nitinol history and its mechanical properties. A detailed overview about biocompatibility and corrosion resistance is then presented, with an extended literature review. At the end of the chapter, Nitinol's major applications are referred.

The experimental methods are described in the Chapter 3, comprising the samples and solutions preparation, and a short description of the electrochemical measurements and surface analysis techniques.

Chapter 4 shows the results, namely the open-circuit potential, anodic polarization curves and electrochemical impedance spectra of treated and untreated Nitinol; a structure of the oxide film formed at the surface of the alloy is proposed. Surface analysis is also depicted.

The final chapter presents the general conclusions from this work, along with a few ideas for future work.

Chapter 2

Background

2.1 Theoretical Overview

The application of a material to a certain purpose depends, naturally, of its properties and the function that it will have. In the biomedical field, it's very important to ensure that the material presents a high corrosion resistance and biocompatibility, because it will be in contact with the human body for periods that can go from a few hours to several years. Nitinol, a nearly equiatomic alloy, composed of nickel and titanium, has been gaining a considerable amount of attention since the late 1980's due to its particular combination of properties: shape memory effect and superelasticity (mechanical properties) and biocompatibility (physical-chemical properties).

The discovery of this Ni-Ti alloy is reported to 1959 by William J. Buehler, from the U.S. Naval Ordnance Laboratory (the name Nitinol is derived from **N**ickel **T**itanium **N**aval **O**rdnance **L**aboratory). NiTi first successful application was coupling hydraulic-fluid lines in F-14 jet fighters. Since that, and with improved manufacturing techniques, the commercial use of NiTi increased during the 1970's and 1980's, being applied into medical, safety and military products [3]. By the late 1980's, the attention focused towards medical applications, particularly implants. Due to Nitinol unique characteristics, combined with the isothermal environment of human body, the introduction of the material into the patient is simple through minimal invasive procedures.

2.2 Nitinol characteristics

2.2.1 Shape Memory Effect (SME)

The shape memory effect refers to the ability of materials to return to their pre-defined dimensions upon heating. This property is a consequence of a martensitic transformation, a solid state phase change from austenite to martensite. In figure 2.1 a schematic picture is represented to help illustrating the SME.

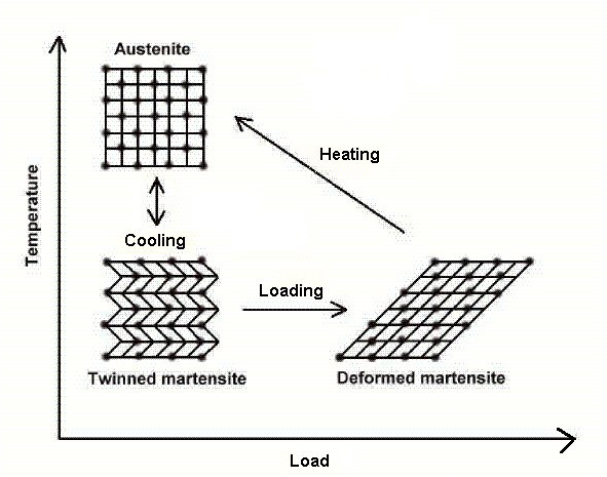

Figure 2.1: Shape Memory Effect [4].

A shape memory alloy can exist in two phases: austenite (at high temperatures and called the *parent phase*, A) and martensite (at low temperatures, *product phase*, M). If a specimen at high temperature, being fully parent phase, is cooled, it will start to suffer a change in its crystal structure, when a certain M_s temperature (martensite start temperature) is reached. As temperature continues to fall, the transformation to a martensitic structure proceeds until M_f temperature (martensite finish temperature), at which the specimen is 100 % martensite.

The reverse transformation can also occur. By heating the material in the martensitic shape, the austenitic structure begins to form at a temperature named A_s (austenite start temperature), being fully transformed at A_f (austenite finish temperature); this reversibility is associated with a temperature hysteresis.

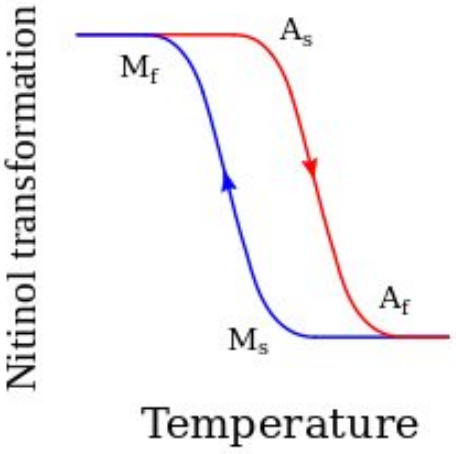

Figure 2.2: Temperature hysterisis of Nitinol [5].

To a proper use of the SME in the biomedical field by NiTi alloys, A_f must be in a value slightly below the human body temperature. Being the martensitic phase very malleable, it can be introduced into

the patient in a shape that facilitates its insertion; by reaching the temperature inside the body, it can assume a totally different shape (as austenite already). Further ahead, in NiTi applications (section 2.6), very clear examples will be given to show how this property is crucial in the success of the alloy.

Several properties of NiTi's austenitic and martensitic state are notably different; although, these A $\rightarrow$ M and M $\rightarrow$ A transformations are not macroscopically noticed, there is a marked change in its inner structure that will confer a different behaviour to each solid phase. NiTi in the austenitic state has a BCC (body centered cubic) structure while as martensite is a rhombohedral crystal, being deformed in the plastic regime when submitted to a certain load. Heating the specimen to a temperature above the A_f, causes the disappearance of that macroscopic deformation, and its return to the initial conditions – shape memory effect (see figure 2.1). Strains on the order of 10% imposed to martensite allow for full shape recovery of NiTi, a very important feature of this type of alloy when compared with classic materials likewise steel or aluminum, which afford a maximum value of elastic strain of about 1% [6, 1].

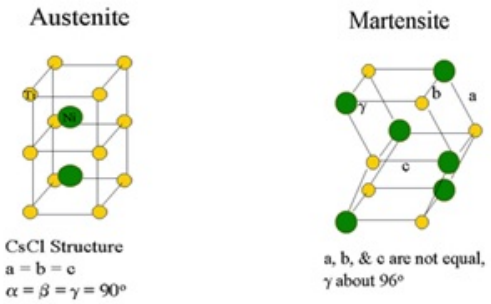

Figure 2.3: Austenitic and martensitic structures of NiTi [7].

As it was said before, the shape memory effect of Nitinol is a result of a martensitic transformation. It can be defined as a displacive, diffusionless transformation where a new phase is obtained, through an atomic reordering at short distances (less than one interatomic spacing); the product phase has the same chemical composition of the parent phase and generally it occurs very fast, being considered independent from time [8]. This type of transformation can occur in many type of metallic and non-metallic crystals, minerals and compounds [9], and its driving force can be either chemical or mechanical, through cooling or loading with an external force, respectively [10].

The atomic movements during a martensitic transformation are known for being ordered and cooperative and most of atoms have the same nearest neighbours in both phases (austenite and martensite), although differently arranged. The manner in which atoms change position in this transformation, orderly, disciplined manner, like regimentation, has led to it being named *military transformation*, in contrast to diffusion-controlled transformations which are termed *civilian*. The truth is that its movements do not happen simultaneously – atomic movement propagates successively in an ordered manner as a transformation front moves across the material, looking like a domino effect, with each atom falling one after

another in succession, rather than a military movement [9, 11].

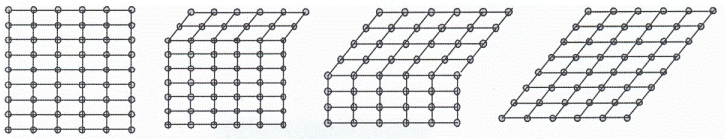

Figure 2.4: Displacive transformation [8].

The change from austenite to a different structure, as illustrated in figure 2.4, produces a vacant volume inside the crystal. This happens due to opposing stresses applied to the transforming region, exerted by the surrounding matrix, to minimize the shape change. Elastic strains are insufficient to relax these stresses, so plastic deformation is considered to be a consequence of this type of transformation. This deformation may be produced by the movement of dislocations, *slip*, or by partial dislocations: *stacking faults* or *internal twins* [11]. Point defects, like interstitial atoms and vacancies, may also be produced [11].

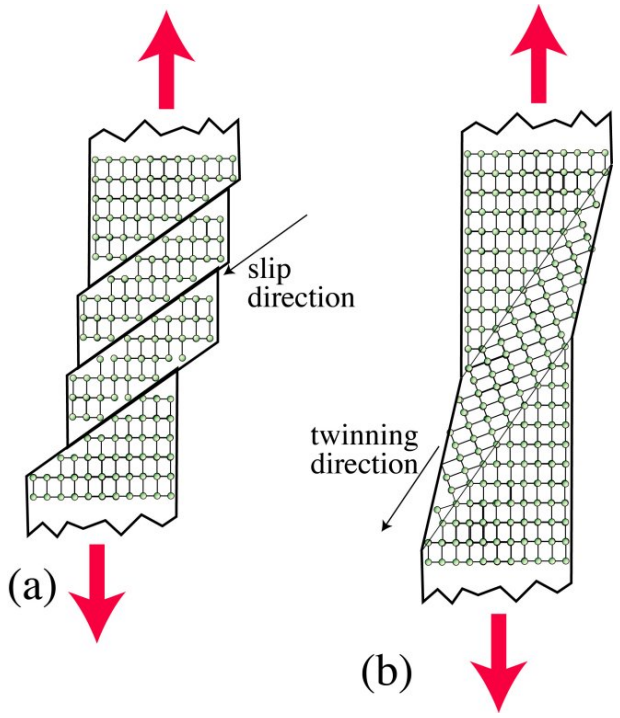

Figure 2.5: (a) Dislocation glide and (b) deformation twinning [12].

In short, the presence of lattice imperfections, which is an important feature of martensite, is a consequence of cooperative atomic movements, and its amount is larger when the transformation strains are large, and smaller when the strains are small. Other main characteristics of martensitic reactions are related with their dependence on time and temperature, among others. The amount of transformation is independent of time – at a constant temperature, a fraction of the parent phase transforms very quickly, after which there is no further change – but it depends on the temperature. The velocity of the reaction is usually very fast, having as limit that of sound [13].

Martensitic transformation is a reversible process, in the sense that an initial atomic structure can be repeatedly obtained - this is the fundamental principle of the SME. A single austenitic crystal can origin one or several crystals of the new phase, through cooling. The reverse reaction, transformation of martensite to austenite by heating, results in a single crystal of the same size, shape and orientation as the original crystal. The martensite crystals are oriented with respect to the original lattice; the plane of the lattice on which they are formed is called the *habit plane*. In general, the volume change between the two phases is not very significant.

2.2.2 Superelasticity

Another property that makes NiTi of special interest is its ability to return to the initial shape, after the release of an induced stress. These type of mechanical behaviour that occurs at a constant temperature $T > A_f$, is called superelasticity, or pseudoelastic effect. It was discovered by the swedish metallurgist Arne Ölander in 1932 concerning a gold-cadmium alloy and reported during a meeting of the Swedish Metallurgical Society. Later, in 1951, Chang and Read were able to give a much clearer explanation about this phenomenon [13].
In Fig. 2.6 a stress-strain curve is represented, illustrating the pseudoelastic behaviour of Ni-Ti alloy. Following Fig. 2.6, when an initial strain is applied to the original material, in the austenitic state, it is possible to observe a proportionality between stress and strain, according to Hooke's law:

$$\sigma = E\varepsilon \tag{2.1}$$

with the constant of proportionality (E) being called the Young's modulus, its value being specific for each type of material [14]. In the region of the stress-strain curve where the Hook's law is observed, the austenitic metal undergoes elastic deformation (path between the origin and point **A**). For strains applied above point **A**, martensite starts to form (stress-induced martensite), and a superelastic plateau is observed, from **A** to **B**, point in which the martensitic transformation is complete. Elastic deformation of martensite occurs (point **B** to **C**) if the material is further strained; if it is strained too much, irreversible plastic deformation may occur.

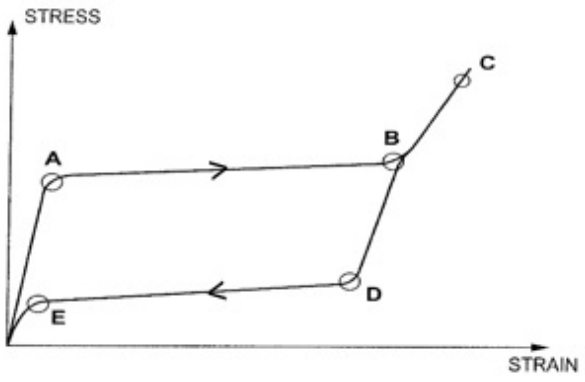

Figure 2.6: Nitinol stress-strain curve [15].

When the stress is reduced, it starts to become thermodynamically more stable for the material to come back to its parent phase and the martensite begins to transform to austenite – point **D** – until transformation is complete, point **E**, followed by elastic unloading [16]. In this way, the net deformation after a load-unload cycle is effectively zero [13]. Stress-strain plots of alloys with this pseudo-elastic behaviour exhibit a pronounced hysteresis, as similarly seen in the thermal cycle, because of the different stress levels at which the forward and reverse transformation happen [16].
As just seen, the two main mechanical properties of NiTi are due to martensitic transformations, although induced by two different manners: SME originates from temperature modifications, while superelasticity relies on a stress-induced martensitic transformation.

2.2.3 Other properties

Beyond the shape memory effect and superelasticity, Nitinol holds other interesting properties, from the mechanical point of view. Young's modulus is one of them, with a value in the range of 30 – 50 GPa. Comparing with other metallic materials used in medical implants, the closest value of Young's modulus to that of cortical bone (between 10 and 30 GPa) is Nitinol's [1].

Table 2.1: Mechanical properties of metallic implant materials and cortical bone [1].

Material	**Young's modulus (GPa)**	**UTS (MPa)**	**Fracture toughness (MPa $\sqrt{m}$)**
CoCrMo alloys	240	900–1540	100
316L stainless steel	200	500–1000	100
Ti alloys	105–125	900	80
Mg alloys	40–45	100–250	15–40
NiTi alloys	30–50	1355	30–60
Cortical bone	10–30	130–150	2–12

Table 2.2: Mechanical properties of NiTi alloys in comparison with 316L stainless steel and cortical bone [1].

Alloys	**Young's modulus (GPa)**	**0.2 yield stress (MPa)**	**Maximal elastic strain (%)**	**UTS (MPa)**	**Elongation at rupture (%)**	**Fracture toughness (MPa$\sqrt{m}$)**
316 L ss	200	200–700	0.20	500–850	10–40	100
NiTi (austenite)	50–80	200–700	10	900–1355	14.3	30–60
NiTi (marten-site)	30–40	70–140	10	NA	NA	NA
Cortical bone	10–30	NA	NA	50–150	NA	2–12

By the analysis of Table 2.1 it is easily seen that stainless steel and cobalt- and titanium-based alloys have much higher Young's modulus than bone (and NiTi), what means that, in order to obtain the same deformation than the last ones, it is necessary to impose very high stresses. For that reason, implants made of those materials, for being very inelastic, can bear almost all the subjected load; this situation

leads to negative effects for the bones around the implant site, because the loading on these bones decreases, causing weakness and atrophy to them. This phenomenon, called *stress shielding effect*, turns desirable to choose an implant with similar Young's modulus to that of bones [1].

Two other general mechanical properties of interest are the yield strength and UTS (standing for *Ultimate Tensile Stress*), which quantify the behaviour of a material under stress. The first one refers to the stress value at which a material begins to deform in the plastic regime while the second one is the maximum resistance to fracture. Table 2.2 shows that these properties for NiTi are not affected by its relatively low Young's modulus, being comparable of those of stainless steel. Another very attractive mechanical property of Nitinol is its large elastic strain, in the order of 10% approximately, much higher than any traditional alloy, like stainless steel that presents a value around 0.20%.

2.3 Biocompatibility

The biocompatibility of a material used in intimate contact with human beings is obviously considered a very sensitive topic; a great amount of experiments must be done in order to ensure that a certain material is not harmful to the host before its application on a large scale. It is considered that NiTi exhibits good biocompatibility, although a few conflicting results published in the literature may question its certainty [17].

The biocompatibility of a device may be defined simply as its ability to perform with an appropriate host response in a specific situation [18]. This means that no harmful effects should be noticed in the human body when in contact with it – the material should be made of elements that minimize the impact that a "strange" body causes. In reality no metals or alloys are completely inert or non-toxic and the degree of biocompatibility is related to the extent of the reaction between the foreign and the host body [19].

The chemical interactions of a medical implant with the physiological environment of the host system (for example, the release of toxic metal ions) is the primary concern regarding the biocompatibility but not the only one. In a minor scale it also includes the mechanical properties of the material, as the physical impacts of the implanted material on the surrounding tissue. There are records of cervical fusion implants and joint replacements procedures that fail due to suboptimal mechanical properties, rather than problems related to the material's components [20, 21].

Another crucial factor is the specific medical application that the implant will have: a device considered appropriate for orthopaedic surgery, for example, may not be used satisfactorily in cardiovascular applications – the requirements for implants biocompatibility are complex, varying from purpose to purpose [1].

2.3.1 NiTi constituents' materials

As it was said before, NiTi is an alloy composed by nickel and titanium, in the same atomic proportion. In terms of weight, Ni has bigger expression, on the order of 55% (Ni and Ti molecular weights are 58.69

and 47.87 g/mol respectively). Ideally, non-toxic elements should be selected to be part of the material in intimate contact with the human body; unfortunately, often this situation is not possible to reach without losing the properties that turn the metal or alloy suitable to a specific application. In the situations that a reactive element is used, it is of special importance the presence of highly corrosion resistant elements [1]. Nitinol is considered to be one of these cases: an alloy made of a toxic and carcinogenic element (Ni) and a non-toxic one, even in large doses (Ti).

Nickel

Nickel is an element present in the human body in a very low quantity. Along with other compounds, such as cobalt, molybdenum and tungsten for example, nickel is needed as a micronutrient, but is considered extremely toxic at doses higher than required (1 mg/day [22]). It is very important in nutrition for the biological functionality of the human body, being present in urease, an enzyme that assists in the hydrolysis of urea, and promotes bone strength by aiding Fe absorption [1, 22], for example.

Problems associated with nickel deficiency are scarce in literature due to the low amount required, but evidence is found of deleterious effects in animals; according to Anke et al [1, 23], lack of nickel in rats caused reduced growth, interferences in lipid metabolism, skin changes and uneven hair development, among others . In another study, held by Denkhaus and Salnikow [23] in 2002, histological and biological changes in animal cells were seen, causing anemia due to weak iron resorption.
Nickel can enter in the human body through the lungs, oral intake, skin contact or via implants. The International Agency for Research on Cancer (IARC) evaluated in 2012 the carcinogenicity of nickel metal and nickel compounds, such as hydroxides, sulphides and nickel acetate and despite of concluding that there were enough evidences for classifying those substances as carcinogenic, the study did not reach an agreement about those effects in humans or animals exposed to nickel-alloys typically used in implanted medical devices [24].

There are several studies in the literature related to the toxicology of nickel, with some reports pointing out the occurrence of dermatitis due to the use of earrings containing nickel [25], inhalation of nickel carbonyl and nickel aerosols causing acute pneumonitis and chronic rhinitis and sinusitis, respectively [1] and local sarcomas caused by implanted nickel alloys inside the muscles of rats [26].
Monteiro [27] performed biocompatibility studies of stainless steel and vitallium implants in 80 patients; 10% accused positive epicutaneous patch tests for metal presence, with 5 of them having a known history of nickel allergy. The author concluded that an induction of sensitization by the implants seemed unlikely.

The high nickel content of Nitinol is the most concerning factor related to its biocompatibility. If a considerable amount of nickel is released by this alloy, it can compromise the stability of the material in contact with the human body, bringing deleterious effects to the host; because of that, several studies were performed in order to evaluate the safety of this type of alloys. Okazaki and Gotoh [28] found negligible the quantity of metals released by NiTi in comparison with other materials used for orthopedic implants

(stainless steel, Co-Cr-Mo and Co-Cr-Mo-Ni-Fe).
Michiardi et al. [29] applied a series of oxidation treatments in low-oxygen atmospheres to NiTi samples and compared their amount of nickel released with untreated ones, during one month of immersion in SBF. In the different surfaces, the peak of Ni released occurred during the first hour and started to slow down with time, stabilizing and tending to zero by the fifth day of immersion. The amount of nickel released by the untreated nitinol within the whole experiment time, way below the critical concentration to induce allergy, was 3 to 10 times higher than the treated surfaces; these results are a consequence of a thick oxide layer formed by the selective oxidation of Ti, avoiding the diffusion of Ni to the near-surface areas.

The presence of nickel even in concentrations that in theory would not cause harm to the human body can bring negative effects to it. Results of Sun et al. [30] show that osteoblasts behaviour may be affected by metal ions in a subtoxic concentration. In other case [31], a patient with a Nitinol stent implanted in the superficial femoral artery developed a severe allergic reaction. At that time, it was the first reported case of a systemic contact dermatitis from nickel allergy caused by peripheral Nitinol stent. According to the author, and referring to a non-allergic patient, the small amount of nickel that may be released from the stent shouldn't be enough to begin a significant allergic reaction, even more when the stent is located intravascularly, diluting a possible severe reaction.

Titanium

Contrary to nickel, titanium is not found naturally in the human body. The material has proven to be suitable as in implant in bone surgery, being applied in osteosynthesis, oral implantology and in joint prosthetics, making good physical connection with the host bone [1, 32]. It is considered a non-allergenic material with suitable mechanical properties, featuring an excellent biocompatibility and corrosion resistance [32]. Möller et al. performed an in vitro test, promoting the contact of zirconium ant titanium implants with osteoblasts. In the same study, the in vivo test was made using domestic pigs, over 4 and 12 weeks. The results showed good biocompatibility and osseointegration [33].
However, a few studies complaining the use of titanium can be found: Hosoki et al. [34] accompanied the case of a 69-year-old man after a dental implantation. The patient suffered of allergic symptoms (eczema) after the surgery, only disappearing completely when the implant was removed. In another work, titanium debris from metal prosthesis caused significant changes in a culture of cells, with the damage persisting on it even when the stimulus was removed [35].

In general, titanium is a material with a significant smaller allergic risk when compared with other metals; however, each patient should be object of tests to access about a potential hypersensitivity to the metal prior to the surgery.

2.3.2 Biocompatibility of NiTi - *in vitro* experiments

In vitro and *in vivo* studies on biocompatibility of NiTi alloys had been made since the late 1970's. One of the first *in vitro* reports was performed by Castleman and Motzkin [36] in 1981 using human fetal

lung fibroblasts and the biocompatibility of NiTi was tested along with 316L stainless steel, titanium and Co-Cr alloy. The cells in contact with 316L stainless steel and Co-Cr alloy presented the same cell growth than the control cultures, while the other two materials reduced cell growth. It was also observed in NiTi and titanium experiments that the morphological changes of cells were more pronounced. In 1994, Assad et al. [37] studied the cytocompatibility of NiTi and other orthopaedic materials of interest using a L-929 fibroblasts culture and observed that all metals induced a mild biological reaction. Pure titanium, 316L stainless steel and Ti-6Al-4V showed less cytotoxic behaviour than NiTi and Co-Cr-Mo, that presented similar results. Furthermore, the authors also tested NiTi samples subjected to plasma surface treatment and concluded that the cytocompatibility of Nitinol had been improved.
Since then, and with the increasing interest in the properties of Nitinol, more studies were conducted to clarify about the safety of the application of this alloy on a large scale. Between 1990 and 2010 the number of reports concerning the biocompatibility of NiTi had a tremendous boom, with some of that results being depicted in Table 2.3 [1, 38].

Table 2.3: *In vitro* studies on biocompatibility of NiTi alloys [1, 38].

Author	**Year**	**Study**
Wever et al. [39]	1997	The short-term biological safety of NiTi was evaluated; the alloy showed no cytotoxic, allergic or genotoxic activity, being regarded as a biologically safe implant material
Assad et al. [40]	1998	NiTi and CP-titanium presented less genotoxic results to metaphase chromosomes than 316L stainless steel. The cell culture response in the presence of NiTi was satisfactory
Kapanen et al. [41]	2002	The results showed low cytotoxicity of NiTi in contact with bone forming cells, from rat osteosarcoma cell line ROS-17. The number of dead cells provoked by NiTi and Ti was substantially lower than by Ni
Michiardi et al. [42]	2007	Oxidized and untreated NiTi showed an excellent cytocompatibility with MG63 cells. Bone formation may be accelerated by oxidizing the surfaces of NiTi
Nie et al. [43]	2010	Using murine fibroblast and osteoblast cell lines, no cytotoxicity was detected in the direct-contact evolution testing. NiTi was considered a novel and promising biomedical material to be used in the future

In spite of the optimistic results from the *in vitro* experiments of the last 20 years, it is very important to say that the releasing kinetics of metal ions from this kind of designed-to-be anticorrosive alloys, such as NiTi, is slow. This means that the toxicity of released ions may only be possible to diagnose several years after material's insertion. Thus, this short-term *in vitro* evaluations shouldn't be considered as a reliable indicator of long-term *in vivo* assessments of the effects of these implantable devices into the human body.

2.3.3 Biocompatibility of NiTi - *in vivo* experiments in animals

To complement the data acquired through the *in vitro* trials, *in vivo* experiments using animals were also done to test the biocompatibility of NiTi. The *in vivo* working conditions are mechanically and biologically complicated. Normal physiological loading causes a combination of various deformation strains in bone

and its vicinity, such as compression, tension, shear and vibration [1]. Biological conditions include changes in pH, low-level infection, inflammation, tissue remodelling and the presence of macrophages and debris.
In that way, besides the realism of performing the experiment in a living aggressive organism, thus observing the overall effects on it, it was also possible to track the changes in the host systems during longer periods – the tests could last between several days and a few years.

The first published *in vivo* study regarding the muscle response to a Nitinol wire was made by Cutright et al. in 1973 [44]. The reaction of the tissue to the wires placed subcutaneously in 45 rats was followed for 9 weeks. The tissue reaction was minimal during that period and "the reparative process was initiated within 1 to 2 weeks and formed a dense, relatively avascular fibrous connective tissue capsule" around the implants [44]. From this study it was concluded that NiTi could be used in deep tissues.
3 years later, another report was released concerning NiTi as a bone implant [45]. Nitinol and Co-Cr alloys were used as bone plates and implanted into the femurs of beagles for periods of 3, 6, 12 and 17 months; after that time, tissue from liver, spleen, lung, kidney and brain was removed for observation. There were no negative evidences caused by NiTi, possibly triggered by the contact of the metallic implant with the surrounding tissue, neither any adverse tissue reaction, such as bone resorption. High nickel concentration was observed but it was considered as contamination during the cutting procedure. The researchers concluded that due to the lack of toxic effects *in vivo*, Nitinol was sufficiently compatible with dog tissue to guarantee further investigation of its potential as a biomaterial; however, the authors also pointed out some failures in their work, such as the small number of test animals (12 in total) that made difficult the statistical analysis due to some considerable variation between the capsules of different specimens of the same material. Also the muscle tissue in dogs exposed to NiTi implants for 17 months presented some variability.

Table 2.4: *In vivo* studies on biocompatibility of NiTi alloys [1, 38].

Author	**Year**	**Study**
Yang et al. [46]	1992	Internal fixing devices made of NiTi and 316L stainless steel plate-screws were applied into fractured femoral shafts of dogs for a maximum period of 12 weeks. The fracture healing was similar between the two materials but the stress-shielding effect in the bone underneath the NiTi device was less visible, due to its lower elastic modulus. The axial compression stress of the fracture line is kept greater and the contact of NiTi with the cortical bone was not so close, which might be beneficial for the recovery of blood supply and bone remodelling

Continuation of Table 2.4		
Author	**Year**	**Study**
Matsumoto et al. [47]	1993	During 4 weeks, a NiTi device for correction of scoliosis was implanted in the paravertebral area of 4 rabbits. The Ni concentration in the blood after 6-9 hours of the insertions was twice the normal level; After 4 weeks the Ni concentration was: 4-fold in the kidneys, 2-fold in the liver and 10-fold in urine. The use of coatings might had been a good method to limit Ni high levels
Simske and Sachdeva [48]	1995	Porous NiTi and hydroxyapatite (a type of calcium phosphate ceramic used for bone repair in maxillo-facial surgery) were placed to either side of the frontal bone of 7 rabbits. No adjacent macrophage cells were observed for either implant type, the materials made bone contact with the surrounding cranial hard tissue and the percentage of ingrowth increased with the recovery time. There were no significant differences in quality between the bone in contact with the implants and the surrounding cranial bone. After 12 weeks porous NiTi implants appear to allow for cranial bone ingrowth and were considered suitable for craniofacial applications
Berger-Gorbet et al. [49]	1996	NiTi screws implanted in tibias of rabbits showed a slower bone-remodelling process when compared with the other control materials (such as vitallium and titanium among others). This slow osteogenesis was characterized by no close contact between bone and implant, disorganized migration of osteoblasts around the implant and a lower activity of osteonectin synthesis
Takeshita et al. [50]	1997	The bone reaction to NiTi, titanium, anodic oxidized titanium (AO-Ti), Ti-6Al-4V and nickel was assessed by inserting these material through the medullary canal of rat tibiae. The implant materials were encapsulated with bone tissues excepting Ni which was encapsulated with connective tissues through the 168-day experimental period. Ni showed no bone contact at any time during the experiment. Histometric analysis revealed no significant differences among the tissue reactions to Ti, AO-Ti and Ti-6Al-4V with nitinol implants showing significantly lower percentage of bone contact and bone contact area than the other titanium-made materials

Continuation of Table 2.4		
Author	**Year**	**Study**
Wen et al. [51]	1997	The corrosion resistance and tissue biocompatibility of NiTi and Ti50Ni50-xCux (x = 2, 6, 8) alloy were investigated by electrochemical and quantitative histomorphometric methods. There were no significant differences on tissue reaction parameters after two and three months between the 4 tested alloys. After the 3-months implantation, no corrosion was observed in the plate surfaces. It was concluded that the 4 alloys present good biocompatibility
Idelshohn et al. [52]	2004	NiTi springs were implanted in 6 female rabbits to induce the bone neo-formation. All the tested animals completed the distraction with success. A continuity in the newly formed bone with similar transversal and horizontal dimensions than the original bone can be observed. The report concludes that the application of a constant force on distraction osteogenesis using SMA springs (NiTI in the case) may be a successful alternative to the conventional gradual distraction
Li et al. [53]	2007	The histological performance of HA (hydroxyapatite) coated NiTi and untreated NiTi was evaluated after two years of implantation by animal model (rabbits). The bioactivity and biocompatibility of NiTi are substantially improved by means of HA coating through chemical treatment; despite this observation, the untreated NiTi shows good biocompatibility after long time implantation
Liu et al. [54]	2010	Bone ingrowth under load-bearing in vivo conditions was investigated through implants into the distal part of the femur/tibia of rabbits for 15 weeks. Porous NiTi materials bond very well to newly formed bone tissues, penetrating deeply into the porous NiTi scaffold compared to one made of porous Ti. Histological analysis revealed that new bone tissues adhere and grow well on the external surfaces and exposed areas on the inner pores of the NiTi scaffold, allowing for fast formation and ingrowth of new bones. Thus, this material is considered suitable for clinical applications under load-bearing conditions

In the majority of the cases depicted in Table 2.4, it is possible to assign a good biocompatible behaviour for NiTi or surface-modified NiTi. However, there are also some conflicting results [47, 49, 50] in which arise some concerns with this alloy, such as inferior properties compared with stainless steel, Co- and

Ti- alloys [49, 50], or a high nickel concentration [47]. In respect to the performance of modified NiTi alloys, the results are positive, with its biocompatibility being similar or better than the untreated Nitinol. The application of coatings proved to be a promising method to improve the biocompatibility of this alloy, as shown in [48, 53] by the deposition of hydroxyapatite. In this way, a considerable attention must be given to this kind of modified alloys (see Chapter 2.5).

2.3.4 Biocompatibility of NiTi - *in vivo* experiments of implants in humans

In addition to the referred *in vitro* and *in vivo* reports, NiTi has also been used as a human implant material either for hard and soft tissue – Table 2.5. The cases found appear to conclude that NiTi presents good potential for its clinical use. However, due to a clear lack of knowledge about Nitinol's biocompatibility, its medical applications have been hindered worldwide [1] and the number of trials is quite scarce – there was only one found in the last 15 years – what makes it harder to reach an agreement about this matter.

Table 2.5: Biocompatibility studies of NiTi alloys in humans [1, 38].

Author	**Year**	**Study**
von Salis-Soglio [55]	1989	The author conducted a study of ventral intercorporeal lumbar spondylodesis with a NiTi implant in 51 patients within an average postoperative period of 9 months. One case of pseudoarthrosis and 11 of delayed bony fusion were observed. It was concluded that, in light of the easier operative technique, the earlier mobilization of the patients and the good fusion rate, the NiTi spondylosis seems to have important advantages over the transplantation of bone chips
Qiu [56]	1993	NiTi urethral stents were implanted in 39 patients with benign prostatic hyperplasia (BPH). A clinical success rate of 89% was achieved and follow-ups of 3-26 months showed no incrustation and migration of the spiral
Tang et al. [57]	1996	36 metatarsal osteotomies using internal fixation made of a NiTi compression staple for hallux valgus were performed in 21 patients. 20 patients had complete relief from pain, while in one foot the pain was transferred under the second metatarsal head. All osteotomies united, and the average angle of hallux valgus and the intermetatarsal angle improved. The time of bone healing was shortened and patients were allowed to bear weight earlier than usual (after 19 and 41 days post-surgery for light and normal work respectively)

Continuation of Table 2.5		
Author	**Year**	**Study**
Itro et al. [58]	1997	A NiTi device was utilized in the surgical correction of maxilla-facial fractures. This study showed that the surgical treatment of maxillo-facial bone fractures by shape memory alloys is simple, ensures a good stability of fracture surfaces, reducing the time period of operative procedures and patient's rehabilitation, by allowing a fast bone healing
Kim et al. [59]	2012	The aim of this investigation was to evaluate the safety and early surgical outcomes of NiTi endoluminal Compression Anastomotic Clip 30 (NiTi CAC 30) for intestinal anastomosis in 50 patients with gastrointestinal malignancy. No early migration or expulsion was observed, neither anastomotic leakage or bleeding occurred. NiTi CAC 30 proved to be safe and feasible for intestinal anastomosis without anastomotic leakage and reoperation compared with the stapling technique

More general conclusions from studies realized carried out on NiTi capability of well-behavins in the aggressive environment of the human body will be given in the NiTi applications and corrosion resistance chapters. At this point, most of the cases analysed seem to point out to a good biocompatibility of the alloy but, due to its unique properties and wide variety of applications, more studies should be conducted (in number and variety) for a better clearance of its safety. According to Ryhänen [38] there are reports from 1980's of NiTi material that has been successfully used in bone-related human applications in Russia and China in a large number of applications. With the advantage of technology and a deeper understanding of these "smart" alloys, there is no apparent reason for what it looks like an underuse of Nitinol potential.

2.4 Corrosion resistance

One of the main properties that a material should possess in order to be maintained in intimate contact with the human body is high resistance to corrosion. Being the human body an aggressive environment for implants, it is vital to select a material that will perform adequately in it, knowing that there are metals very corrosion-resistant in air but corroding severely in the human body. For example, high corrosion resistant stainless steels usually cause chronic allergy and toxic reactions in the host body [1].
Even the conditions inside the human being are different from region to region (for example, blood vs buccal cavity), having each own different pH values and oxygen concentrations; because of this, implants with a good performance in one part of the body can suffer an high degree of corrosion due to acidic erosion or oxidation in another one [1].

Aqueous ions also help the acceleration of corrosion. Under normal conditions, human tissue fluid and blood plasma contain high ion concentrations, mostly Na^+ and Cl^- but also traces of K^+, HCO^{3-} and Ca^{2+} among others. Amino acids and soluble proteins exist as well in most body fluids. At normal body temperature, around 37℃, and 1 atm, these fluids present a pH value between 7.2 and 7.4; however, corrosion of implants may increase the acidity within human body [60].
In short, the ideal corrosion resistance for an implant would be such that minimize the release of metal ions in any part of the body over a long period of service (several decades), remaining at a satisfactory level under normal physiological conditions [1].

2.4.1 Corrosion

Definiton of corrosion

Before heading to the corrosion resistance of NiTi and studies about it, it is important to clarify some concepts about corrosion, like what is it, in which conditions does it happen and how can it be avoided.
Corrosion can be defined as the deterioration of materials due to chemical interactions with their environment. Generally the term is applied to metals, and in that case, corrosion is caused normally by their oxidation due to electrochemical processes. However, there are other materials that can also corrode, such as plastics, concrete and wood [61].
In a study [62] released by NACE International (National Association of Corrosion Engineers) in March 2016, the estimated global cost of corrosion was around 2.5 trillions US dollars, equivalent to roughly 3.4% of the global Gross Domestic Product. There are also other disastrous consequences difficult to quantify, like human losses or interruption of communications, caused by corrosion in safety devices of bridges, aeroplanes or cars or in telecommunication cables, respectively [61]. Figures 2.7 and 2.8 illustrate some examples of materials affected by corrosion.

Figure 2.7: Rusty car [63].

Mechanisms of corrosion

The process of corrosion for metallic materials can be explained by an electrochemical process, in which there is a transfer of electric charges through an aqueous environment, denominated *electrolyte*.

(a) Rusted struts of a bridge

(b) Corrosion in a master phone socket

Figure 2.8: Other cases of corrosion [64, 65].

Equation 2.2 represents a standard *oxidation* reaction, characterized by a loss of electrons by the metal:

$$Me \longrightarrow Me^{n+} + ne^{-} \tag{2.2}$$

The oxidation reaction involves an increase of the oxidation state of the metal (in this case, from 0 to +n) and the electrode in which this reaction occurs is called *anode*; that is why oxidation can also be called as *anodic reaction*. The electrons coming out from the metal in the oxidation reaction are conducted to another chemical species, becoming part of it, in a reaction called *reduction*. The oxidation state of the species that consume electrons will also change, decreasing. *Cathode* is the name of the electrode where the reduction, also called *cathodic reaction*, takes place.

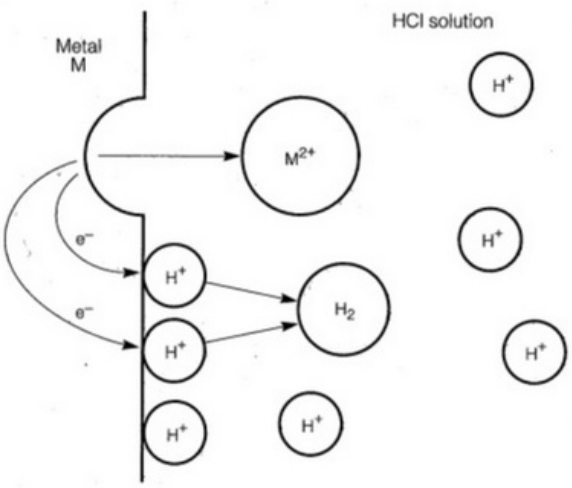

Figure 2.9: Schematic diagram of metal M dissolution [66].

Figure 2.9 shows a corrosion process scheme of a metal in an acidic solution. The metal M dissolves according to the oxidation reaction 2.2, releasing electrons into the bulk of the metal and M^{2+} ions into the surrounding solution (HCl). The electrons then move through the metal into an adjoining surface (functioning as cathode) where they reduce H^{+} ions from the acid, with the formation of molecular hydrogen:

$$2\,H^+ + 2\,e^- \longrightarrow H_2 \tag{2.3}$$

Examples of anodic reactions involved in corrosion are typically of the 2.2 type, such as iron oxidation:

$$Fe \longrightarrow Fe^{2+} + 2\,e^- \tag{2.4}$$

$$Ni \longrightarrow Ni^{2+} + 2\,e^- \tag{2.5}$$

$$Al \longrightarrow Al^{3+} + 3\,e^- \tag{2.6}$$

Cathodic reactions with significant interest for corrosion are quite scarce. The most common one consists in the reduction of H^+ into hydrogen gas, in acidic solution (eq. 2.3). In solutions exposed to ambient air, the reduction of dissolved oxygen is often observed, with equations 2.7 and 2.8, showing the reactions for basic/neutral and acidic solutions, respectively [61]:

$$O_2 + H_2O + 4\,e^- \longrightarrow 4\,OH^- \tag{2.7}$$

$$O_2 + 4\,H^+ + 4\,e^- \longrightarrow 2\,H_2O \tag{2.8}$$

Electrode Potentials

When there is more than one metallic species in contact with an electrolyte, the question of which one will corrode can emerge; knowing that each metal has a certain tendency to suffer corrosion in a specific environment, the one with a lower value for the *reduction potential* will oxidize. The reduction potential can so be defined as the tendency of a chemical species to acquire electrons, being reduced. Considering the case of iron immersed in a solution with copper ions, reactions 2.9 and 2.10 will take place

$$Fe \longrightarrow Fe^{2+} + 2\,e^- \tag{2.9}$$

$$Cu^{2+} + 2\,e^- \longrightarrow Cu \tag{2.10}$$

with iron dissolution (eq. 2.9) generating the release of electrons, which in turn reduce Cu^{2+} ions (eq. 2.10), resulting in the deposition of metallic copper on the iron. In this situation and according with what was said, the metallic component with bigger reduction potential, copper, was reduced. A list based on the reduction potentials for each species can be formulated, the so called *electrochemical series*, measured in standard conditions - 25 ºC, at atmospheric pressure - and assigning a value of 0 to the electrode used as reference to the others, called *standard hydrogen electrode* (SHE). The substances

at the top of Table 2.6, like gold or platinum, are nobler, having less tendency to oxidize than those below them in the table.

Table 2.6: Standard electrochemical series.

Reaction	Standard Reduction Potential (V)
$Au^{3+} + 3\,e^- \longrightarrow Au$	$+1.498$
$Pt^{2+} + 2\,e^- \longrightarrow Pt$	$+1.118$
$Ag^{+} + e^- \longrightarrow Ag$	$+0.799$
$Fe^{3+} + e^- \longrightarrow Fe^{2+}$	$+0.771$
$Cu^{2+} + 2\,e^- \longrightarrow Cu$	$+0.337$
$2\,H^{+} + 2\,e^- \longrightarrow H_2$	0
$Pb^{2+} + 2\,e^- \longrightarrow Pb$	-0.126
$Sn^{2+} + 2\,e^- \longrightarrow Sn$	-0.136
$Ni^{2+} + 2\,e^- \longrightarrow Ni$	-0.250
$Co^{2+} + 2\,e^- \longrightarrow Co$	-0.277
$Cd^{2+} + 2\,e^- \longrightarrow Cd$	-0.403
$Fe^{2+} + 2\,e^- \longrightarrow Fe$	-0.440
$Cr^{3+} + 3\,e^- \longrightarrow Cr$	-0.744
$Zn^{2+} + 2\,e^- \longrightarrow Zn$	-0.763
$Ti^{2+} + 2\,e^- \longrightarrow Ti$	-1.630
$Al^{3+} + 3\,e^- \longrightarrow Al$	-1.662
$Mg^{2+} + 2\,e^- \longrightarrow Mg$	-2.372

The standard conditions, however, are not seen very frequently due to several reasons such as temperatures different from 25 ℃, impurities in the metal, activities of ionic species different from unity, formation of an oxide layer on the metal's surface, among others [61]. Being the reduction potentials dependent of the environment, the relative position of each cathodic reaction in the electrochemical series can change for each surrounding medium. For example, in flowing seawater and NaCl 3% solution, the titanium electrode potential is about -0.1 and $+0.37$ V respectively, being one of the most oxidizing-resistant species, while in the standard conditions is one of the bottom elements of the electrochemical series. This kind of series, different from standard conditions, are named *galvanic series* and a metallic species will be dissolved If there's an existing element in that environment with a higher value of potential to consume the released electrons of the oxidation [61].

Passivity

Some metals, such as aluminium, nickel, chromium, titanium and cobalt, have the ability to form a thin oxide or oxyhydroxide layer on its surface, that confers an increase of surface's stability by protecting the bulk material from corrosion. By this, in situations where corrosion was expected to dissolve the material, a loss of reactivity is observed, through a drastic decrease in corrosion rate. This phenomenon is called *passivity* and it's exhibited under certain environmental conditions by those metals; for alloys, usually one element is enriched in the film (for instance, films on Fe-Cr alloys are enriched in Cr). The formed passive film, usually with a nm thickness, does not cause a complete suppression of the corrosion, but

it slows it considerably: a reduction of 10^3 to 10^6 times below the corrosion rate is often seen [61].

The corrosion resistance reliability of some metals or alloys used in construction is based on its capacity to passivate, with aluminum being one of these common cases; without the formation of thin passive layers that isolate the surface from the surrounding environment, the majority of the structural materials wouldn't be stable and could react violently with drastic consequences [61].
Another important metal is chromium, frequently used in alloys because of the resistant passive oxide film formed on its surface. For being brittle it is not used alone, but enhances passivity when alloyed with other metals, such as iron and nickel in stainless steels [66]; steels with $>$ 12% Cr improve substantially its corrosion resistance with the formation of a protective Cr-rich film, becoming stainless steels.

In spite of its enormous contribution to the stability of the materials, passivity has also some collateral dangers. Often this thin films are susceptible to local breakdown and accelerated localized attack, with some of the most dangerous forms of corrosion being precisely due to the rupture of oxide layers.

Forms of Corrosion

Several types of corrosion exist and will be succinctly described next, being different from each others in terms of their mechanisms, targeted materials and protection measures.

Uniform Corrosion

Figure 2.10: Uniform Corrosion [67, 68].

The uniform attack is a type of corrosion that affects the material evenly along its surface, normally leaving behind roughness on it. The corrosion environment has the same access to all parts of the metal, with its surface being either metallurgically and compositionally uniform; in practice, these two last requirements are quite difficult to achieve, and some degree of non-uniformity is tolerated in the definition of uniform corrosion.

Familiar examples of this kind of corrosion are easily seen, such as general rusting of steel and iron and tarnishing of silver ware, by atmospheric corrosion. Other frequent case is the corrosion of steel in acidic solution.
Uniform corrosion is responsible for the greatest amount of metal consumed and, despite being a type of corrosion that can cause a decrease in the material's thickness, weakening it, is not considered one of the most problematic cases for being easily detected and predicted; in this way, *localized* corrosion is more difficult to control and avoid, and although not so material-consuming, its action is quite fast in penetration and failure of the target.

Galvanic Corrosion

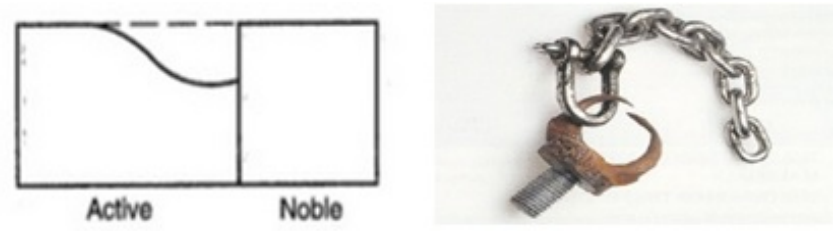

Figure 2.11: Galvanic Corrosion [66, 69].

Also called *bimetallic* corrosion, it occurs when two different metals are coupled in a corrosive environment; the less noble one will be corroded, protecting the other. Different materials have different electrochemical potentials in the same electrolyte; this difference will be the driving force for the destructive attack on the active metal, acting as anode. The metal with a more positive or noble potential in the respective galvanic series will act as the cathode, being protected from corrosion (see 2.4.1 subsection). The most aggressive attack occurs at the joint between the two distinct metals, calming down in zones away from this.

As an example of galvanic corrosion, if copper and steel tubing are joined in a domestic water heater, the steel will corrode in the vicinity of the junction, with a cathodic reaction occurring on copper.
A bimetallic pair can have different behaviours depending on the environment in which is inserted. Considering the steel/zinc pair, this last one will corrode preferentially in aqueous mediums at low temperatures, while for temperatures above 60℃ the zinc act as cathode, oxidizing the steel. Galvanic series are very useful for predicting which material will be attacked over others, counting on phenomena like passivity, for a specific environment [61].

The rate of this type of corrosion depends also on the relative anode-to-cathode surface areas exposed to the electrolyte. For a very small anodic area when compared with the cathode, this last one will continuously receive electrons to proceed the cathodic process at the expense of electrons released by the anode, which may lead to its complete consumption. For that reason, it is advisable to use anodic areas far larger than cathodic ones.
Other prevention methods to avoid galvanic corrosion may be the choice of two metals (if coupling of different materials is required) close together in the galvanic series, the use of electrically insulators between the metals or coatings. A third metal can also be used, less noble than the other two in order to be ”sacrificed”, a process known as *cathodic protection*.

Crevice Corrosion

Crevice corrosion is a type of localized attack that occurs in passive materials due to a difference in oxygen’s concentration. In crevices and gaps between two metallic surfaces or under deposits of dirt or corrosion products, there are volumes of stagnated solution that turn difficult its renovation or oxygenation. This crevice must be wide enough for the solution to penetrate but narrow enough for its stagnancy;

Figure 2.12: Crevice Corrosion [70, 71].

outside the gap both metals can be resistant to corrosion.
With the lack of oxygen inside the small crevices, the oxide layer is destroyed, functioning as an anode; the rest of the metal's surface, with a constant renovation of oxygen, behaves as the cathode of the system (so being protected from corrosion). The big difference between the anode/cathode area (with anodic area being considerably smaller) promotes fast corrosion rates inside the crevice.

Crevice corrosion can occur in different environments, such as chlorides, sulphates or nitrates, being the attack more efficient in the presence of H^+ and Cl^- ions that destroy the passive protective films. Stainless steel's crevice corrosion is widely known in aerated salt solutions, such as seawater; the main products of stainless steel (iron, chromium and nickel) accumulate in the crevice and form very acidic chloride solutions in which corrosion rates are considerably high [66].
The use of welded butt joints rather than riveted or bolted joints is one way of crevice corrosion prevention, as well as to avoid the creation of stagnant zones by ensuring a complete drainage of the metals and the remotion of accumulated deposits frequently.

Pitting Corrosion

Figure 2.13: Pitting Corrosion [66, 72].

Likewise crevice corrosion, pitting attacks passive materials, causing damages in the form of cavities or pits; these pits may be deep, shallow or undercut, like is depicted in Fig. 2.13 [66]. It is considered one of the most damaging forms of corrosion, often going undetected and with just an insignificant loss of material until failure happens, occurring while in presence of aggressive ions (mainly chlorides).
Its mechanism is also similar to what was seen in the case of crevice corrosion; once the pit is formed, its interior will act as the anode of a corrosion cell and release electrons to the cathode, which is the exterior surface of the material and is protected by an oxide layer. Once again, the relation between anodic/cathodic areas is very adverse, promoting the attack of the material by deepening the pits. The density of pits is also important: a single one can grow up and deep very quickly rather than a lot of

small pits (the total anodic area will be higher).

Stainless steels are some of the most susceptible materials to pitting corrosion, due to the rupture of their natural oxide/hydroxide protective films; alloying with approximately 2% molybdenum enhances their resistance substantially.
The main factors to be taken into account for this type of corrosion are the material's composition, their microstructure (the existence of heterogeneous zones promote the nucleation of pits) and the environment's conditions, such as pH, chloride concentration and temperature [61].

Intergranular Corrosion

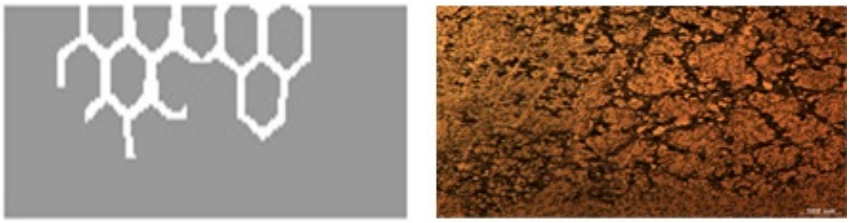

Figure 2.14: Intergranular Corrosion [73, 74].

Another type of localized attack is the intergranular corrosion, and as the name suggests, it occurs preferentially along grain boundaries for some alloys and in specific environments; the mechanical properties of the material are severely affected, and in the presence of tensile stress, cracking may occur.

This form of corrosion is a common problem in some austenitic stainless steels when subjected to heat treatments between 450 and 800℃; chromium situated near the grain boundaries reacts with existing carbon, forming $Cr_{23}C_6$ and depleting the grain boundary and nearby structure of chromium - the decrease in this element causes the so-called intergranular corrosion in that kind of materials.
Intergranular corrosion can be prevented by using a very low-carbon grade of stainless steels (like 304L or 316L for example), by subjecting the material to a high-temperature heat treatment in which all the chromium carbides are dissolved, followed by quenching, or by alloying the stainless steel with a stabilizing element such as titanium or niobium, which will form carbides with the existing carbon rather than chromium.

Selective Leaching

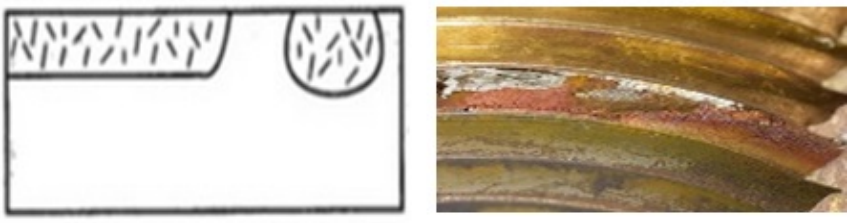

Figure 2.15: Selective Leaching [66, 75].

Selective leaching, also known as *dealloying*, is defined as the selective corrosion (dissolution) of one or more components of a solid solution alloy. The most common example of this kind of phenomenon

is seen in brass, in which zinc is selectively leached from the copper-zinc alloy. This process, called *dezincification*, is explained by the difference in the electrochemical potentials of the two species, being attacked the less noble one (zinc), leaving behind a copper-rich surface layer that is porous and brittle. Dezincification can be identified by a change in brass's colour, changing from yellow to a red color (typical from copper).

Besides brass, selective leaching can affect other alloys, based of cobalt, nickel or iron. Those corrosion attacks can be prevented by selecting more resistant metals and less aggressive leached-environments, or by cathodic protection.

Erosion, cavitation and fretting corrosion

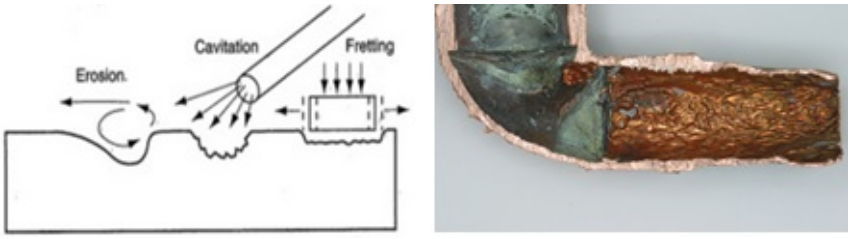

Figure 2.16: Erosion, cavitation and fretting corrosion scheme and erosion corrosion example [66, 76].

Erosion corrosion is a type of attack that arises from the combined action of a corrosive environment and wear as a consequence of fluid motion; a stagnant or very slow-flowing fluid will cause a subtle attack on the material, but rapid movement of that corrosive fluid erodes and removes the protective surface film, exposing the reactive alloy beneath and accelerating corrosion. The attack generally follows the direction of localized flow and turbulence around surface irregularities [66].
This type of problem is usually found at high flow rates around tube blockages, tube inlet ends, or in pump impellers, being especially harmful to alloys that passivate, and soft materials such as copper and lead; erosion-corrosion is enhanced by the existence of sand or suspended slurries.

Like erosion, *cavitation corrosion* involves a fluid's acceleration over the surface of a material; it is caused by the appearance of water vapor bubbles, provoked by a decrease of the fluid's pressure while in high velocities. The bubbles collapse and causes roughened pits, which may result in penetration on the surface. In addition, a synergistic effect of electrochemical corrosion and cavitation has been shown to exist where corrosion rates are increased in corrosive solutions, as a consequence of passive films breakdown [77].
Fretting corrosion is a consequence of repeated small movements between the corroding metal and another contacting solid under load; the metal's protective passive film suffers from a severe wear due to heavily loaded surfaces that move slightly but repeatedly against each other. This relative motion creates an abrasive wear on the metal's surface oxide film, removing the passive layer and again exposing the reactive material to increased oxide formation. The effect is compounded by the oxide debris, which contributes to the wear process.
These type of corrosion problems may be prevented by streamlining the pipes to minimize turbulence,

reducing flow's velocity, using more resistant materials, removing bubbles and particulates from the solution or by lubricate the surfaces.

Environmentally Induced Cracking

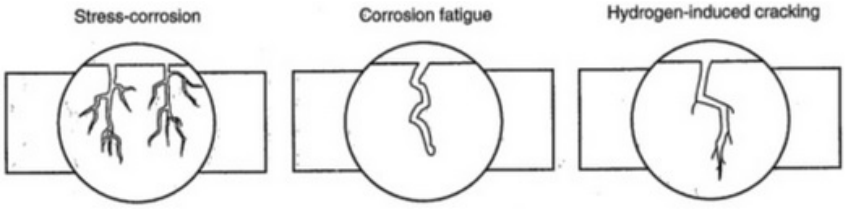

Figure 2.17: Environmentally Induced Cracking [66].

Environmentally Induced Cracking (EIC) is a a kind of corrosion that takes into account the simultaneous effect of a corrosive environment and an applied tensile stress in the susceptible material, with three types of failure included in EIC: stress corrosion, corrosion fatigue and hydrogen-induced cracking; brittle fractures are seen in normally ductile materials, with the environment being a causative factor.

Stress Corrosion Cracking (SCC) attacks materials with a static tensile stress in the presence of a certain environment. In fact, specific conditions are necessary to this type of problem to occur, (1) with materials virtually inert in a particular corrosive medium becoming susceptible with an applied stress or (2) materials under stress suffering from SCC in specific environments.
Small cracks form and propagate through perpendicular directions to the stress; since this phenomenon occurs in passive materials, with low-corrosion rates, the loss of material can be unnoticed until the moment of failure. This type of corrosion affects stainless steel in solutions containing chloride ions, brass in ammonia solutions and carbon steel in nitrates [66].
SCC may be prevented, among other measures, by lowering the magnitude of the stress, using alloys less susceptible to SCC or by coatings to avoid the direct metal/medium contact.

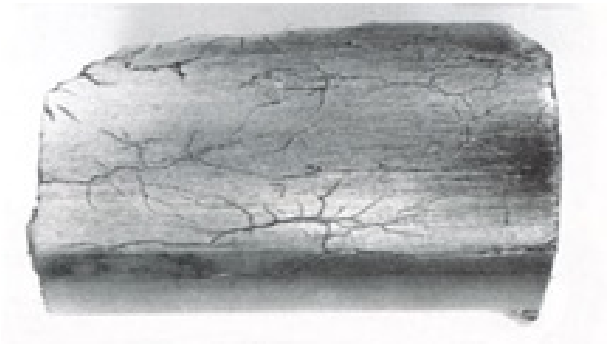

Figure 2.18: Stress Corrosion Cracking [78].

CFC, standing for *Corrosion Fatigue Cracking*, occurs under cyclic stresses in a corrosive medium. The difference between simply mechanical fatigue and corrosion fatigue relies on the aggressive environment, making the material more susceptible; macroscopically, the first fracture zone, corresponding to its beginning, is smooth in the mechanical fatigue, while in CFC is characterized by the presence of

corrosion products.

In the presence of a corrosive environment (water sea, for instance), the susceptibility and rate of fatigue will be increased; however no specific environment is required with variables such pH, temperature, or oxygen concentration having influence on the medium's aggressiveness, and so in the fatigue of the material.

Prevention of CFC can be made by using equipments that don't produce accumulation of alternate tensions, by heat treatment that release the metals from residual tensions, by using corrosion inhibitors or through coatings [61].

Figure 2.19: Fatigue Corrosion Cracking [79].

The other concerning EIC is the *Hydrogen Induced Cracking* (HIC), which results from the diffusion of atomic hydrogen into an alloy lattice, in particular that coming as intermediate from the reduction reaction of H^+ present in corrosion processes:

$$2\,H^+ + 2\,e^- \longrightarrow 2\,H \longrightarrow H_2 \tag{2.11}$$

The small size of atomic hydrogen facilitates its progression through the metal's lattice, which affects the properties of the material; in the presence of some specific species, likewise sulfide or cyanide ions, the normal formation of molecular hydrogen is slowed down, and hydrogen in the atomic form remains longer on the surface of the material [61]. HIC may occur during thermal treatments at high temperatures, during electroplating, through contact with maintenance chemicals, in presence of H_2S, corrosion reactions, cathodic protection, and operating in high-pressure hydrogen-containing environments.

Ways of preventing this type of environmentally induced cracking focus basically on reducing hydrogen content, by avoiding the hydrogen source, through thermal treatments that remove the accumulated hydrogen, application of coatings, using more resistant materials or by raising pH of the environment.

2.4.2 Corrosion Resistance of NiTi

Besides good biocompatibility, NiTi devices should present high resistance to corrosion in order to be safely used. This issue has been investigated since it was considered to be potentially applied in the medical field; one of the first studies was performed by Buehler and Wang [81] in 1968 and the results showed a good corrosion resistance for NiTi in an aggressive environment (seawater). Through the

Figure 2.20: Hydrogen Induced Cracking [80].

following years and until the beginning of the new millennium, more studies have been performed, as summarised in Table 2.7; most of reports consist of *in vivo* studies of dental arch wires and *in vitro* trials, being the corrosion behaviour of Nitinol inside the human body still limited [38].

Table 2.7: Corrosion behaviour of NiTi [1, 38].

Author	**Year**	**Study**
Speck and Fraker [82]	1980	Titanium and its alloys (such as NiTi) proved to be more corrosion resistant than 316L stainless steel, Co-Cr-Mo and Co-Ni-Mo alloys in Hanks' physiological solution at 37 ℃ and a pH of 7.4. The breakdown potential of NiTi is lower than of titanium; still, is more resistant to corrosion than the other materials. Lowering the solution's pH causes a negative shift in the breakdown potential of Nitinol
Edie et al. [83]	1981	Corrosion of orthodontic wires made of NiTi and stainless steel were examined and it was concluded that there is no reason to believe that NiTi wires are more subject to corrosion than stainless steel in a typically clinical environment
Sarkar et al. [84]	1983	Potentiodyanmic cyclic polarization in a 1 % NaCl solution within -500 mV and $+300$ mV (SCE) indicated that NiTi is more sensitive to corrosion than Ti. Pitting corrosion was observed in NiTi; X-ray analysis of the pitted surface indicated that it could have been due to selective dissolution of nickel from Nitinol
Barrett et al. [85]	1993	*In vitro* trials in prepared artificial saliva medium at 37 ℃ were conducted using stainless steel and nickel-titanium arch wires. The release rate of nickel from both arch wires materials were not significantly different; how much of that element is actually absorbed by patients undergoing orthodontic treatment still needed to be determined

Continuation of Table 2.7		
Author	**Year**	**Study**
Cragg et al. [86]	1993	44 Nitinol intraluminal stent were implanted in the iliac arteries of 22 sheeps. Minimal corrosion was seen at 6 months of experiment, with pitting being the predominant type; the main pitting product was found to be a titanium-bearing compound, probably an oxide. The authors concluded that NiTi stents can be safely deployed in the vascular system, with human trials being justified
Rondelli [87]	1996	Corrosion performance of NiTi was evaluated in physiological simulating fluids, with the release of nickel ions being three times higher for NiTi than for austenitic stainless steels. Under passive conditions, NiTi exhibited passivity current density higher than other materials commonly used as implants; localized corrosion tests in which the passive film of NiTi is abruptly damaged pointed out that its characteristics are not so good when compared with those of Ti6Al4V and sometimes even with stainless steels
Wever et al. [88]	1998	Tested in Hank's solution at 37°C, NiTi showed passive behaviour, with a better resistance to chemical breakdown of passivity compared with 316L ss. The passive diffusion of nickel from NiTi reduced through time, from an initial release rate of 14.5 x 10^{-7} μg cm^{-2} s^{-1} to an undetectable value 10 days after; it was concluded than Nitinol presents good corrosion properties

From the results of Table 2.7 it can be said that, in general, NiTi alloys present better corrosion resistance behaviour than other tested alloys, such as Co-Cr-Mo and 316L stainless steel (with the exception of Rondelli report [87]); in comparison with commercially pure titanium, NiTi proved to be more sensitive to corrosion, according to [82, 84]. This different behaviour is justified, obviously, by the presence of nickel in NiTi alloys.

The corrosion resistance of NiTi alloys relies on the presence of a passive oxide film that covers its surface and inhibits the development of uniform corrosion. Nitinol becomes protected from aggressive physiological environments due to the formation of a Ti-enriched oxide layer with low amounts of nickel, which is in contact with a Ni-enriched sub-layer; the big amount of nickel present in this sub-layer is responsible for turning NiTi resistance against passivity breakdown much poorer when compared with pure titanium, resulting in the onset of pitting corrosion. Ni cations are released from the Ni-enriched sub-layer through pores in the outermost TiO_2 film, with possible hazardous consequences due to the adverse effects associated with Ni^{2+} species, as material's degradation proceeds [89].
Another negative aspect that comes out from that fraction of nickel still existing in the Ti-enriched layer relates with passive film behaviour when damaged: in contrast to other medical materials, likewise pure

Ti and Ti4Al6V, which easily repassivate after surface damage, the Nitinol oxides have a lower self-healing ability in scratch tests, and so a lower resistance to localized corrosion [90].

The preferential TiO_2 film formation is corroborated by thermodynamic data, through the analysis of Gibbs free energy (ΔG) values. ΔG of a reaction gives a measure of the driving force that makes that reaction to occur: a negative value indicates that the reaction can proceed spontaneously without external inputs, while a positive value indicates that it will not.
At 25℃, free energy of formation for TiO_2, TiO and NiO is, respectively, -889.5, -495 and -211.7 kJ mol^{-1}, what seems to favour the formation of titanium dioxide over other possible oxides [90]; in theory, this external porous Ti oxide film should serve several purposes: to increase the stability of the surface layers by protecting the bulk material from corrosion, to create a physico-chemical barrier against Ni oxidation, providing stability to the material even under high anodic polarizations in physiological environments, to promote osseointegration, facilitating the growth of the bone, as well as its bonding with the implant [17].

In the last 15 years, more studies concerning the corrosion resistance of NiTi have been conducted, characterized by similar problems of those reported before such as the lack of *in vivo* experiments; Table 2.8 exhibits some recent studies, with the *in vitro* studies having been made using physiological solutions.

Table 2.8: Recent studies of NiTi's corrosion behaviour.

Author	**Year**	**Study**
Stepan et al. [91]	2005	A prosthetic heart valve using thin film NiTi was developed and tested under *in vitro* and *in vivo* conditions, immersing thin samples in Hank's solution for 1 month and by implantation in pigs using stents. No signs of corrosion were seen from immersion in Hank's solution and tissue and organ samples explanted from pigs after 2, 3, 4 and 6 weeks of NiTi film's implantation showed no disease. The authors concluded that thin film NiTi may be very well suited for use in artificial heart valves, although long term testing is still required

Continuation of Table 2.8		
Author	**Year**	**Study**
Pértile et al. [92]	2008	*In vivo* trials with 6 human patients were conducted in order to assess the OCP to which a NiTi alloy is subjected upon contact with bloodstream. The average *in vivo* OCP value was -0.334 $\pm$ 0.030 V/SCE, in agreement with *in vitro* OCP values measured in artificial saliva and urine, and in Ringer's solution. NiTi is not susceptible to active dissolution (at rest) as long as the breakdown potentials reported so far (0.0 V/SCE) remain above the measured OCP. These results highlight the importance of conducting tests under realistic conditions (such as under mechanical loads, wear and fatigue)
Figueira et al. [93]	2009	The corrosion behaviour of NiTi was object of study and compared with other materials, using Hank's solution at 37°C. It was concluded that NiTi presents a good corrosion behaviour, although slightly less resistant to that of Ti and Ti-6Al-4V, and being sensitive to crevice corrosion. XPS analysis showed that, after immersion in Hank's and MEM solution, the passive film was constituted by TiO_2 (mainly) and $Ni(OH)_2$
Kassab and Gomes [94]	2013	NiTi corrosion resistance was assessed and compared with that of beta titanium, through EIS and anodic polarization in NaCl 0.15 M with and without addition of NaF. In NaCl solution with 0.02 M NaF, NiTi showed to be susceptible to localized corrosion, while beta titanium didn't. Addition of fluoride proved to have negative effects on NiTi corrosion resistance: when 0.02 and 0.04 M of NaF were added to the NaCl solution, NiTi presented localized corrosion; for higher concentrations (0.05, 0.07 and 0.12 M), the alloy presented general corrosion. There is no galvanic corrosion between the two materials

Continuation of Table 2.8		
Author	**Year**	**Study**
Mirjalili et al. [95]	2013	The corrosion behaviour of NiTi and stainless steel (SS304) orthodontic wires in simulated saliva solution in presence of fluoride ions was assessed. SS304 showed pitting corrosion in simulated saliva solution while NiTi showed passive behaviour. The presence of fluoride ions caused a decrease of NiTi breakdown potential, while it had an inverted effect on that of SS304; artificial crevice had no effect on breakdown potential of solution containing fluoride ions. Pre-passivation of the two materials in nitric acid showed to had a positive influence on pitting corrosion in the presence of F^- ions
Izquierdo et al. [89]	2016	Surface electrochemical analysis of titanium and NiTi in naturally aerated Ringer's solution was investigated. The slower corrosion rate shown by Nitinol in that medium arises from the formation of a more insulating and nobler passive layer; however, this film may undergo pitting corrosion at quite low anodic polarizations. At higher anodic polarizations, NiTi passive layers experience breakdown, characterized by the release of metal cations from the material surface. XPS data showed that NiTi surface was spontaneously covered by an inner Ti dioxide layer, whereas the outer layer was constituted by a mixture of TiO_2 and NiO

In general, from the data exposed on Table 2.8 it's possible to assign a good corrosion behaviour for NiTi alloys. The *in vivo* experiments showed promising results, with the authors highlighting the importance of performing more complete tests, through longer periods and by subjecting the samples to loading/unloading situations [91, 92]. With respect to the *in vitro* trials, NiTi experienced some corrosion in aggressive environments, such as in presence of fluoride ions.
In order to obtain the best possible conditions for the performance of NiTi, several treatments may be considered, and will be object of discussion next.

2.5 Coatings and surface treatments

The relation between a biomaterial and the surrounding environment is largely controlled by its surface chemistry. In the case of NiTi, its corrosion resistance and biocompatibility relies not only on the protective TiO_2 passive layer spontaneously formed but also on the surface features of the material.
NiTi mechanical properties, such as superelasticity and shape recovery, are related to the bulk of the material, while biocompatibility response is dependent of its surface. The optimization of the last is

necessary in order to trigger osseointegration and to minimize the release of Ni^{2+} ions, ensuring a proper service from the devices; several methods can be used to modify the surface of NiTi alloys by deposition/remotion of materials on/from the substrate or by surface transformation [96].

Efforts are continuing to be made towards the development of new coatings and surface modifications for NiTi alloys, with the goal of improving the stability of the material in contact with the human body; there are plenty of studies done with different approaches that makes it difficult to enumerate and talk about each of one.

There is a class of methods that can be regarded as surface preparations used to enhance the adhesion of the subsequent coating or final surface treatment; however, they are frequently the only modification made to the material's surface and their main purpose is to remove material, in order to get a regular surface. The most common ones used in NiTi alloys are:

- Mechanical grinding and polishing - griding is considered the first step of mechanical material removing, which removes damaged or deformed surface material, while limiting the amount of additional surface deformation. The goal is a plane surface with minimal damage that can easily be removed during polishing for the shortest possible time. Next step is usually polishing, used to remove the damage remaining from griding by using abrasive particles of successively finer size, commonly SiC paper. Diamond paste or Al_2O_3 is used as an abrasive to accomplish the fastest material removal and the best possible planeness for the final polishing step; due to its hardness, diamond cuts extremely well through all materials and phases. Polishing permits to obtain a smooth surface.

- Chemical etching - this surface treatment consists in chemical dissolution of the material, without causing any mechanical stress to it (like as in grinding and polishing). The process cleans the surface, removes cracked, discontinuous surface layers, oxidizes the surface and removes nickel from the surface; however, under highly oxidising conditions, passivation can prevent further dissolution of the material. One example of an etching solution useful for NiTi is composed of 10 ml of HF, 20 ml of HNO_3 and 30 ml of H_2O [97, 98].

- Electropolishing - in electropolishing, the sample to be polished is anodically polarised in a solution that chemically dissolves the material; this polarisation drives the equilibrium of the equation $Me \longrightarrow Me^{n+} + ne^-$ to the right, resulting in the dissolution of the alloy. The main advantage of this method is the easy control of the dissolution conditions or dissolution rate, increasing the latter with the increased potential until a saturated layer is formed in the direct vicinity of the metal; the concentration gradient between this saturated layer and the bulk electrolyte will provoke a levelling and a smooth surface is achieved. Electropolishing of NiTi can be performed in mixtures of 70% methanol/30% nitric acid or 10% perchloric acid/90% acetic acid for example [97].

Milošev and Kapun [99] concluded that the corrosion stability of Nitinol is strongly affected by the type of surface preparation; ground samples (G) were susceptible to localized corrosion, while polishing (MP)

and chemical etching (CE) improved localized corrosion attack and shift the breakdown potentials by almost 600 mV. The surface roughness decreased in the order CE $>$ G $>$ MP. The concentrations of titanium and nickel at the surface also vary substantially depending on surface treatments; the ratio Ti/Ni by grinding was 2.6, what suggests that nickel is preferentially removed using SiC papers, leaving behind a surface rich in Ti. Etching, although increasing the concentrations of those 2 elements at the surface, presented also an Ti-enriched layer (Ti/Ni = 1.9). Finally, polishing the materials using a 1 μm diamond paste caused an higher concentration of Ni with respect of Ti (Ti/Ni = 0.4), and a decrease in oxygen concentration, proving that this method removes Ti and TiO_2 from the NiTi surface.
In a previous study [100], from 2006, the effect of surface preparation on corrosion properties and nickel release of a NiTi alloy was studied. Electropolishing exhibited better results in both parameters, leading as well to a lower surface roughness, compared with chemical etching, mechanical polishing and thermal oxidation at 500 ℃.

Another approach in the surface treatments of NiTi is to promote the formation of oxide films by taking advantage of the high oxygen affinity of titanium. Treatments are performed to increase the thickness of the oxide layer, functioning as a bigger barrier against corrosion and nickel ion release. Figure 2.21 illustrates a scheme of oxide formation on NiTi; the surface of the alloy is covered by a thin oxide layer, which is in contact with water or air, the potential suppliers of oxygen. A chemical gradient or an electrical field drives the metal cations through the oxide towards the outer oxide surface, while O^{2-} anions are driven under the same conditions in the opposite direction, inward to the metal/oxide interface. Titanium, being less noble than nickel, will have a higher chemical gradient and its driving force will be also higher; this causes a reduction of nickel's quantity in the outer part of the oxide, being richer in the metal/oxide interface or at the inner part of the oxide. The oxide grows according to the stoichiometry between cations and anions; otherwise, local space charge layers would exist within the oxide [97].

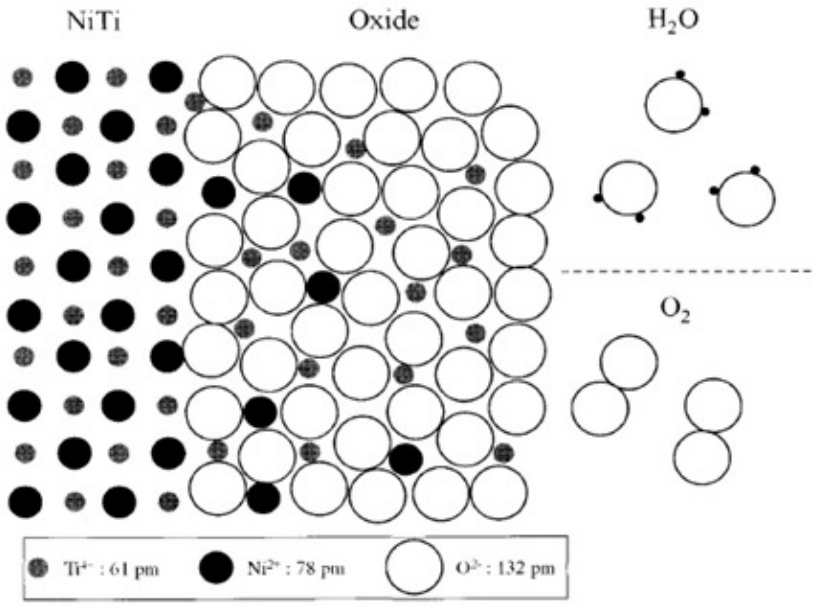

Figure 2.21: Oxide formation on NiTi [97].

- Anodization - this electrochemical technique at low temperatures improves the corrosion resistance of NiTi by increasing the thickness of the passive layer formed over the alloy, due to an anodic reaction. The electrolyte must not be very aggressive, in order to allow the alloy to passivate; aqueous solution of sulphuric acid, a solution of near neutral pH-value or a buffered solution may be used. The anodization can be performed in a two or three electrode arrangement, with NiTi being polarised anodically; during anodization process, Ti from the alloy gets preferentially oxidized and nickel dissolves in the medium, which decreases the pH of the solution. In general, an anodized-NiTi surface is amorphous and the nature of the formed oxide layer, such as the presence of cracks, pore size and pore density often decides the corrosion performance: if the oxide layer thickness is higher, the conductivity of the surfaces is poor and therefore it exhibits good resistance to corrosion [97, 101]. Advanced anodizing procedures permit to control the gradients of nickel and titanium within the oxide.

- Plasma electrolytic oxidation (PEO) - this anodizing process permits to obtain the formation of a uniform crystalline TiO_2 based coatings with excellent wear resistance, adhesive strength and bioactivity. The application of high potentials that exceed the breakdown limit of the material causes localized rupture of the coating, leading to plasma formation consequently, which promotes suitable conditions for the adhesion of oxide layers on the substrate's surface. Another advantage of this method is that the electrolytes used in PEO are weak alkaline solutions, being friendly to the environment [102, 103].

- Thermal oxidation - although a thin stable film of TiO_2 is formed on the surface of NiTi at room temperature, it does not give so much protection to the alloy, due to its low thickness and the possibility of NiO formation; increasing the temperature in oxidizing environments will accelerate the oxidation of NiTi and permits Ti to migrate readily towards the surface, due to the higher thermodynamic stability of TiO_2 compared with NiO. In this way, temperature, oxidation time and source's composition have a great influence in the thickness and composition of the layer formed during thermal oxidation, with prolonged times resulting in thicker films. Normally this type of treatment is used with temperatures above 200 ℃, with a TiO_2-enriched and Ni-depleted surface oxide layer being the ideal result of thermal oxidation [97].

Several studies have been conducted about the above reported methods of oxide films formation. Bernard et al. [104] applied with success an anodization treatment to a laser processed NiTi and improved the cell-material interactions and reduction of Ni ion release; the hydrophilic character of NiTi was also improved due to an increase in the polar component of surface energy. In another study [105], corrosion resistance in Hank's solution of anodized NiTi thin films, using voltages up to 6 V, was improved when compared with untreated NiTi.
In recent works [106, 107] Ca and P coatings by PEO treatments where examined and it was found that their porous and rough morphology favoured adhesion of osteoblasts. Corrosion resistance of NiTi was improved, so as its bioactivity, what made the authors to conclude that this material is suitable as long term hard tissue replacement implants [107].

Finally, there is also a lot of reports referring to thermal treatments. Vojtech et al. [108] performed experiments with NiTi alloys heated at 500 ℃ for 5−10 min in different environments; they were able to produce surface oxides of a thickness ranging from 15 to 50 nm. The authors concluded that low pressure environments would be a good choice to improve corrosion resistance and that releasing of Ni is more susceptible with thicker passive layers. Recently, a study was released [109] in which thermal treatments at 400 and 600 ℃ for 1 hour were done, and a reduction of Ni content on the surface and formation of oxide layers were induced. The final conclusion, after a 7-day incubation in SBF solution, was that the sample treated at an higher temperature presented a thicker titanium dioxide coating, less Ni content on the surface and a more bioactive surface, being much better than the treated at 400 ℃. In another report [110] the functional properties of NiTi wires were modified by heat treatments at moderate temperatures of 450 - 600 ℃ for a period of 10 minutes. Although fatigue life is found to improve with increasing heat treatment temperature, its effect on the corrosion resistance is negative due to the formation of thick and defect-containing oxide layers which worsen the protective effect.

The improvement of the features of NiTi, such as biocompatibility or resistance to wear or corrosion, can be achieved by depositing materials on the substrate, thus obtaining a coating between the alloy and the surrounding environment; there are plenty of possible options to constitute a coating for Nitinol alloys, each method being selected according to the property to enhance.

- Calcium phosphate - calcium-phosphate (Ca-P) based compounds, such as hydroxyapatite (HA), with the formula $Ca_{10}(PO_4)_6(OH)_2$, offer a good environment for living body cells growth, in spite of having poor mechanical properties; for that reason, they cannot be used as bulk materials in implants. HA, being the main constituent of the human bone, is able to accelerate bone ingrowths onto the surface of biomedical implants, having excellent biocompatibility and bioactivity, which complements with the good mechanical properties of NiTi. Ca-P coatings can be deposited using different methods like electrochemical deposition, plasma spraying and sol-gel method [96, 111].

- Sol-gel method - process that involves conversion of small molecules, named precursors, into a colloidal solution and then into an integrated network that will be used as a coating on the surface of the metal. Different coatings can be prepared through this method, usually of titanium oxides or silicium in the case of NiTi alloys. Sol-gel method has the advantages of being processed at low-temperatures and the possibility to cast coatings in complex shapes; however, long periods of time are usually needed to process functional coatings. A TiO_2 flexible film capable of sustaining high-deformations normally imposed on NiTi alloys may be prepared starting from precursor solutions containing an alkoxide, such as etrabutylorthotitanate, and diethanolamine dissolved in ethanol and mixing them with water (with or without additives) in a certain ratio [96].

Coatings with different Ca/P stoichiometry were object of study in a recent work [111] and it was observed that HA film presented the best cell attachment; the coating with the highest Ca/P value proved to have a moderate wettable surface, which promotes the cell growth, while stiffness and hardness of the lowest Ca/P stoichiometry was considered not-suitable to resist against the stresses produced by the

cells. In a work from 2011 [112], a hydroxyapatite coating was deposited onto a porous NiTi alloy using a sol-gel procedure; the coating showed good stability in Tris buffer solution (TBS) and the rate of Ni release in SBF from it was much smaller than that of an uncoated sample. Based on the observations, they concluded that the sol-gel method provided an effective way of producing the HA coating on porous NiTi alloys with the enhanced apatite forming ability beneficial for biomedical applications. In another sol-gel method, but with deposition of TiO_2 on endodontic instruments [113], measurements showed that corrosion behaviour and fatigue resistance were improved; in general, the flexible oxide film keeps the corrosion rate low, and that should be maintained for strained samples, since TiO_2 layer is able to tolerate relatively large deformations.

- Plasma immersion ion implantation (PIII) - PIII is a low-temperature process that involves simultaneous ion implantation and deposition, usually resulting in a robust, atomically intermixed, surface ceramic layer that improves the corrosion behaviour, biocompatibility and tribological surface properties of NiTi alloys. Some advantages of this technique when compared with conventional ion implantation are the capacity to provide a uniform dose rate over a non-planar surface, higher efficiency and larger area, among others. There's an high bonding strength between the metallic substrate and the coating, with a thickness of the latter varying between $100-900$ nm; however, there are studies that attribute the efficiency of the barrier more to its density than to the thickness. This referred high bonding strength avoids delamination between coating and substrate under load-bearing conditions, which often happens with coatings formed by electrochemical deposition or sol-gel processes [114, 115].

PIII process was used to synthesise composite coatings on NiTi alloys [114]; thickness of (Si, O, N)/(Ti, O, N)/Ti coating was around 0.84 ± 0.05 μm and because of it, there was no evidence of Ni presence on the alloy's surface. Shape-memory effect of Nitinol was not affected by the processing of the coating and in comparison with uncoated and (Ti, O, N)/Ti coated samples, the (Si, O, N)/(Ti, O, N)/Ti one showed the best wear and corrosion resistance, as well as an enhanced bioactivity. (Ti, O, N)/Ti coating also showed promising results in another study [116], with a surface roughness not so different from the uncoated sample. There was also no Ni on its surface, with a thickness of about 1.0 μm for the coating; due to high bonding strength, neither cracking nor delamination was observed for the composite coating after large deformation. Cell proliferation on coated samples was substantially higher than that of uncoated ones, after 1, 3 and 7 days of cell culture.

- Nitriding - since nickel cannot form nitride compounds, the diffusion of nitrogen into the surface of NiTi would result in the removal of Ni from it, forming a protective and wear resistant free-nickel TiN layer on the surface of the alloy, in the absence of oxygen sources. However, one drawback of this method is that TiN is very brittle and breaks when deformed; as consequence, cracks form on the surface of nitrided NiTi what leads to the exposure of the inner layers to the environment, and specifically the release of hazardous nickel ions [117].

Surface nitriding of NiTi [118] brought positive effects to the alloy in terms of biocompatibility. Compared with untreated samples, the nitrided ones showed an enhancement of the adhesion of human umbilical

vein endothelial cells (HUVECs), cell spreading and proliferation. Dynamic tests would be more precise to examine the fatigue response of these treated NiTi alloys, due to the already mentioned brittleness of TiN.

Almost every treatments that were referred improved Nitinol's mechanical and physical-chemical properties, and many other more could have been mentioned; this seems to foresee that NiTi is relatively easy to manage with, being compatible with a lot of different elements/techniques. More different tests are although needed to get a complete evaluation about all the potential of NiTi alloys to be used in the biomedical field without any constraints.

2.6 Applications

Shape memory alloys (SMA's) is a class of metallic compounds that have very special capacities, with recovering from apparent permanent strains being the most distinctive one; Nitinol is the most used SMA and, due to its unique mechanical properties, specifically shape memory effect and superelasticity, has been exploited through the years as orthodontic archwires, vascular stents and orthopedic devices for closure and fixation, among others forms, and in many different fields.
In the following paragraphs the most widely used applications will be presented, starting from the self-expandable stents that, by providing minimally invasive treatments instead of major surgeries, are probably the most successful ones.

2.6.1 Self-expandable stents

Self-expandable stents consist of tubular NiTi mesh, coated with a polymer or uncoated, that can be introduced into body conduits to treat dangerous obstructions; its most exciting clinical application is for cardiovascular surgery, but it can also treat biliary, intestinal, and esophageal conduits.

Cardiovascular applications

In situations of coronary heart diseases, in which there is a narrowing of the blood vessels, a filter is inserted as a straight thin wire via a small bore catheter.

Upon reaching the interior of the blocked artery and sensing its body temperature, the stent reverts to its complex filter shape and locks into place permanently, trapping any further stenosis. Pulmonary embolism is other cardiovascular problem that can be treated by these self-expandable stents [1].

Gastrointestinal applications

Esophageal NiTi stents can improve dysphagia of patients in case of malignant esophageal obstructions; however, reports of negative results have already came out, such as tumor ingrowth/overgrowth, incomplete expansion or stent migration [1, 120]. Self-expandable stents are also used (with efficient long-term results) in the treatment of malignant biliary obstructions.

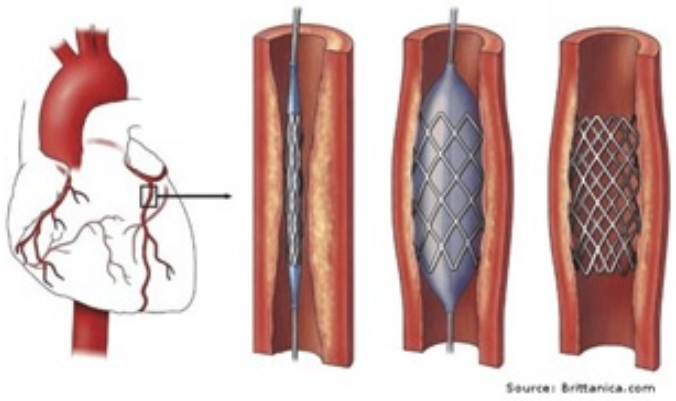

Figure 2.22: Intra-vascular stent [119].

Urological applications

In the field of urology, flexible and resistant urethral and prostatic stents have already been used to treat urinary duct or prostatic obstructions; for patients with high operative risks, the insertion of a permanent and temporary NiTi stent proved to offer a useful alternative in treatments for prostatic hyperplasia [121] and urethral strictures [122], respectively.

Other stent applications

Since the mid 1990's, SMA's have been used in several applications in neurosurgery, and in the form of very different devices, stents included. In addition to coils, a ball-shaped wire made of the same material, NiTi stents can be used to treat intracranial aneurysms, in cases that the aneurysm has a large neck: after the placement of the coil in the aneurysm, a stent is released in the corresponding zone of the artery to prevent coil's migration [120].
In a study performed by Luo et al. [123] in 2011, tracheal reconstruction of 8 animals with a mesh patch of NiTi as extraluminal stents was assessed and good results were obtained; because of that, the researchers used the same method to repair a tracheal wall defect in a human victim of a traffic accident, and the results were positive as well. To prevent airway occlusions, besides from trachea problems, self-expandable NiTi stents may also be used in inoperable bronchial stenoses, result of intraluminal tumor invasion [1].

2.6.2 Orthodontics

The first medical use of NiTi alloys was in the orthodontic field, in the form of *archwires*; Andreasen and Hilleman, in 1971, observed that NiTi wires were able to produce constant and lighter forces than the traditional used stainless steel wires, and so were considered more effective than the latters [120].
Currently, the most used NiTi-based orthodontic applications are the archwires (Fig. 2.23 (a)) and *palate expanders* (Fig. 2.23 (b)), that take advantage of Nitinol's superelasticity property.

The successful use of NiTi relies on its ability to apply to the teeth almost constant forces, and low in magnitude, during dental repositioning, obtained as a consequence of the bone-remodeling process,

(a) Archwire (b) Palate expander

Figure 2.23: Orthodontic applications of NiTi alloys [124, 125].

due to the alloy's extended elastic domain, which allows it to recover from large deformations. In this way, the device induces physiological dental movements without damaging the underlying tissues and causing minimal discomfort to the patient, as opposed to other classic materials that by applying discontinuous forces can cause hyalinization, a deleterious process caused by tissue disintegration.
As a consequence of such a high biological and clinical effectiveness of NiTi wires, the frequency of readjustments by the attending orthondist drops from every month (the interval usually needed for retensioning stainless steel wires) to a few times per year, and with a pain decrease during the entire treatment period [120].

Besides these two devices, there are more used in orthodontical practices. NiTi *dental drills*, for example, are used for root canal procedures and their good fatigue resistance and high elasticity prevents undesirable failures. *Fixators* for mounting bridgework are devices based on a small SMA element notched on both sides; with the temperature's increase, the notched area expands, what causes a permanent hold of bridgework. NiTi fixators may also be used to prevent a loose tooth from falling out. *Dental prostheses* and *implants* are other devices commonly used in orthodontics and made of NiTi alloys [120].

2.6.3 Orthopedics

SMA alloys have also an enormous variety of applications in the orthopedic branch, namely in fixation and compression for treatment of disjoint bone segments. A very simple fixation device, and one of the first ones to be studied for orthopedic procedures, is the NiTi *staple* (Fig. 2.24); at room temperature, the staple can be easily shaped to facilitate the insertion in the human body, since it is in the martensitic phase.

When inside and already installed in the human body, the staple tends to close and to unite the two disjoint bones, inducing a constrained shape recovery, caused by the temperature's increase and consequently the transformation from martensite to austenite. Fixation staples made of NiTi have already been applied for fixation of mandibular fractures, metatarsal osteotomies, spinal deformity treatments and intra-articular fractures, along several other problems.

Figure 2.24: NiTi fixation staple [120].

A NiTi *plate* is another fixation device, which needs to be fixed with screws to maintain bone alignment, and is normally placed on fractured regions such as face, nose, and jaws [1, 120].

Correction *rods* for scoliosis (sideways curvature of the spine) have also been one of the first devices with clinical trials, having ambiguous results: in some reports, improvements were not found when compared with traditional implant systems [47], whereas a more recent one [126] reported a satisfactory performance of NiTi rods in correction of scoliosis in 38 patients.
Specific types of rods, denominated *intramedullary nails*, are used to treat long-bones or ankle fractures, with the metal being fixed into the medullary cavity of the bone. Again, advantage is taken of the shape memory effect to manipulate the device and get an easy insertion, obtaining then a tight fixing when the NiTi rod is heated inside the human body (to a temperature higher than the austenitic transformation temperature).

Very good clinical results were obtained by using NiTi *rings* to model mal-formed cranium of children[127]; by fixing the ring to the osseous margins, the superelastic device expands, being able to reshape the cranium vault. Porous NiTi proved to have an exciting potential in orthopedic applications; besides of the well-known mechanical properties, its structure has low density, high permeability, and high surface area, providing high osseointegration and osteoconductivity [120].

2.6.4 Other applications

In addition to the main applications referred, shape memory alloys (and specifically NiTi) have many other fields in which they can be employed. *ColonRing* is a Nitinol *expansion device* used for laparoscopic colorectal surgeries; in otolaryngology, a surgical field that involves operation in deep cavities with complex shapes, NiTi *stape prosthesis* is used to replace the natural stapes when the stapes footplate is fixed in position.
A quite usually seen application in every-day-life are *superelastic eyeglass frames*, different from the conventional frames due to their capacity of being twisted and deformed, undergoing unconstrained recovery of their original shape on unloading. Other minor applications of NiTi can be found in gynecology and physiotherapy [120].

2.7 Tribology and other considerations

There's a set of conditions that a metallic device in contact with the human body should possess in order to serve successfully for long periods of time: (1) excellent biocompatibility, (2) high corrosion resistance, (3) suitable mechanical conditions, (4) high wear resistance and, in case of bone prosthetics, (5) osseo-integration [1]. Since the first 3 characteristics have already been evaluated, it's still important to mention the mechanical working conditions that NiTi devices are subjected inside the human body.

The mechanical working conditions within the human body are quite complex, with many simultaneous concerns: for example, human beings walk normally several thousand steps per day at a rate of 1 Hz. As such, possible NiTi skeletal bone implants, such as spinal fixations, plates and wires suffer from fatigue due to cyclic loading; dental implants are also subjected to cyclic stress during chewing, and so are pacemaker electrodes, which require a conductive material that can undergo very high numbers of flexing motions without failing.
The fatigue life of the well-known self-expandable stent, for example, is strongly influenced by the pulsating blood response and by everyday life activities, from which they can experience up to 40 million loading cycles each year, what makes the fatigue lifetime a major design criterion for NiTi devices. In each case, its understandable that cyclic loading promotes easier material fatigue than static fixed loading [1, 120].

It's difficult to make predictions about Nitinol's fatigue behaviour since those alloys exhibit *nonstandard fracture* and *fatigue responses* compared with other materials; a consequence of that is that well-known theoretical models and standard fatigue testing procedures cannot be applied, and a universal description of NiTi fatigue behavior remains an open issue even today [120].

A material subjected to cyclic loading can fracture below its UTS and even below the yield strength of the material (see subsection 2.2.3); fractures of this kind are a very dangerous concern because they occur under normal service conditions with no prior warnings. Fatigue fracture is considered the major cause of premature failure in most biomedical implants, and those devices require a constant scrutiny in order to survive the expected years of service.
Fatigue usually initiates at a location that acts as a stress concentration, with the stress focusing mainly in imperfections of the material, such as inhomogeneity of the microstructure or surface imperfections, when the material is subjected to external loading; the stresses may lead to the initiation and growth of a crack, that cannot be removed by unloading, which upon reaching a critical size leads to complete fracture.

In the case of NiTi, fatigue properties depend sensively on the deformation temperatures, whether in austenite or martensite, with the fatigue strength of the first phase (maximal amplitude of cyclic stress that can be applied to a material without causing fatigue failure) being higher, and increasing at high temperatures [1]. Niinomi [128] compared the fatigue properties of NiTi alloys with those of stainless steel, Cobalt- and Titanium-based alloys and observed that the first ones did not show better results than the others, explaining why they are not the choice for joint replacements, for example.

There are some others aspects that contribute to aggravate the occurrence of fatigue; the concurrent phenomenons of cyclic stress and friction is called *fretting fatigue*, and happens when a foreign body is pressed to the surface of the specimen (metallic device) to which cyclic stress is applied. Fretting fatigue results from relative movements of low amplitude, and causes the production of oxide debris and fresh metal surfaces. Corrosion can also complicate fatigue issues, with the surface wear of biomedical materials leading to the damage of its surface film and the consequent release of metal ions, compounds and debris [1].

Due to what was said, clinical tests about NiTi performance in the human body, in order to be the most demanding possible, should evaluate parameters like devices geometry, and existing stresses and deformations due to the dynamic conditions that the implants face inside the human body. The majority of the published data evaluates biocompatibility and corrosion behaviour of the alloys without counting with the loading-unloading conditions and the possible consequences of that in the materials; in many cases, the degradation of the biomedical implants is severely accelerated due to tribological issues. In Table 2.9 the results of a few recent reports found in literature are summarized. In general, there are differences in the corrosion behaviour from stressed and unstressed NiTi samples, what confirms the importance of these dynamic tests and requires the performance of an higher number of *in vivo* trials to achieve more conclusions; further research is indeed needed to reach more results about this exciting shape memory alloy.

Table 2.9: NiTi behaviour in dynamic conditions

Author	**Year**	**Study**
Habijan et al. [129]	2011	Biocompatibility of NiTi alloys under cyclic dynamic strains was investigated through their reaction with a human mesenchymal stem cells culture (hMSCs). Dynamic loading of NiTi-SMAs didn't influence the viability of adherent hMSCs compaired with the non-strained samples; the dynamic loading/unloading cycles didn't lead to significant difference in nickel release compared with the unstrained specimen. It was concluded that NiTi alloys are compatible under cyclic mechanical loading

Continuation of Table 2.9		
Author	**Year**	**Study**
Yoshida et al. [130]	2012	In this work, the authors investigated the fracture and corrosion behaviours of NiTi alloys under sustained tensile loading in neutral 2% NaF aqueous solutions containing different concentrations of H_2O_2, from 0.001 to 1 M. In solutions containing 0.001, 0.01 and 1 M H_2O_2 the samples revealed a shorter time to fracture compared with the absence of that compound; in the case of 0.1 M concentration, the time to fracture was longer due to the change from localized to general corrosion. The corrosion behaviour was successively improved by the addition of H_2O_2. By those observations, it was understood that the relationship between fracture and corrosion doesn't straightforwardly correspond to the H_2O_2 concentration
Pedullà et al. [131]	2012	Assessment of NiTi cyclic fatigue resistance files after immersion in NaOCl solution was done. The results showed that the aggressive enviroment where the samples were immersed did not reduce significantly that Nitinol's parameter
Dragoş et al. [132]	2013	NiTi corrosion behaviour was analyzed in Ringer solution before and after a thermo-mechanical solicitation. Both samples suffered from pitting corrosion, with the deformed one showing a decrease on its corrosion resistance, characterized by a bigger amount of Ni released, after 5000 cycles of mechanical solicitation
Kosec et al. [133]	2014	Tribocorrosion tests were conducted in ambient air, distilled water and artificial saliva and in two microstructurally different NiTi alloys: with and without surface oxide films. The experiments showed that corrosion is accelerated when combined with mechanical wear and inside an aggressive enviroment (artificial saliva), resulting in higher total wear rate. Comparing the mechanical and corrosion contributions to the total tribocorrosion wear, the first one prevailed in the cases of surfaces with a passive layer, whereas the other contribution prevailed in the NiTi sample without an oxide film

Continuation of Table 2.9		
Author	**Year**	**Study**
Racek et al. [134]	2015	Electrochemical methods were used to investigate the corrosion fatigue of NiTi wires/springs subjected to cyclic mechanical loadings in simulated body fluids. It was shown that the localized corrosion of NiTi alloys is substantially facilitated by cracking of the surface oxide film, crack opening/closing and passivation, mutually competing during cyclic mechanical loading in fluids

Chapter 3

Experimental Methods

3.1 Overview

The focus of this work was to modify the surface of NiTi alloys through thermal treatments, conducted at two different temperatures, 250 and 350 ℃, and in two types of environment, air and N_2, and to compare the resulting corrosion behaviour with that of the untreated material.
With the aim of better understanding the corrosion resistance of the different types of specimens, electrochemical measurements were performed on NiTi samples subjected and not subjected to thermal treatments. The electrochemical characterization consisted of anodic polarization curves, open circuit potential and electrochemical impedance spectroscopy, carried out in two different physiological solutions (Hank's and PBS) at body temperature (37 ℃).

Apart from the electrochemical studies, superficial analysis were made to examine the surface layers composition, through X-ray Photoelectron Spectroscopy (XPS) and Auger Electron Spectroscopy (AES).

The materials and experimental techniques used during this work will be described through this chapter, apart from a brief explanation of them.

3.2 Materials and solutions

The used material was a rod-shaped NiTi alloy, with 8.509 mm of diameter and 50.2-50.4 at% of Ni, commercially designated as alloy B and supplied by *Memory-Metalle GmbH*.
Hank's and phosphate-buffered saline (PBS) solutions were prepared in the laboratory, using the reagents listed in tables 3.1 and 3.2 (with the respective composition), and demineralized water.

3.3 Sample preparation

The first step in the preparation of samples was to cut them from the long rod-shaped material, obtaining disks with 6 mm of thickness, approximately; for that it was used a *Minitom* cut-off machine, from *Struers*

Table 3.1: Hank's physiological solution composition.

Reagent	Composition (g/L)	Brand
KCl	0.40	Sigma-Aldrich
KH_2PO_4	0.06	Laboratory Chemicals
$Na_2HPO_4.2H_2O$	0.06	Merck
$NaHCO_3$	0.35	Laboratory Chemicals
NaCl	8.0	Sigma-Aldrich
$C_6H_{12}O_6$	1.0	Ridel-deHaën
$CaCl_2.2H_2O$	0.185	Merck
$MgCl_2.6H_2O$	0.10	Merck
$MgSO_4.7H_2O$	0.06	Sigma-Aldrich

Table 3.2: PBS solution composition.

Reagent	Composition (g/L)	Brand
NaCl	8.0	Sigma-Aldrich
Na_2HPO_4	1.44	Merck
KCl	0.2	Sigma-Aldrich
KH_2PO_4	0.24	Laboratory Chemicals

(figure 3.1). The following procedures are different for the thermally treated/untreated samples - and a separate description will be given for each other.

Figure 3.1: *Minitom* cut-off machine.

3.3.1 Untreated samples

After being cut from the rod, a sample that is not going to be submitted to heat treatment is connected to a bare copper wire tip, by gluing it with a little drop of superglue (an excess of that can interfere with the electrical wire-metal contact); after a few minutes, this side is covered by silver paint and left to dry for 24 hours. When dried, the electrical contact between the sample and the copper wire was assessed using a multimeter.

Next step was to attach the sample to a plastic mould and then soak it on epoxy resin (*EpoThin Epoxy Resin*, from *Buehler*) for a period of at least 12 hours; after that the mould was removed, resulting on the metal sample with a free-surface surrounded by the insulating resin (fig. 3.2).

Figure 3.2: Sequence of sample preparation.

The alloy surface, which would be later tested in electrochemical experiments, was mechanically polished using a sequence of SiC papers with different grain sizes (starting from 240 mesh and until 2400 mesh) in a *LaboPol-25* machine, from *Struers* and then with 1 μm diamond paste (from *microdiamant*). After polishing, any impurities from the past treatments were removed by cleaning the samples in 2-propanol through an ultrasonic bath (*Branson 1200 Ultrasonic Cleaner*) for 4 minutes.

Finally, and with the goal of minimizing possible occurrences of crevice corrosion, a mask of beeswax and colophony resin mixture (3:1) was used to isolate the edges, and defining by that a small active area on the alloy's surface.

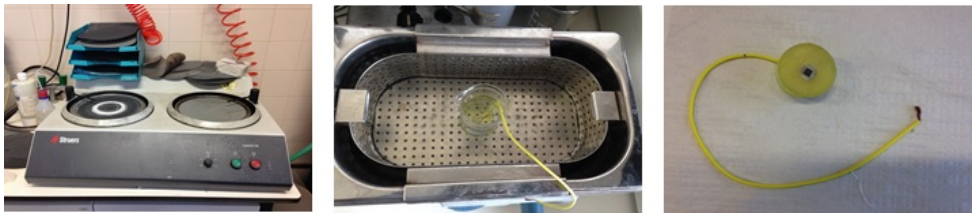

Figure 3.3: Polishing, ultrasonic bath and final sample

3.3.2 Thermally treated samples

The metallic pieces subjected to thermal treatment were directly polished after being cut, in the same way as explained in subsection 3.3.1, and then cleaned in the ultrasonic bath. Done this, they were sent to Polytechnic Institute of Setúbal (IPS) where the sample's surface modification was performed through thermal treatments in two types of atmosphere (air and nitrogen) at two different temperatures (250 and 350 ℃).

Bare copper wire tip was glued to the rear face of the already treated samples and covered by silver paint. When dried, the whole specimen was covered with a beeswax and colophony resin mixture, except for a window corresponding to the area to be tested.

The attached copper wire was introduced through a thin glass tube (with 20 cm of length); the glass-metal contact zones were covered with the mixture mask, leaving only free the metal surface area earlier delimited (fig. 3.4).

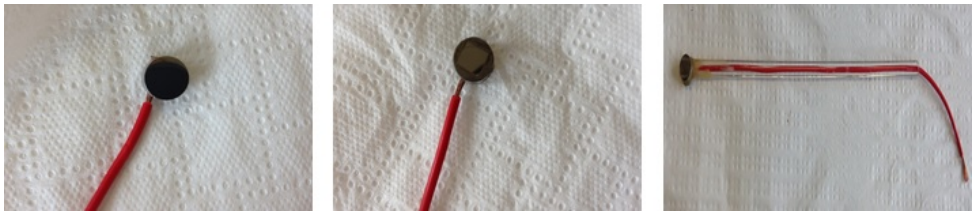

Figure 3.4: Final preparation of thermally treated samples.

3.4 Electrochemical Measurements

The different electrochemical experiments made in the course of this work were performed in a 3-electrode cell, composed by the sample under-study (the *working* electrode), a *Saturated Calomel Electrode* (*reference* electrode) and a Pt coil acting as *counter-electrode*; the role of these two last electrodes is to support as point of reference for the potential control and measurement and to close the circuit in the electrochemical cell, respectively.
The cell was introduced in a Faraday cage, in order to minimize external interferences, with the solution contained in the cell kept at 37 ℃ (to simulate the human body temperature) through a thermostatic bath system, with natural aeration (fig. 3.5).

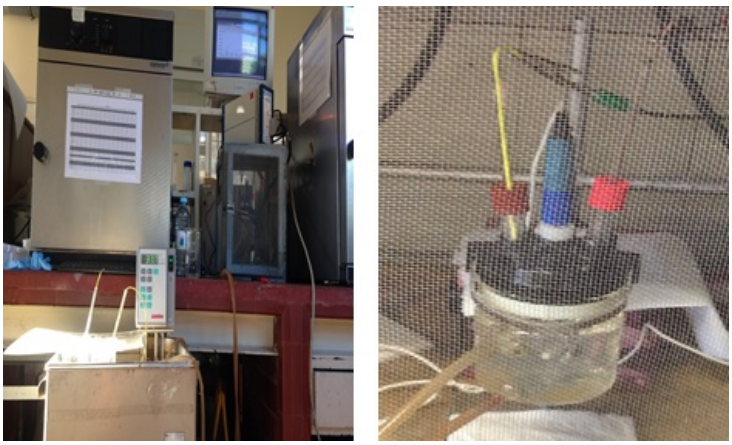

Figure 3.5: Configuration of the 3-electrode cell used in the electrochemical experiments.

3.4.1 Open-Circuit Potential

Open-circuit potential measurement (OCP), normally the first step of most electrochemical experiments, consists in the metal's corrosion potential (E_{corr}) evolution through time and it is measured by the potential difference between the metal immersed in a certain electrolyte (without electric current application) and an appropriate reference electrode (normally, the *Saturated Calomel Electrode* - SCE).

E_{corr} corresponds to the established potential's value on the surface of the metal and is dependent of the inherent reactivity of the metal and the oxidizing power of the solution, with the rates of anodic and cathodic reactions being equal.
The open-circuit potential measurement allow the samples to stabilize before other measurements and provides information about the tendency of metallic materials to participate in the electrochemical corrosion reactions with the surrounding medium.

3.4.2 Anodic Polarization Curves

The relationship between the potential of a metal and current density (corresponding to the rates of the corrosion reactions) is given by *polarization curves*. It allows to study the corrosion behaviour for a specific electrode-electrolyte combination by changing the metal's potential from the stable E_{corr} value as the result of the flow of current.

In the specific case of *anodic polarization*, there is a potential shift away from the open-circuit potential (previously measured) towards positive directions, that is, through values above E_{corr}; by that, oxidation reactions are being induced and the metal's response to it is under observation.
A typical anodic polarization curve for a passive material (such as NiTi) is depicted on fig. 3.6, starting from the open-circuit potential. With the increasing potential from E_{corr} there is also an increase of current until the passivation potential E_{pp} is reached at which there is an abrupt decrease of the current density (from the critical current value, i_{crit}), and so of the corrosion rate, due to the passivation of the material.

The current density in the passive region, i_{pass}, is almost constant with the increasing potential values, until a possible breakdown of the passive layer, which allows high currents to pass again. This is called the *transpassive* region and may be due to pitting or crevice corrosion, among other processes [136].

To obtain the polarization curves (after the previous stabilization of the open-circuit potential) a potential scan was performed starting from 20 mV below E_{corr} upward to 1.5 V/ECS, with a scan rate of 1 mV/s. For that, a potentiostat from *Gamry Instruments*, *Reference 600* was used, coupled to a computer and through DC105 software.

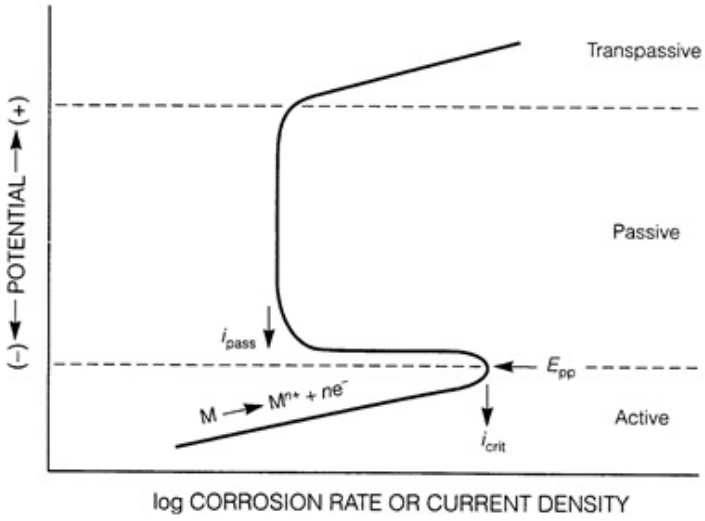

Figure 3.6: Anodic polarization curve for a typical passive material [135].

3.4.3 Electrochemical Impedance Spectroscopy (EIS)

Introduction

Resistance is the ability of a circuit element to resist to flow of electric current, and can be defined by Ohm's law by the voltage applied across that element (E) and the current flowing through it (I):

$$R = \frac{E}{I} \tag{3.1}$$

This simple relationship is limited to only one circuit element - the ideal resistor - having properties such as having a value independent from frequency, with the Ohm's law being valid at all current/voltage levels and with AC current and voltage signals through the resistor being in phase with each other. In reality, there are circuit elements much more complex, and the concept of *impedance* is used over resistance [137].

Electrochemical Impedance Spectroscopy (EIS) consists of applying an AC potential difference to an electrochemical cell and then measuring the current through the cell; through this, the response of the electrochemical system is studied to a small imposed perturbation (the applied potential difference) and the frequency dependence of the impedance can reveal underlying physical/chemical processes.
It is a powerful technique of simple application, that requires proper software to data analysis and has a broad range of research fields like corrosion studies, coatings, fuel cells, plating and catalytic reaction kinetics study, among others.

EIS Theory

In EIS, a small excitation signal is applied in the form of a sinusoidal potential difference, the system responding with a sinusoid current at the same frequency but shifted in phase (fig. 3.7 and equations. 3.2 and 3.4):

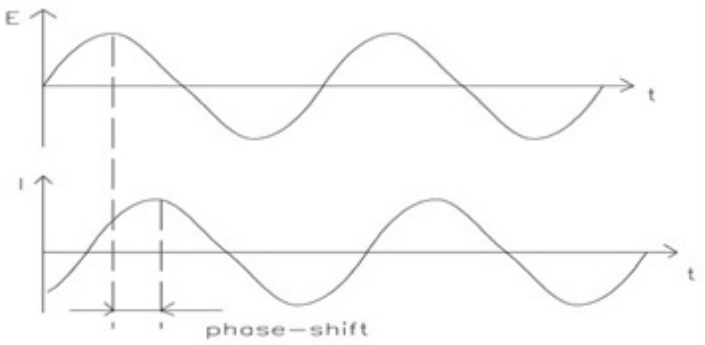

Figure 3.7: Current response to a sinusoidal potential [137].

$$E = E_0 \sin(\omega t) \tag{3.2}$$

$$I = I_0 \sin(\omega t + \phi) \tag{3.3}$$

where ω is the angular frequency, t the time, ϕ is the phase-shift, E_0 the amplitude of the potential difference signal and I_0 the current's amplitude; analogously to Ohm's law, the impedance is defined by the ratio of E and I, being expressed in terms of magnitude, Z_0, and phase shift.

$$Z = \frac{E}{I} = \frac{E_0 \sin(\omega t)}{I_0 \sin(\omega t + \phi)} = Z_0 \frac{\sin(\omega t)}{\sin(\omega t + \phi)} \tag{3.4}$$

Expressing the impedance as a complex function is possible (and turns data interpretation easier) by Euler relationship (eq. 3.5). The representations of potential, current response and impedance as function numbers are, respectively, in eqs. 3.6, 3.7 and 3.8.

$$e^{j\phi} = \cos(\phi) + j \sin(\phi) \tag{3.5}$$

$$E = E_0 e^{j\omega t} \tag{3.6}$$

$$I = I_0 e^{j(\omega t + \phi)} \tag{3.7}$$

$$Z = \frac{E}{I} = \frac{E_0 e^{j\omega t}}{I_0 e^{j(\omega t + \phi)}} = Z_0 e^{-j\phi} = Z_0(\cos(\phi) - j \sin(\phi)) = Re + jIm \tag{3.8}$$

Impedance equation contains a real and an imaginary part. A *Nyquist* plot can be obtained by representing the real part on the x-axis and the imaginary part on the y-axis, corresponding each point of the diagram to the impedance at a different frequency. Another very used representation in EIS experiments is the *Bode* plot, in which the frequency information is showed (on the x-axis, as log(ω) or log(f)) along with impedance modulus ($Z_0 = |Z|$) and phase-shift.

Electrical Circuit Elements and Equivalent Circuits

EIS data is examined by fitting it to an equivalent electrical circuit model using the three common electrical elements: *resistors*, *capacitors* and *inductors*. The goal is to collect data after imposing perturbations with different frequencies, and with that trying to build a model with the same response and based upon the physical electrochemistry of the system (for example, a model containing a resistor that models the cell's solution resistance) [137, 138].

Most EIS models consist of a number of circuit elements (opposed to a single equivalent element) connected in a network and combining either in parallel or in series; the impedance of a circuit can be determined, knowing the impedance value of each element ($Z_{1,2,3,...}$) and the combination between them. For impedance elements in series and in parallel (3.9 and 3.10, respectively):

$$Z_{\text{eq}} = Z_1 + Z_2 + Z_3 + ... \tag{3.9}$$

$$Z_{\text{eq}} = \frac{1}{Z_1} + \frac{1}{Z_2} + \frac{1}{Z_3} + ... \tag{3.10}$$

To determine the value of impedance of a total circuit, the impedance equations for the mentioned standard elements must be known, starting from the relation between current and potential for each one. In a resistor, and being valid Ohm's law, there will be a direct proportionality between the applied potential difference and the current, with the response to a potential sinusoidal wave being also a sinusoidal current having the same frequency and phase (therefore with ϕ = 0) [139]:

$$R = \frac{E}{I} \Leftrightarrow E_0 e^{j\omega t} = I_0 e^{j(\omega t+\phi)} R \Leftrightarrow E_0 e^{j\omega t} = I_0 e^{j\omega t} R \Leftrightarrow E_0 = I_0 R \Leftrightarrow Z = R \tag{3.11}$$

Being C the capacitance, the impedance of a capacitor is given by:

$$I = C\frac{dE}{dt} \Leftrightarrow I_0 e^{j(\omega t+\phi)} = C\frac{d(E_0 e^{j\omega t})}{dt} \Leftrightarrow I_0 e^{j(\omega t+\phi)} = E_0 j\omega C e^{j\omega t} \Leftrightarrow \frac{1}{j\omega C} = Z_0 e^{-j\phi} \Leftrightarrow Z = \frac{1}{j\omega C} \tag{3.12}$$

At least, the impedance equation 3.13 for a inductor (with L being the self-inductance) is:

$$E = L\frac{dI}{dt} \Leftrightarrow E_0 e^{j\omega t} = L\frac{d(I_0 e^{j(\omega t+\phi)})}{dt} \Leftrightarrow E_0 e^{j\omega t} = I_0 L j\omega e^{j(\omega t+\phi)} \Leftrightarrow Z_0 e^{-j\phi} = j\omega L \Leftrightarrow Z = j\omega L \tag{3.13}$$

Table 3.3 summarizes the formulas used and obtained for the three common electrical elements, with some facts being easily noticed through its visualization; the resistor's impedance is independent of frequency, having no imaginary part and so having its potential and current in phase. The impedance of a capacitor/inductor decreases/increases with the raise of frequency, having only an imaginary component and with the current through it being shifted in phase of 90 °/ - 90 ° with respect to the potential [137].

Table 3.3: Electrical elements impedance.

Element	Potential vs. Current	Impedance
Resistor	R = E/I	Z = R
Capacitor	I = C dE/dT	Z = 1/(jωC)
Inductor	E = L dI/dt	Z = jωL

Examples of common equivalent circuit models, with the corresponding Nyquist diagram, can be seen in figures 3.8 and 3.9 for a metal covered with an undamaged coating (presenting a very high impedance) and a *Simplified Randles* cell, respectively. The former one is formed by a resistor connected to a capacitor in series (representing the electrolyte resistance and the coating capacitance) while the last one includes a solution resistance, and a double layer capacitance in parallel with a charge transfer resistance; although being useful models, they're normally a starting point for more complex models [137].

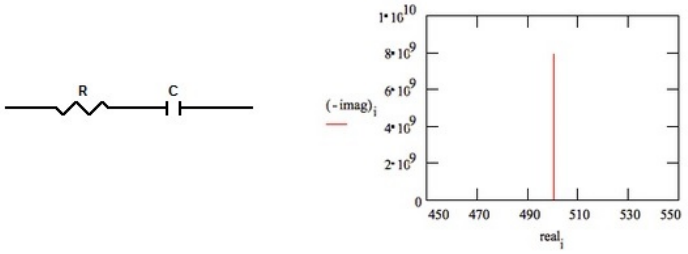

Figure 3.8: Equivalent circuit and Nyquist plot for an excellent coating [137].

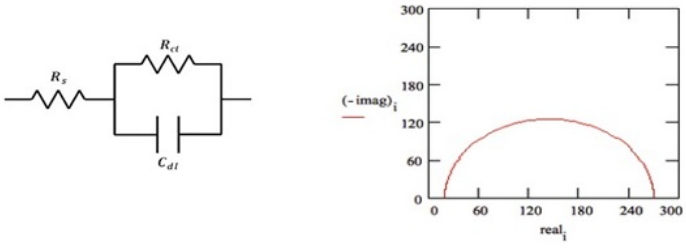

Figure 3.9: Equivalent circuit and Nyquist plot for a simplified Randles cell [137].

EIS applied to corrosion studies

Considering a typical corrosion reaction, $Me \Longleftrightarrow Me^{n+} + ne^{-}$, carried on a 3-electrode electrochemical cell in which there is a single charge transfer process, the total impedance of that system can be explained in terms of 3 elements: the *solution resistance*, *double layer capacitance* and *charge transfer resistance*.

Solution resistance (R_s) is considered a significant element in an electrochemical cell's impedance, due

to the need of a medium to exist in redox reactions, and is given by the combined effect of the electrolyte resistance, electrical wires resistance and the internal resistance of the electrodes; in general, these last two parameters are considered negligible (modern potentiostats compensates for the solution resistance between counter and reference electrodes) but any solution resistance between the reference and the working electrode must be considered in the model's formulation [137].

An electrical double layer exists on the electrode/electrolyte interface and is formed due to the separation of charges between the metallic electrode and ions of opposite charge that are attracted to it. This double layer behaves like a parallel-plate capacitor (C_{dl}) and allows the passage of current discontinuously, through the occurrence of charges and discharges. The value of the double layer capacitance depends on several variables, such as the thickness of its separation, ionic concentrations, temperature and of the existing dielectric constant [137, 138].

The charge transfer resistance (R_{ct}) is defined as the resistance to electron addition or removal, being the expression of the reactional (or faradaic) component of the system. It is related with the kinetic constant k_0, the symmetry coefficient α and the concentrations of the oxidized and reduced species, C_{ox} and C_{red} respectively, through expressions valid for the equilibrium potential such as [139]:

$$\sigma = \frac{RT}{n^2F^2k_0C_{ox}^{\alpha}C_{red}^{(1-\alpha)}} \tag{3.14}$$

In addition to these three elements, it is also common to use two other different ones: the *Warburg* impedance (W) and the *Constant Phase Element* (CPE).
The Warburg impedance refers to mass transfer phenomena and depends largely on the frequency of the potential perturbation: at high frequencies, the value of W is small since diffusing reactants don't have to move very far; at low frequencies, with the reactants having to diffuse farther, the Warburg impedance increases (eq. 3.15) [137].

$$W = \sigma(\omega)^{-1/2}(1-j) \tag{3.15}$$

The σ present in eq. 3.15 corresponds to the Warburg coefficient:

$$\sigma = \frac{RT}{n^2F^2A\sqrt{2}}\left(\frac{1}{C_{ox}\sqrt{D_{ox}}} + \frac{1}{C_{red}\sqrt{D_{red}}}\right) \tag{3.16}$$

with D_{ox}/D_{red} being the diffusion coefficient of the oxidant/reductant, A the electrode surface area, n the number of electrons involved, F the Faradays constant, R the gas constant, T the temperature and C_{ox}/C_{red} the concentration of oxidant/reductant in the bulk. The Warburg impedance shows up on a Nyquist diagram as a diagonal line with a slope of 45° for low frequencies.

In the case of a constant phase element, it can be considered a deviation from ideal conditions of a double layer capacitor: with a constant phase-shift value but different from 90 °. Equation 3.17 expresses the impedance of that non-ideal capacitor:

$$CPE = \frac{1}{(j\omega)^nY_0} \tag{3.17}$$

being Y_0 the admittance and the n exponent a value between 0 and 1 (generally 0.9-1 for a non-ideal capacitor); depending on the value of n, CPE will act like other common elements: a resistor (for n = 0), a capacitor (n = 1), a Warburg element (n = 0.5), or an inductor (n = -1). n is a parameter dependent of the surface roughness and the integrity of the oxide film for a corrosion system.

With all these information from existing elements needed to construct an adequate equivalent circuit model that could match with the response of the system under-study, it is necessary to fit the circuit to the experimental data. For this, a dedicated software was used, ZView® from *Scribner Associates*, using a non-linear least-squares method.
In some cases, more than one equivalent circuit seems to fit well with the experimental data; in those situations, the choice must rely on the physical electrochemistry of the system [139].

Measurement

The electrochemical impedance spectroscopy trials were performed using the EIS300 software, from *Gamry Instruments*, controlled by a computer. The measurements were taken after the stabilization of the open-circuit potential and by imposing a sinusoidal perturbation, through an AC voltage perturbation of 10 mV rms, from 100 kHz to 10 mHz. Successive spectra were acquired through time, until the stabilization of the system.

3.5 Surface Analysis Techniques

Every detail of a device used in the biomedical field must be examined meticulously. One of them is related with which kind of elements will contact with the human physiological environment, even more knowing about the substantial presence of nickel in NiTi alloys. To clarify these type of concerns, surface analysis - the study of the outermost layers of materials - is an important tool to give a microstructural characterisation of materials.
Two different, but very similar, techniques were used to evaluate the surface of NiTi alloys: X-ray Photoelectron Spectroscopy (XPS) and Auger Electron Spectroscopy (AES).

3.5.1 X-ray Photoelectron Spectroscopy

XPS, also denominated ESCA (from *Electron Spectroscopy for Chemical Analysis*) is a widely used technique to characterize the chemical composition of surfaces, providing information about the existing elements on material's surface, as well as their oxidation states.

The principle of XPS is based on the photoelectric effect, using an X-ray source to emit photons with an energy high enough to excite the constituent atoms on the surface (figure 3.10). The most commonly used anodes are made of Al or Mg, providing Al-K_α and Mg-K_α photons with 1486.6 and 1256.6 eV line energies, respectively [140].

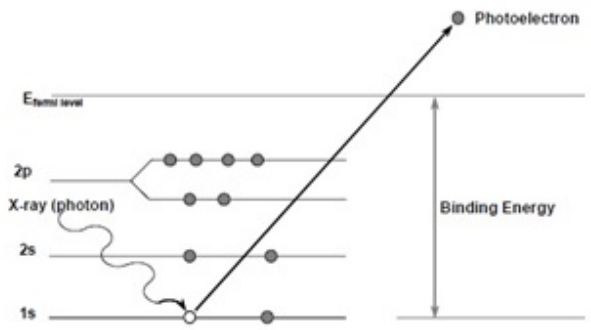

Figure 3.10: Schematic representation of the XPS process [141].

The incident beam provokes the removal of an inner shell electron, a photoelectron, which energy will be analysed by a spectrometer; this instrument measures the kinetic energy of the removed electron, given by the difference between the photon and the binding energy. Since each element has a unique electronic structure, its binding energy is also a characteristic parameter, which allows to collect information about the chemical species on a XPS spectrum, such as type, concentration or chemical state.

3.5.2 Auger Electron Spectroscopy

The Auger Electron Spectroscopy, analogously to XPS, is based on the utilization of a spectrometer to measure the kinetic energy of electrons emitted from the target sample, with the main difference being related with the source of the primary radiation, necessary to provoke the ionisation of the atoms, and the type of analyzed electrons [141]. Figure 3.11 shows a schematic representation of the Auger electron emission process, and its comparison with X-ray fluorescence process:

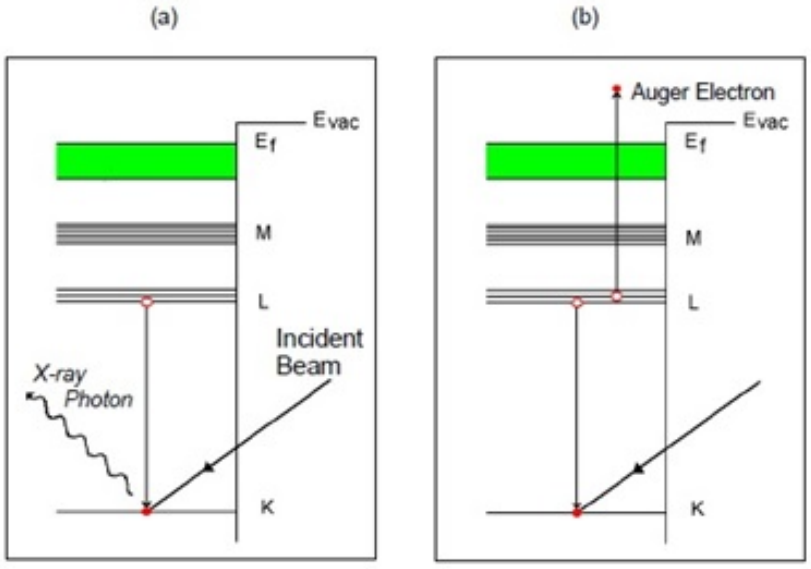

Figure 3.11: Schematic representation of X-ray fluorescence (a) and AES (b) processes [141].

In AES, an electron beam strikes the solid sample, promoting the formation of a vacancy due to the

removal of an inner shell electron; a second electron comes from an outer level and fills that vacancy, resulting on the existence of an excess energy that must be released.
In order to balance the process, X-ray photons can be emitted (leading to X-ray fluorescence) or, alternatively and more likely, a third electron can escape from the atom - the so-called Auger electron - which will be examined by the spectrometer.

The detection of the kinetic energy of Auger electrons enables to identify the present elements, based on the principle that the kinetic energy is only a function of the atomic energy levels, and so all elements of the periodic table have a unique spectrum. For a proper measurement, the electrons must leave the surface without energy losses during the process.
AES spectra can be very useful to quantify the presence of chemical elements on a surface, since the area of the Auger peaks is proportional to elemental concentration; nevertheless, is often considered a low-sensitive technique concerning chemical shifts caused by different atomic surrounding atoms [141, 142].

XPS and AES analysis was performed using a Microlab 310F from *Fisons Instruments* (*VG Scientific*), a field-emmission Auger microprobe, represented in figure 3.12.

Figure 3.12: Auger and XPS laboratory [142].

XPS spectra of treated and untreated NiTi were acquired in CAE mode (*Constant Analyser Energy*), using an Mg non-monochromated anode as X-ray source, and working at an energy of 15 keV.
In Auger spectroscopy, the concentration profiles were obtained by means of a Ar^{+} beam of high purity, at the energy of 1 keV, 1x10^{-7} mBar of pressure and with a current density range of 0.5-0.6 μA/mm^2. The Auger spectra was acquired in CRR mode (*Constant Retard Ratio*) using an energy of 10 keV and a current of 50 nA (approximately) for the electron beam.

Chapter 4

Results

The results of the experimental methods explained in chapter 3 are shown in the course of this chapter. The electrochemical measurements, involving open circuit potential, anodic polarization curves and electrochemical impedance spectroscopy, are analyzed first, followed by the surface analysis techniques (XPS and AES). A discussion of the represented results is made, along with a comparison with similar published works.

4.1 Electrochemical measurements results

4.1.1 OCP and Anodic polarization curves

The corrosion behaviour of untreated NiTi samples was evaluated through open-circuit potential and anodic polarization curve measurements, in two physiological solutions at 37 ºC: Hank's and PBS. The use of these electrolytes is quite common in the evaluation of biomaterials' corrosion resistance, with Hank's presenting ionic concentrations similar to human plasma; PBS, from *Phosphate Buffered Saline*, is a balanced salt solution used in many cell culture applications that maintains the osmotic balance and pH in a value of approximately 7.4 (ideal blood pH).

Figure 4.1 illustrates the results of the measured OCP, performed for a period of 1 hour and prior to the polarization curves. Similar values of the stabilized E_{corr} are obtained for Hank's and PBS (-0.342 and -0.343 V, respectively), what seems to indicate a similar corrosion behaviour of NiTi in both electrolytes. A discrete trend to reach more positive values was also verified, enhancing the passive behaviour of the material. This meets with data presented by Andreeva [143] in a 1964 report, in which a titanium oxide film formed in air (at room temperature) was steadily grown from a thickness of around 1 nm to 25 nm total, over a period of 4 years.
Figueira [138] performed open-circuit measurements of Ni, Ti and NiTi in Hank's solution for longer time periods (24h); the author observed that E_{corr}(NiTi) (lower than -0.4 V) stabilized in a value between the other two compounds, which is no surprise being the alloy equally constituted by nickel and titanium. The higher E_{corr} obtained in the present work compared with that of [138], may indicate a good surface

quality preparation before testing.

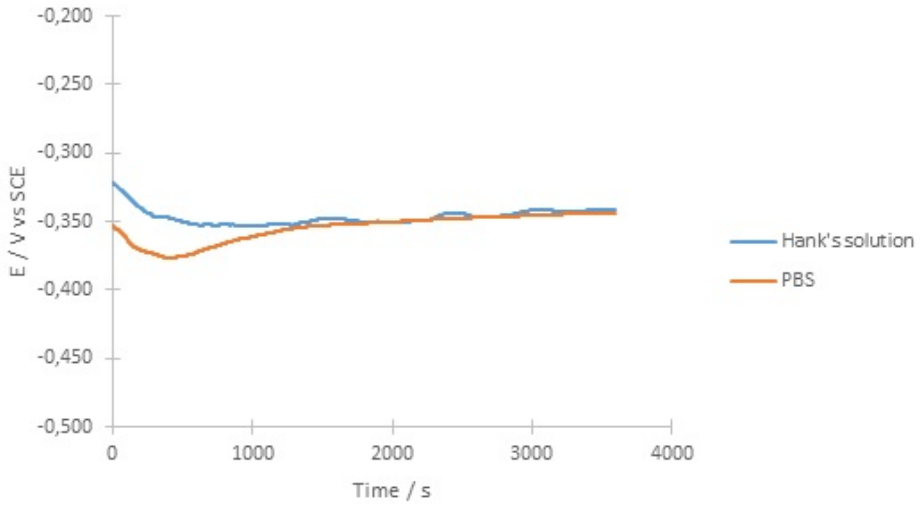

Figure 4.1: Open-circuit potential for NiTi immersed in two physiological solutions at 37℃.

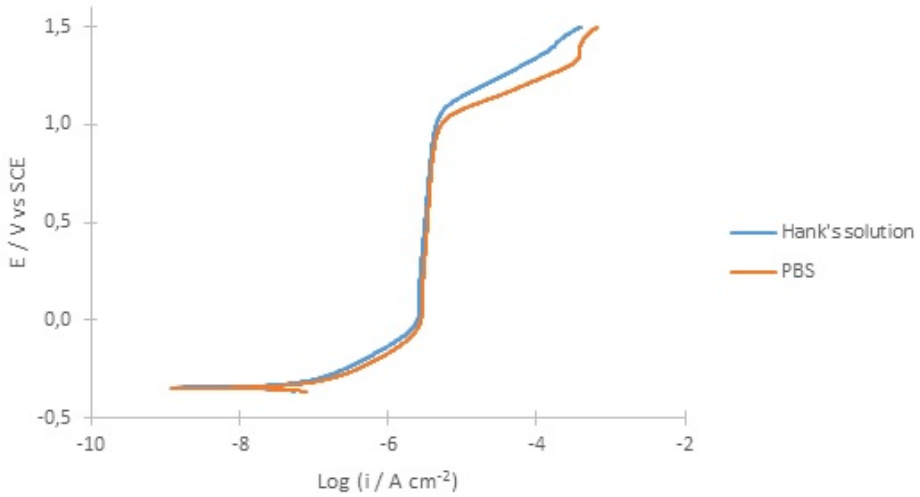

Figure 4.2: Anodic Polarization Curves for NiTi immersed in two physiological solutions at 37℃.

Starting from 20 mV below the E_{corr}, anodic polarizations were performed until the potential reached 1.5 V (figure 4.2), with table 4.1 resuming the main parameters obtained from the curves. NiTi presents a similar behaviour in both environments, with a passive region plateau of 1V approximately, indicating the presence of an oxide layer formed on the surface of the sample that prevents the advance of material degradation. According to published literature, the transpassive potentials for untreatd NiTi samples are normally in the range of 0.8-1.2 V [144], which is observed as result of these experiments (E_b of 1.046 and 1.023 V in Hank's and PBS respectively).

The passive region, characterized by tiny variations of the current density with the increasing potential, ends with an abrupt increase of current values, corresponding to a possible breakdown of the protective

passive layer. This phenomenon, occurring at the denominated *breakdown potential* (E_b), could be caused by pitting or crevice (resulting in localized corrosion), or by oxygen evolution due to oxidation of water; but in the present case is believed to be a consequence of oxygen evolution [145], as no corrosion evidences were found in any of the specimens, for both simulated environments.

Table 4.1: Anodic polarization curves parameters for untreated Nitinol.

Solution	**E_{corr} (V)**	**i_{pass} (μA/cm^2)**	**E_b (V)**	**E_b - E_{corr} (V)**
Hank's	- 0.342	2.62	1.046	1.388
PBS	- 0.343	2.83	1.023	1.366

These observations seem to be in line with results from a study performed by Pound [146], in which it was determined that the breakdown behaviour of NiTi in PBS is similar to Hank's solution. Liang and Mou [147] attributed a better corrosion resistance of biometallic materials in Hank's than in PBS due to the presence of glucose and SO_4^{2-} ions and Liu et al. [148] concluded that the presence of glucose (until 10 mmol/L) improved the corrosion resistance of titanium; in another work [149], the authors state that calcium-phosphate surface films can naturally form on Ti alloys in biological environments, acting as barrier to ion diffusion from the surface material. Taking into account the compositions of the two solutions (see section 3.3), it seems reasonable to admit that the presence of glucose, Ca and SO_4^{2-} may provide an extra stabilization to NiTi alloys in Hank's solution.

After NiTi corrosion behaviour had been analyzed in two different environments, the focus centered on trying to get better results by modifying the surface of the alloy, with the measurements being performed only in Hank's solution from now on; for that, some samples were subjected to thermal treatments, varying temperature and oxidation atmosphere, through four different surface modification types: oxidation in air and in nitrogen atmosphere, at 250 and 350 ℃.

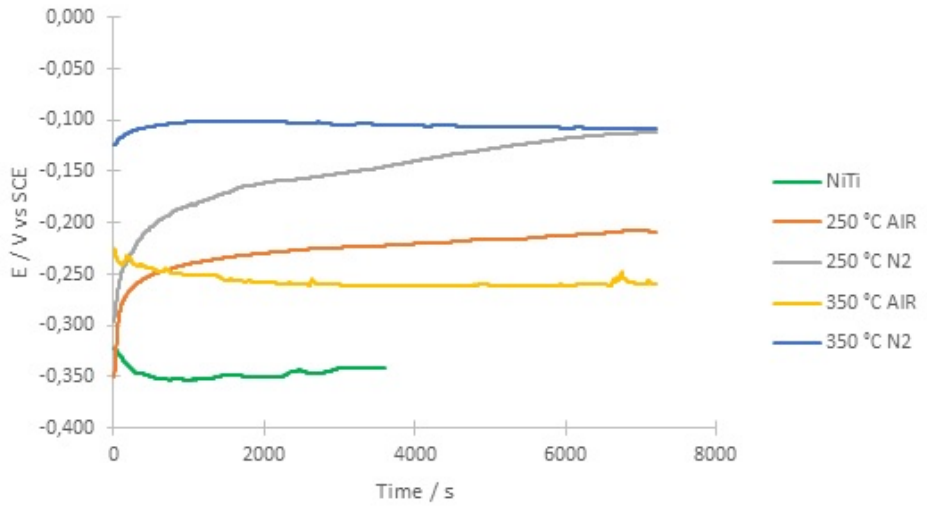

Figure 4.3: Open-circuit potential for thermally treated and untreated NiTi in Hank's solution at 37℃.

The open-circuit potential curves of the treated samples and the respective comparison with that of previous measured untreated NiTi are depicted in Figure 4.3. An higher testing duration was used at this

time (2 hours) to get more stable values. In general, the thermal treatments provoked a considerable increase of E_{corr}, with 3 different identified plateaus: under N_2, air atmosphere and raw NiTi. The increase of the potential values (in comparison with that of NiTi) is related with the presence of passive layers; the ones treated at 350 ℃, more stable during the monitoring, and those at 250 ℃, with an asymptotical increase in E_{corr}, indicating a continuous build-up of their oxide layer after immersion.
A stable value of around -0.110 V was reached for the N_2 treated Nitinol, while more negative values were obtained under air oxidation (-0.209 and -0.259 V at 250 and 350 ℃, respectively) suggesting that treatments in N_2 atmosphere enhance NiTi corrosion resistance more than in air.

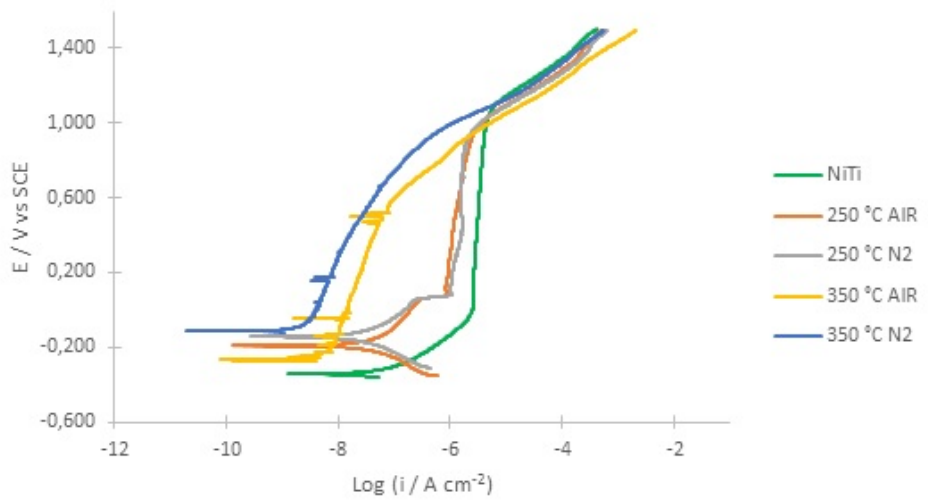

Figure 4.4: Anodic Polarization Curves for thermally treated and untreated NiTi immersed in Hank's solution at 37℃.

In the same manner as before, anodic polarization curves were obtained after the OCP measurement, being represented in fig. 4.4. The current densities observed for the treated NiTi are significantly lower than that of untreated ones, showing an improvement of the corrosion resistance. Furthermore, the current density at the passive region of the samples treated at 350 ℃ is substantially lower than for the others (in about two orders of magnitude), what is an indication of the enhanced protection conferred by the passive film formed under these conditions. With respect to the 250 ℃ samples, a more similar behaviour with the standard alloy is observed, with a visible passive region between 0.08 and 1.0 V; by this, it's plausible to assume that the protective character of the oxide film formed at 250 ℃ is slightly higher than the native film of NiTi but substantially lower than the ones treated at 350 ℃.

4.1.2 Electrochemical Impedance Spectroscopy

In order to analyze with more detail the corrosion resistance of NiTi alloys and to get more specific informations about its formed passive layer, EIS measurements were performed over a period of 1 week, in Hank's solution at 37 ℃, and after stabilization of the open-circuit potential. Figures 4.5-4.9 represent the typical Nyquist and Bode plots for the five different types of samples, with figure 4.5 corresponding to the untreated Nitinol.

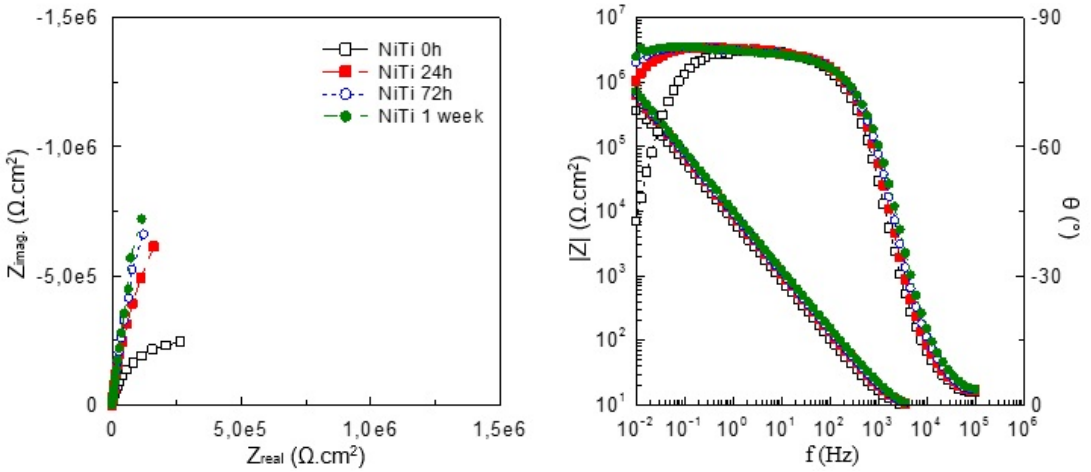

Figure 4.5: Nyquist and Bode plots of untreated NiTi.

In the case of the native material, it is possible to observe an enhancement of the corrosion resistance with time, with impedance values getting higher as the time goes on; this result is a consequence of a progressive improvement of the oxide's film protection on NiTi's surface.

The corrosion behaviour of the alloy turns to be substantially different with the thermal treatments. A common feature from all of them (figures 4.6-4.9) is related with the immediate corrosion resistance, with higher resistances and phase angles close to -90° over a wider frequency range (illustrating a near-capacitive response), for t = 0 h in comparison with untreated NiTi.

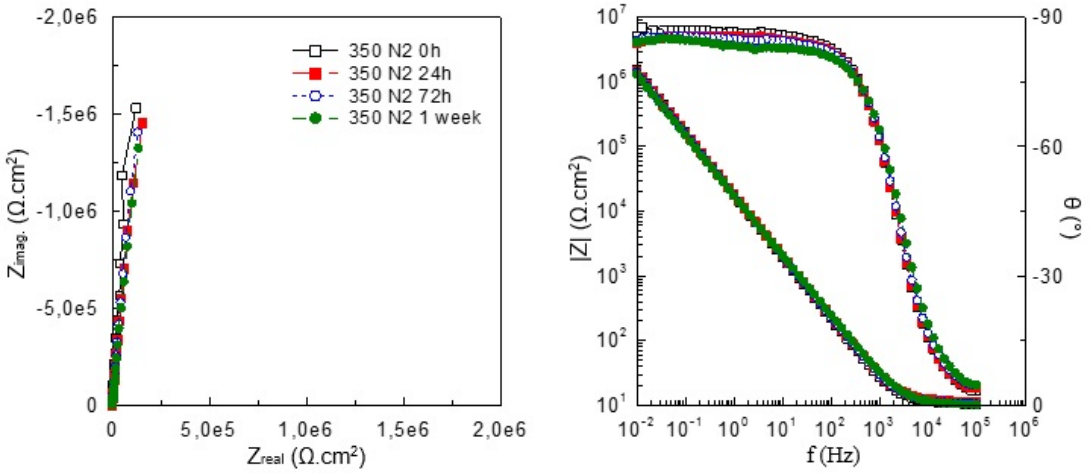

Figure 4.6: Nyquist and Bode plots of NiTi treated in N_2 environment at 350 ℃.

Among the subjected treatments, different behaviours on Nitinol's surface were obtained. Oxidation at 350 ℃ in N_2-controlled environment seems to be, by far, the most promising tested treatment, with high impedance values and a phase angle very close to -90° at medium and low frequencies, being independent from time (figure 4.6). Figures 4.7 and 4.8 illustrate also an enhancement in the corrosion resistance compared with untreated NiTi for t = 0h, for 350 ℃ in air and 250 ℃ under nitrogen environment, respectively (with the first having higher impedance values); although presenting a high resistance against corrosion, the protective behaviour of the formed passive films seems to be slightly decreasing

over time.

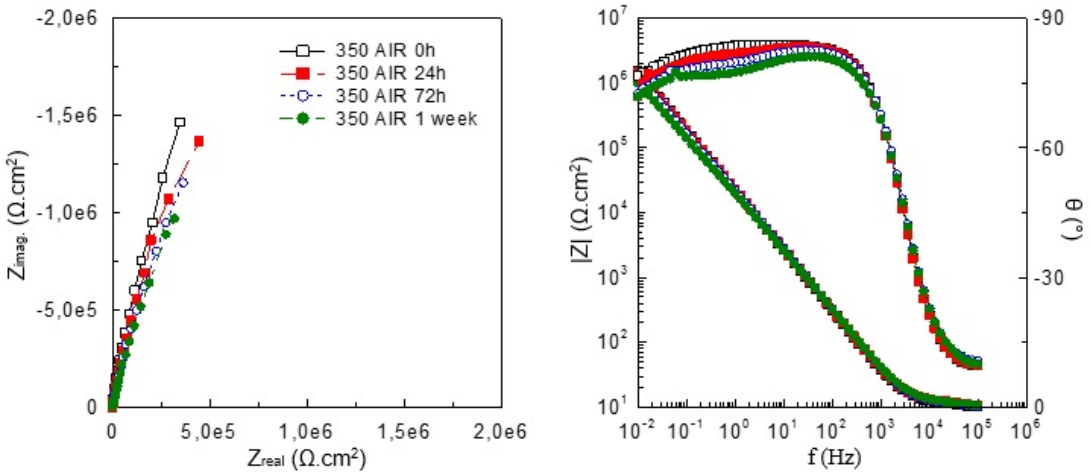

Figure 4.7: Nyquist and Bode plots of NiTi treated in air at 350 ℃.

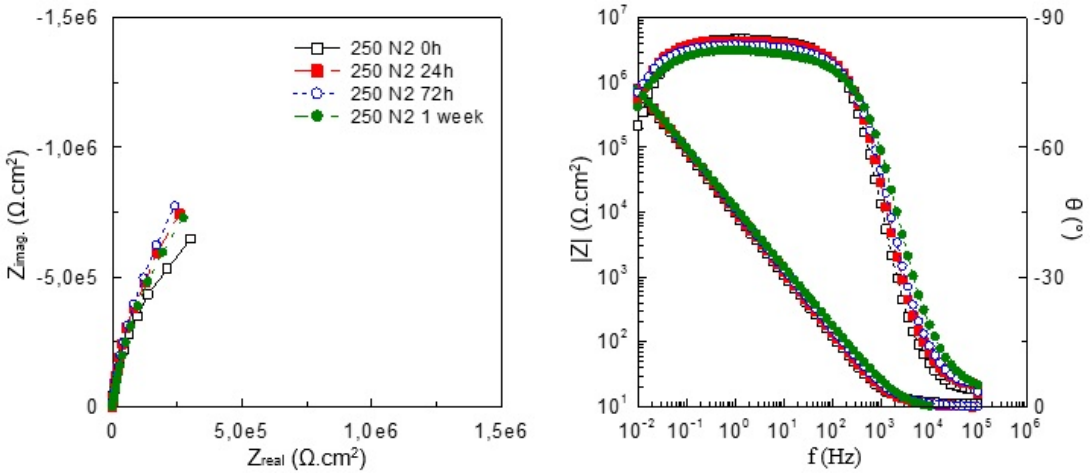

Figure 4.8: Nyquist and Bode plots of NiTi treated in N_2 environment at 250 ℃.

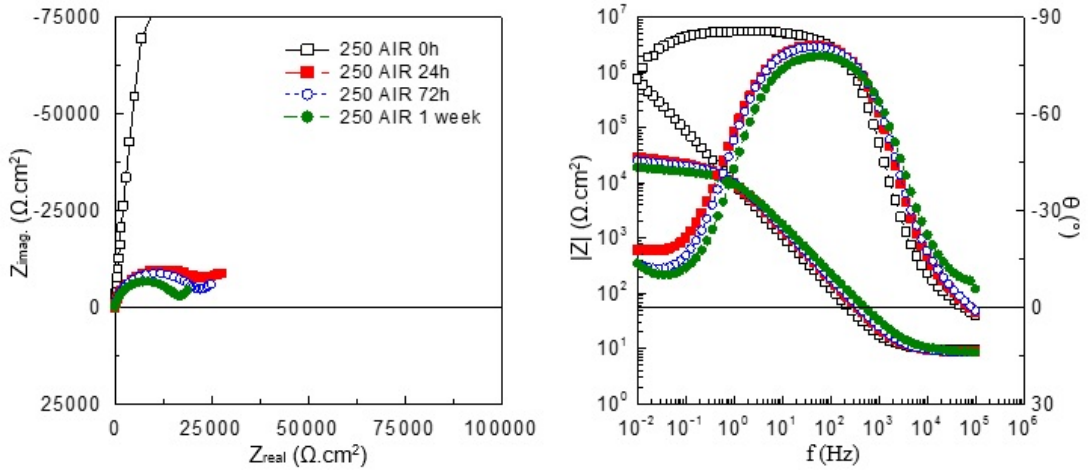

Figure 4.9: Nyquist and Bode plots of NiTi treated in air at 250 ℃.

Finally, impedance spectroscopy results indicate that one of the performed treatments does not improve

the corrosion resistance of the alloy at a medium/long term. In spite of showing a slightly higher resistance against corrosion in the beginning of the experiment (in comparison with the untreated material), the oxide layer of NiTi treated in air at 250 ℃ loses quickly its protective character (figure 4.9).

As it was said in subchapter 3.4.3, the concept of equivalent circuit means that an electrochemical process can be represented through an electrical model. By the analysis of the different plots obtained from EIS, a proposal to explain the structure of NiTi surface was suggested, represented in figure 4.10:

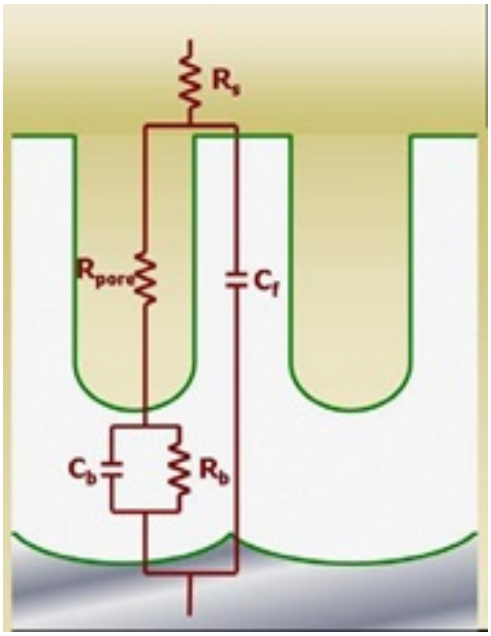

Figure 4.10: Proposed structure for the oxide film on NiTi and its equivalent circuit [138].

with the exposed equivalent circuit being constituted by three resistances - R_s, the solution resistance measured between the working and reference electrodes, R_{pore}, the additional resistance of the solution inside the pores, and R_b corresponding to the barrier layer resistance - and two capacitances, representing the barrier layer and the overall film in the porous walls. Constant phase elements (CPE) are used instead of pure capacitances in the fitting of EIS spectra to show the deviation from the ideal behaviour.

The proposed model of figure 4.10 assumes a ”duplex” structure for the oxide film on the surface of NiTi: an inner and dense barrier layer followed by a porous one. According to Mieluch [150], it is common to use a two-layer model, composed by an inner compact layer (acting as a barrier) and an outer porous one, when studying the oxide films on passive materials. In this model, it is possible to assume that the outer layer basically consists of the same oxide as the inner layer, but possesses microscopic pores which are filled by the surrounding solution.
Given this structure, the charge transfer can be conducted through two different ways:

- in pore direction, counting on the contributions of the electrolyte resistance inside the pores (R_{pore}) and the crossing of the thin barrier layer, characterized by its resistance and capacitance, R_b and C_b, respectively;

- crossing of the entire film thickness outside the pores, represented by it capacitance, C_f - the respective resistance is not represented because the flow of electrons is not expected to occur due to the very high resistance in parallel with the capacitance.

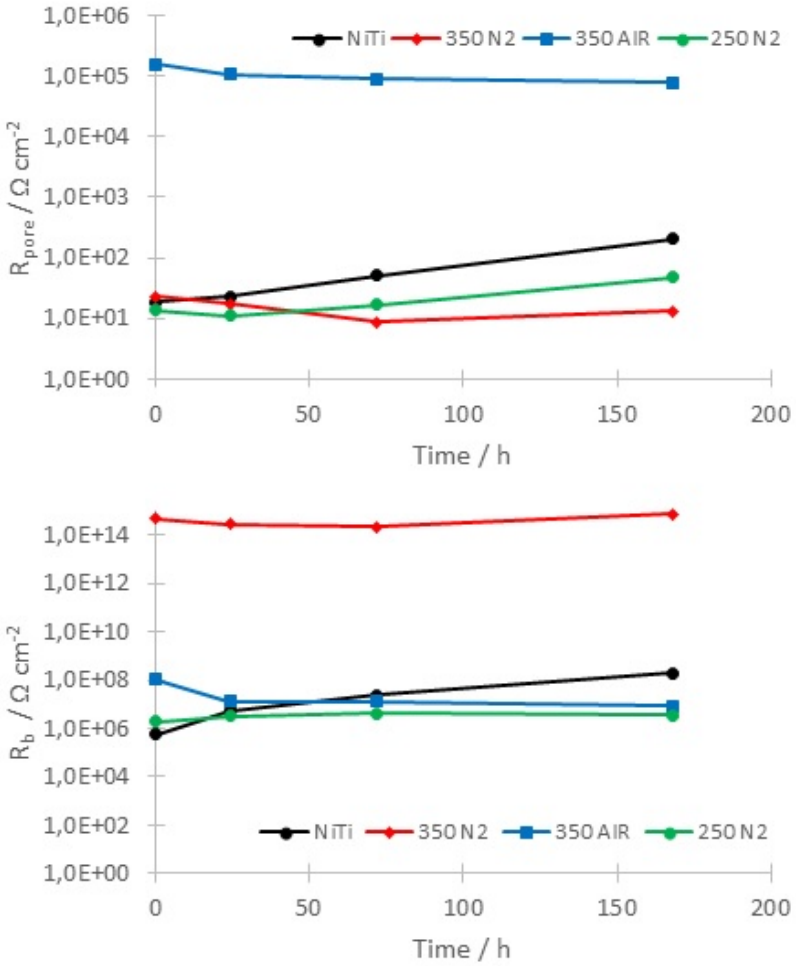

Figure 4.11: R_{pore} and R_b evolution through time.

Figures 4.11 and 4.12 and table 4.2 show the results from the fitting of the EIS data with the duplex model, through the variation of the resistances R_{pore} and R_b, capacitances C_f and C_b and the values of each component of the equivalent circuit along the experimental time, respectively; representation of NiTi treated in air at 250 ℃ was excluded due to the negative impedance results when compared with the untreated alloy.

The resistance and capacitance values of the native NiTi match with what was observed in the EIS spectrum, in which the corrosion resistance was improved through time. Both resistances substantially increase, while C_f and C_b decrease, although in a less pronounced way; assuming an oxide's film capacitance expressed by $C = \varepsilon\varepsilon_0 A/d$, being d the oxide thickness, A the surface area, ε_0 the absolute permittivity in vacuum and ε the oxide's dielectric constant (with a value around 100 [151]), the native alloy's behaviour can be explained as being due to an increase of the porous and internal layer's thick-

ness (since both capacitances decrease), enhancing the protective capacity of the material. A reduction in the pore's area (caused, for example, by pore's sealing) may also result in the same evolution.

The high corrosion resistance of the samples treated at 350 ℃ relies, according to figure 4.11, on different layers: while the treatment in N_2 produces very high values of R_b, with an average of 4.3x10^{14} Ω cm^{-2}, the one treated in air shows high resistance in pore direction, comparing with the other samples; this last observation can be related with a small area from the pores, a big tortuosity of them (which relates to the low values of the respective n parameters, in the 0.5 - 0.7 range) or a considerable thickness of the outer layer. Both R_{pore} and R_b from 350 ℃ oxidation in air slightly decrease along the experiment, being in agreement with the slight loss of protection observed in fig. 4.7.

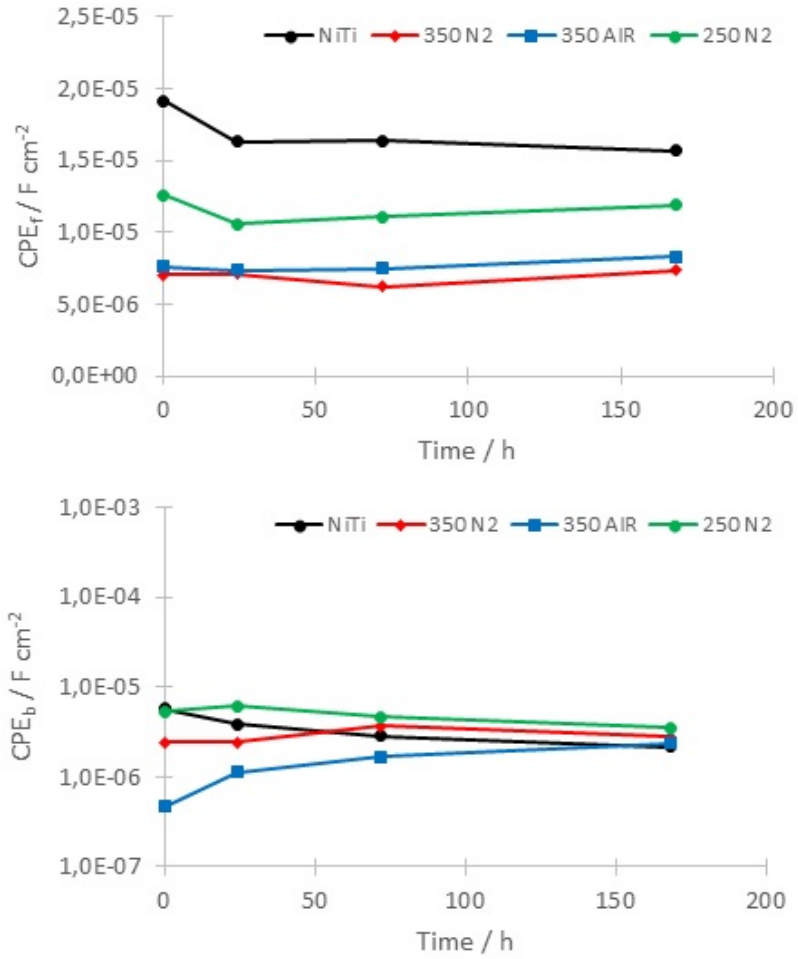

Figure 4.12: C_f and C_b evolution through time.

In terms of capacitances, the behaviour of all samples present a very similar trend, specially those related to the pores' wall, with almost no variation of C_f through time. In which concerns C_b, although with relatively different values at t = 0h, they tend to reach approximately the same values by the end of immersion. Moreover, almost no time evolution is observed for the samples treated in N_2, whereas a decrease of C_b is noticed for the untreated material (in line with the corresponding increase of R_b, as discussed above) and an increase of C_b is observed for the samples treated in air at 350 ℃. In this last

case, and as already discussed, tortuous pores may have been formed, leading to quite low initial values of capacitance and very high R_{pore} due to the long solution pathways, so the observed variations could be attributed to the degradation of that porous layer, with short-circuiting of the pores. It is important to stress that the present discussion refers to capacitances, although being based on the Y_0 values of the respective CPE's, as the respective n values are normally very close to 1.

The values of χ^2, depicted in table 4.2, give a measurement of the goodness of fit; being in the 10^{-4} range, the proposed equivalent circuit is considered a good model. The n values lie between 0.90 and 0.96, indicating a near capacitive behaviour of the oxide films, with the exception for the n(CPE_b) of 350 ℃, which increases from 0.47 to 0.76, possibly a consequence of the high tortuosity of its oxide layer.

Table 4.2: Fitting of the EIS to the equivalent circuit.

Sample/Time	χ^2	R_s (Ωcm^{-2})	$Y_{0,f}$ (F cm^{-2})	n($Y_{0,f}$)	R_{pore} (Ωcm^{-2})	$Y_{0,b}$ (F cm^{-2})	n($Y_{0,b}$)	R_b (Ωcm^{-2})
NiTi 0h	4.04E-04	7.8	1.92E-05	0.92	18.6	5.72E-06	0.91	5.48E+05
NiTi 24h	6.66E-04	8.2	1.63E-05	0.92	22.7	3.83E-06	0.91	5.32E+06
NiTi 72h	8.18E-04	7.9	1.64E-05	0.92	51.6	2.87E-06	0.91	2.45E+07
NiTi 168h	8.91E-04	7.7	1.57E-05	0.92	202.8	2.16E-06	0.91	2.01E+08
350 N_2 0h	9.29E-04	10.5	7.06E-06	0.96	23.2	2.43E-06	0.95	4.94E+14
350 N_2 24h	5.50E-04	11.2	7.11E-06	0.95	17.7	2.44E-06	0.94	3.00E+14
350 N_2 72h	6.03E-04	10.4	6.19E-06	0.95	8.7	3.65E-06	0.94	2.14E+14
350 N_2 168h	9.92E-04	10.2	7.38E-06	0.93	13.1	2.78E-06	0.93	7.28E+14
350 air 0h	6.46E-04	11.3	7.62E-06	0.94	1.56E+05	4.67E-07	0.47	1.04E+08
350 air 24h	7.67E-04	12.0	7.35E-06	0.94	1.08E+05	1.11E-06	0.69	1.24E+07
350 air 72h	6.31E-04	11.5	7.50E-06	0.93	9.07E+04	1.68E-06	0.70	1.31E+07
350 air 168h	9.18E-04	11.8	8.29E-06	0.92	7.96E+04	2.38E-06	0.76	8.47E+06
250 N_2 0h	1.37E-04	11.1	1.26E-05	0.95	13.6	5.35E-06	0.94	1.97E+06
250 N_2 24h	1.56E-04	10.0	1.06E-05	0.95	11.0	6.07E-06	0.94	3.28E+06
250 N_2 72h	1.57E-04	10.2	1.11E-05	0.93	16.8	4.65E-06	0.92	4.15E+06
250 N_2 168h	4.57E-04	9.0	1.19E-05	0.92	48.4	3.49E-06	0.90	3.55E+06

4.2 Surface analysis results

The surface of the most-promising samples, in terms of corrosion resistance, the ones thermally treated at 350 ℃, was analysed through XPS and AES and compared with the native passive layer of NiTi.

Naturally, some differences are expected to be noticed between each treated sample. The treatment in air atmosphere promotes (in theory) the oxidation of both constituents of the alloy (Ni and Ti), with the outer surface of NiTi being richer in Ti, due to its higher affinity to be oxidized. In this case, nickel is localized mostly in the metal/oxide interface or at the inner part of the oxide (see figure 2.21).
The use of an oxygen shortage atmosphere, such as the N_2 one, will cause a selective oxidation of titanium atoms, having a protective oxide barrier mainly made of TiO_2, with the goal of avoiding the nickel presence in NiTi surface and its release to the surrounding environment.

The XPS spectra are depicted in figures 4.13 and 4.14, in Ti 2p and Ni 2p region respectively, while the results of Auger Electron Spectroscopy are shown in fig. 4.15

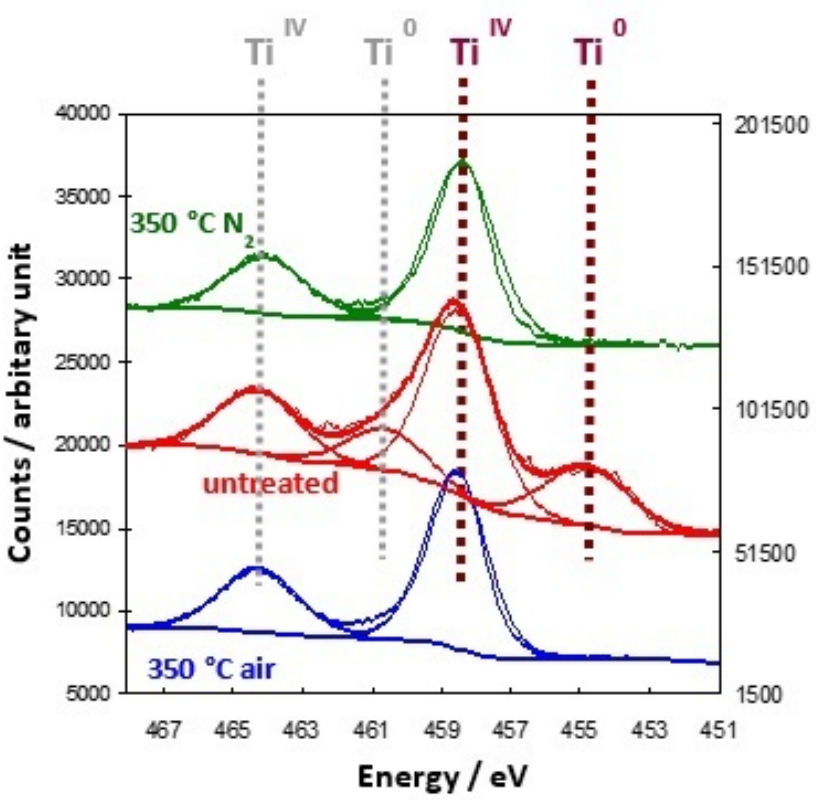

Figure 4.13: XPS spectrum in Ti 2p region for untreated and treated NiTi in air and N_2 environment at 350 ℃.

The observation of the XPS spectra reveals the existence of Ti and Ni in the oxidised state (Ti^{IV} and Ni^{II} respectively) in the three different samples, indicating the presence of a protective oxide layer. Furthermore, the presence of the constituent elements in the metallic form (Ti^0 and Ni^0), is only detected in the case of untreated NiTi: although presenting a passive layer that confers stability to the alloy, that native film is very thin when compared with the treated samples.
As a result of the N_2-controlled environment treatment, the peak's area of Ti^{IV} is substantially bigger than that of Ni^{IV}, meaning that the formed oxide layer is mostly made of TiO_2. In the other two cases, the area of the peaks of the oxidized elements are more similar, result of a bigger presence of nickel in the passive layer.

Referring to the Auger concentration profiles, it is possible to see that the Ni concentration is much lower than that of Ti in the three different samples surfaces, especially for the one treated in N_2 environment, which is approximately half of that for the other situations. The very similar value of Ni/Ti for the untreated and treated in air at 350 ℃ sample is related with the same oxide formation mechanism, being a result of the tendency of each element to form oxides and their respective diffusion coefficients.

Analogously of what was concluded from XPS results, the native's film thickness is found to be small, justified by the strong increase of Ni with the worn depth, reaching the ratio of 1 (corresponding to the alloy's substrate) for a relatively short depth.

A sub-surface region very poor in nickel is detected as a result of oxidation in air; however, for more

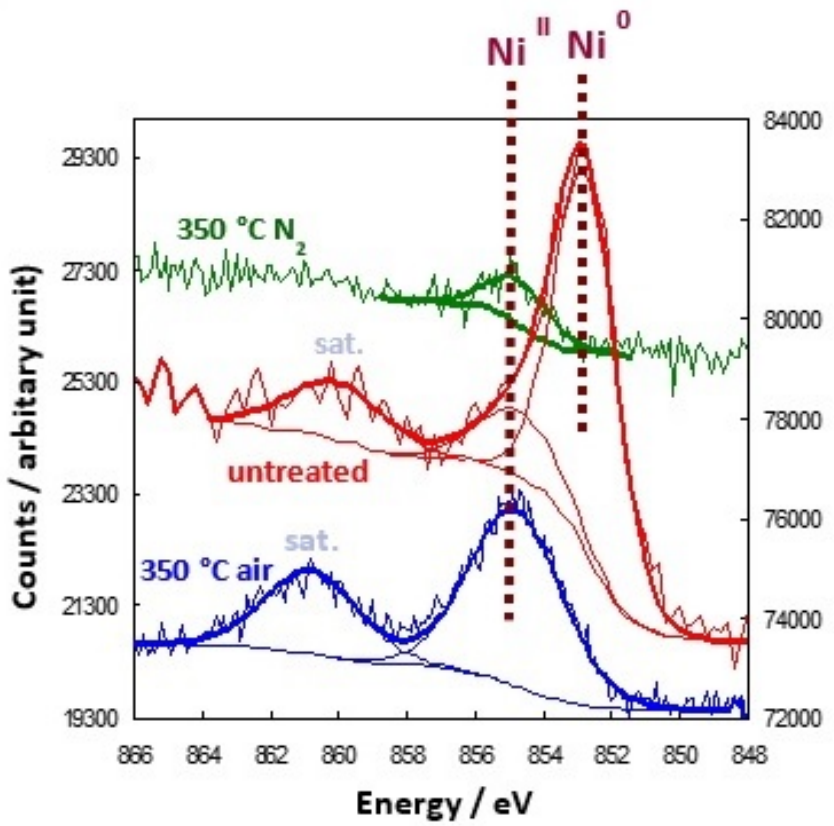

Figure 4.14: XPS spectrum in Ni 2p region for untreated and treated NiTi in air and N_2 environment at 350 ℃.

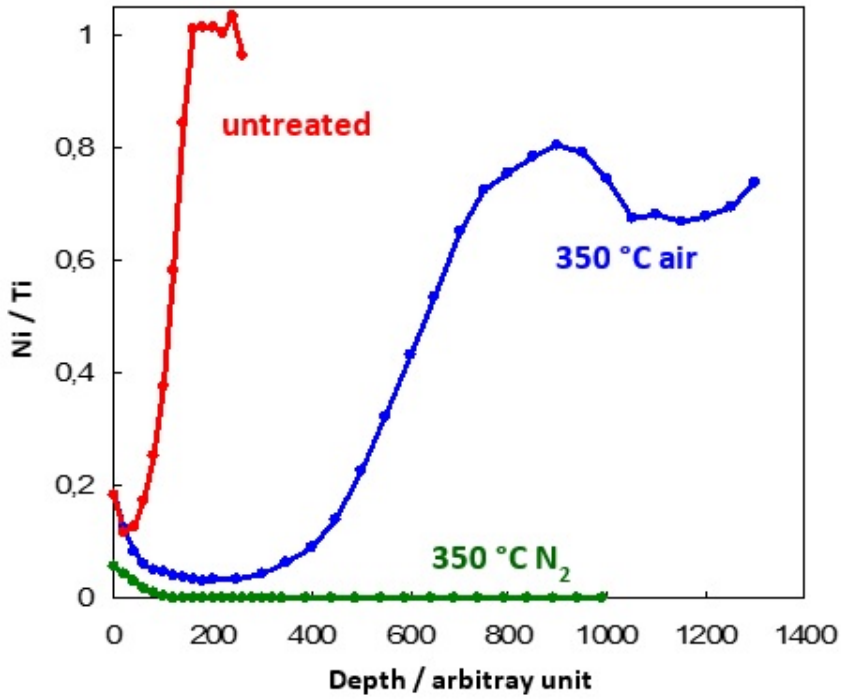

Figure 4.15: Evolution of Ni/Ti ratio along the worn depth for untreated and treated NiTi in air and N_2 environment at 350 ℃.

internal layers, the concentration of Ni starts to become more and more significant, although never reaching the same quantity than titanium. This means that the passive layer formed through this method is thicker than that of untreated NiTi, but not chemically constant in its composition.

The selective oxidation of Ti in N_2 environment, in addition to having reduced the nickel concentration of the oxide layer surface, almost provokes an elimination of that element for all the examined depth; in case of corrosion, Ni ions release will be extremely minimized from the implant simply, because there is a lack of them in the outermost regions of the material.

This preferential oxidation of titanium over nickel, enhanced in environments with low-oxygen concentration, can be explained through an Elligham diagram [152], which is a plot of ΔG versus temperature, and displays the free energy of formation for several metal oxides (figure 4.16). Through its visualization it is easily seen that $\Delta G(TiO_2)$ is substantially lower than ΔG(NiO) within the entire temperature range, what confirms the higher tendency of Ti to form oxides.

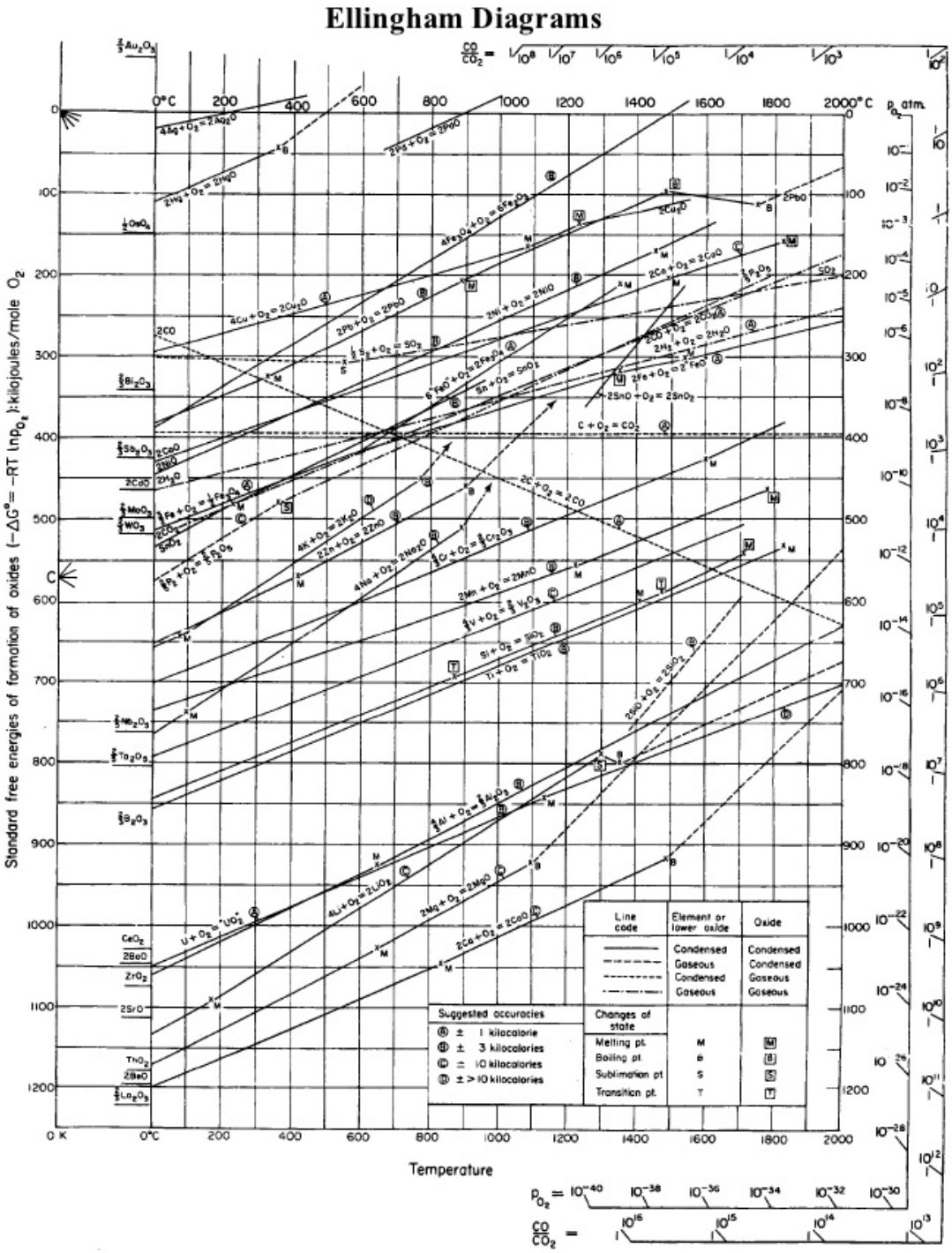

Figure 4.16: Ellingham Diagram [152].

Chapter 5

Conclusions and Future Work

The corrosion behaviour of surface modified Nitinol was investigated in a simulated physiological solution through electrochemical measurements and compared with the untreated alloy. The samples with the most exciting results were characterised by XPS and AES in order to assess the distribution of nickel and titanium in the materials passive films.

NiTi's corrosion behaviour has been intensively studied since its promising properties were found suitable for biomedical implants. In general, an high resistance to corrosion is attributed to NiTi alloys, in comparison with other materials used as implants, like 316L stainless steels and cobalt-based alloys, [36, 82], but presents worse results than commercially pure titanium [84].
Indeed, the high presence of nickel in this kind of alloys is a concerning matter due to the inflammatory and allergic reactions that nickel's release may cause in the host body.

The open circuit potential measurements have shown an enhancement of the passive behaviour of the alloys subjected to thermal treatments, with oxidation in N_2 environment providing more positive E_{corr} stable values. The potentiodynamic polarization curves illustrate a marked passive region for all samples, with the untreated NiTi presenting a higher current density at the passive region. This means that the thermal treatments provide a more protective character to the oxide film on NiTi's surface, in which relies its resistance to corrosion; among the four different treatments, the ones performed at higher temperatures (350 ºC) lead to the best corrosion performance.

From the EIS results, the resistance to corrosion is extremely improved by oxidation at 350 ºC in nitrogen atmosphere, with high and constant impedance values along the whole experiment. In the other modified alloys, the corrosion resistance is very high for t = 0h, but their passive layer starts to become less protective over time, with resistance decreasing in the order 350 ºC air $>$ 250 ºC N_2 $>>$ 250 ºC air. The native NiTi's oxide film presents a very different behaviour: although starting with a low corrosion resistance, it increases over time.
A "duplex" structure was proposed for the Nitinol passive oxide, composed by a dense inner layer and an outer porous one, leading to an equivalent circuit that fits the experimental data.

The surface analysis results show different concentrations of nickel and titanium within the passive films, for untreated and treated NiTi at 350 ºC. The spectrum demonstrate that the native film is quite thin, as proved by the presence of Ni and Ti in the metallic form (by XPS) and in an equiatomic proportion for relative low depths (seen in AES depth profile).
The treatments conducted in two different environments brought different oxide films constitutions, with almost no presence of nickel in the outermost oxide layers obtained from oxidation in N_2 atmosphere; in this situation, the release of that element is minimized in case of corrosion.

The selective oxidation of titanium over nickel is related with the low Gibbs free energy of TiO_2 in comparison to that of NiO. In this way, and in a situation of oxygen shortage, Ti will have higher tendency to form oxides than Ni, which will provoke an enrichment of the former species on the outermost layers of the passive film.
With respect to the differences observed for oxidation at 250 and 350 ºC, kinetic reasons can be invoked. Being the oxidation reaction closely dependent on the temperature, being accelerated with T increase, it is understandable to obtain thicker oxide layers for 350 ºC, enhancing the material's protection.

It is possible to conclude from this work that the performed thermal treatment in nitrogen environment at 350 ºC brings undoubtedly improvements, in comparison with the native alloy, in terms of corrosion resistance and nickel content reduction at NiTi's surface, which can also be interpreted as a biocompatibility optimization. To get a more complete evaluation, a study of the mechanical and fatigue properties should be opportune, in order to understand the effects of the thermal oxidation at all levels, including in the transition temperatures.
In fact, as has been referred several times in chapter 2, *in vivo* tests give a broader perspective of a device's performance, since it is conducted in a realistic environment, in which the material face dynamic conditions as it would naturally inside the human body.

Since the thermal treatments at 250 ºC did not bring considerable advantages, a suggestion for a future work would be to perform those treatments at a temperature closer to 300 ºC and to check if the corrosion resistance is comparable with those treated at 350 ºC; in theory, a thicker film, despite minimising the nickel release to the surrounding medium, might affect considerably the mechanical properties of the material, jeopardising its application. In principle, and in case of similar corrosion behaviours, alloys thermally treated at lower temperature may be better. To quantify the thickness of the formed oxide film, the observation of the material's cross-section by electron microscopy (SEM or TEM) would be an interesting choice.

Bibliography

[1] Q. Chen and G. A. Thouas. Metallic implant biomaterials. In *Materials Science and Engineering: R: Reports*, volume 87, pages 1–58. 2015.

[2] L. Petrini and F. Migliavacca. Biomedical applications of shape memory alloys. *Journal of Metallurgy*, 2011:1–15, 2011.

[3] G. B. Kauffman and I. Mayo. The story of nitinol: The serendipitous discovery of the memory metal and its applications. In *The Chemical Educator*, volume 2. 1996.

[4] Shape memory alloys. https://webdocs.cs.ualberta.ca/∼database/MEMS/sma_mems/sma.html. Last access on: 26-07-2016.

[5] Nickel titanium. https://en.wiki2.org/wiki/Nickel_titanium, . Last access on: 26-07-2016.

[6] M. W. M. van der Wijst. Shape memory alloys featuring nitinol, 1992.

[7] Memory metal - mrsec education group. http://education.mrsec.wisc.edu/148.htm. Last access on: 28-07-2016.

[8] R. F. Silva. Metais com memória de forma. Technical report, Universidade de Aveiro.

[9] D. A. Porter and K. E. Easterling. *Phase Transformations in Metals and Alloys*. CRC Press, 3^{rd} edition, 2009.

[10] T. Silva, T. M. e Silva, M. J. Carmezim, and J. C. S. Fernandes. Nitinol – a new material for biomedical applications. *Ciência Tecnologia dos Materiais*, 17(1–2):34–37, 2005.

[11] Z. Nishiyama. *Martensitic Transformation*. Academic Press, 1978.

[12] Shape changes in a shear transformation. http://www.doitpoms.ac.uk/ldplib/shape_memory/ background.php?printable=1, . Last access on: 02-08-2016.

[13] J. W. Christian. *The Theory of Transformations in Metals and Alloys*. Pergamon, 3^{rd} edition, 2002.

[14] W. D. Callister. *Materials Science and Engineering: An Introduction*. Wiley and Sons, 5^{th} edition, 1994.

[15] K. Schussler. Damping apparatus, use of a shape memory alloy and method for changing damping characteristics. http://www.google.com/patents/US20090025833. Last access on: 02-08-2016.

[16] Superelasticity - strain accommodation by martensite formation. http://www.doitpoms.ac.uk/tlplib/superelasticity/superelasticity1.php, . Last access on: 01-09-2016.

[17] C. Trepanier and A. R. Pelton. *Biocompatibility and Corrosion Resistance of NiTi*. Cordis - NDC, 47533 Westinghouse Drive Fremont CA 94539.

[18] J. Black. *Biological Performance of Materials: Fundamentals of Biocompatibility*. CRC Press, 4^{th} edition, 2005.

[19] A. R. Pelton and T. Duerig, editors. *Shape Memory and Superelastic Technologies*, May 2003. Asilomar Conference Center.

[20] T. Okamoto, M. Neo, S. Fujibayashi, H. Ito, M. Takemoto, and T. Nakamura. Mechanical implant failure in posterior cervical spine fusion. *European Spine Journal*, 21(2):328–334, 2012.

[21] F. D'Angelo, L. Murena, E. Vulcano, G. Zatti, and P. Cherubino. Seven to twelve year results with et cementless stem. a retrospective study of 225 cases. *Hip International*, 20(1):81–86, 2010.

[22] U. C. GUPTA and S. C. GUPTA. Sources and deficiency diseases of mineral nutrients in human health and nutrition: A review. *Pedosphere*, 24(1):13–38, 2014.

[23] C. Klein and M. Costa. *Handbook on the Toxicology of Metals*, volume 1, chapter 48 - Nickel, pages 1091–1111. Elsevier, 4^{th} edition, 2015.

[24] R. P. Brown, B. A. Fowler, S. Fustinoni, and M. Nordberg. *Handbook on the Toxicology of Metals*, volume 1, chapter 5, pages 113–122. Elsevier, 4^{th} edition, 2015.

[25] B. Santucci, P. Ferrari, A. Cristaudo, C. Cannistraci, and M. Picardo. Nickel dermatitis from cheap earrings. *Contact Dermatitis*, 21:245–248, 1989.

[26] K. Takamura, K. Hayashi, N. Ishinishi, T. Yamada, and Y. Sugioka. Evaluation of carcinogenicity and chronic toxicity associated with orthopedic implants in mice. *Journal of Biomedical Materials Research*, 28(5):583–589, 1998.

[27] J. Monteiro. *Estudos de biocompatibilidade de implantes de aço inoxidavel 316L em cirurgia ortopédica*. PhD thesis, Faculdade de Medicina de Lisboa, 1993.

[28] Y. Okazaki and E. Gotoh. Metal release from stainless steel, co-cr-mo-ni-fe and ni-ti alloys in vascular implants. *Corrosion Science*, 50(12):3429–3438, 2008.

[29] A. Michiardi, C. Aparicio, and J. A. P. anda F. J. Gil. New oxidation treatment of niti shape memory alloys to obtain ni-free surfaces and to improve biocompatibility. *Journal of Biomedical Materials Research*, 77(2):249–256, 2006.

[30] Z. L. Sun, J. C. Wataha, and C. T. Hanks. Effects of metal ions on osteoblast-like cell metabolism and differentiation. *Journal of Biomedical Materials Research*, 34(1):29–37, 1997.

[31] J. V. M. P. P. Jetty, S. Jayaram. Superficial femoral artery nitinol stent in a patient with nickel allergy. *Journal of Vascular Surgery*, 58(5):1388–1390, 2013.

[32] O. E. M. Pohler. Unalloyed titanium for implants in bone surgery. *Injury*, 31(4):D7–D13, 2000.

[33] B. Möller, H. Terheyden, Y. Açil, N. M. Purcz, K. Hertrampf, A. Tabakov, E. Behrens, and J. Wiltfang. A comparison of biocompatibility and osseointegration of ceramic and titanium implants: an in vivo and in vitro study. *International Journal of Oral and Maxillofacial Surgery*, 41(5):638–645, 2012.

[34] M. Hosoki, K. Nishigawa, Y. Miyamoto, G. Ohe, and Y. Matsuka. Alergic contact dermatitis caused by titanium screws and dental implants. *Journal of Prosthodontic Research*, 60(3):213–219, 2016.

[35] N. Coen, M. A. Kadhim, E. G. Wright, C. P. Case, and C. E. Mothersill. Particulate debris from a titanium metal prosthesis induces genomic instability in primary human fibroblast cells. *British Journal of Cancer*, 88:548–552, 2003.

[36] L. S. Castleman and S. M. Motzkin. The biocompatibility of nitinol. In D. F. Williams, editor, *Biocompatibility of Clinical Implant Materials*, volume 1, pages 129–154. CRC Press, 1981.

[37] M. Assad, S. Lombardi, S. Berneche, E. A. Desrosiers, L. H. Yahia, and C. H. Rivard. Citotoxicity testing of the nickel-titanium shape memory alloy. *Annales de Chirurgie*, 48(8):731–736, 1994.

[38] J. Ryhänen. *Biocompatibility evaluation of nickel-titanium shape memory metal alloy*. PhD thesis, University of Oulu, 1999.

[39] D. J. Wever, A. G. Veldhuizen, M. M. Sanders, J. M. Schakenraad, and J. R. van Horn. Cytotoxic, allergic and genotoxic activity of a nickel-titanium alloy. *Biomaterials*, 18(16):1115–1120, 1997.

[40] M. Assad, L. H. Yahia, C. H. Rivard, and N. Lemieux. *In vitro* biocompatibility assessment of a nickle-titanium alloy using electron microscopy in situ end-labelling (em-isel). *Journal of Biomedical Materials Research*, 41(1):154–161, 1998.

[41] A. Kapanen, J. Ilvesaro, A. Danilov, J. Ryhänen, P. Lehenkari, and J. Tuukkanen. Behaviour of nitinol in osteoblast-like ros-17 cell cultures. *Biomaterials*, 23(3):645–650, 2002.

[42] A. Michiardi, E. Engel, C. Aparicio, J. A. Planell, and F. J. Gil. Oxidized niti surfaces enhance differentiation of osteoblast-like cells. *Journal of Biomedical Materials Research*, 85A(1):108–114, 2008.

[43] F. L. Nie, Y. F. Zheng, Y. Cheng, S. C. Wei, and R. Z. Valiev. In vitro corrosion and cytotoxicity on microcrystalline, nanocrystalline and amorphous niti alloy fabricated by high pressure torsion. *Materials Letters*, 64(8):983–986, 2010.

[44] D. E. Cutright, S. N. Bhaskar, B. Perez, R. M. Johnson, and G. S. M. Cowan. Tissue reaction to nitinol wire alloy. *Oral Surgery, Oral Medicine, Oral Pathology*, 35(4):578–584, 1973.

[45] L. S. Castleman, S. M. Motzkin, F. P. Alicandri, and V. L. Bonawit. Biocompatibility of nitinol alloy as an implant material. *Journal of Biomedical Materials Research*, 10(5):695–731, 1976.

[46] P. J. Yang, M. Z. G. J. C. Ta and, Q. M. Yang, H. B. Yang, and Q. Sun. Ni-ti memory alloy clamp plate for fracture of short tubular bone. *Chinese Medical Journal*, 105(4):312–315, 1992.

[47] K. Matsumoto, N. Tajima, and S. Kuwahara. Correction of scoliosis with shape-memory alloy. *Nihon Seikeigeka Gakkai Zasshi*, 67(4):267–274, 1993.

[48] S. J. Simske and R. Sachdeva. Cranial bone apposition and ingrowth in a porous nickel-titanium implant. *Journal of Biomedical Materials Research*, 29(4):527–533, 1995.

[49] M. Berger-Gorbet, B. Broxup, C. Rivard, and L. H. Yahia. Biocompatibility testing of niti screws using immunohistochemistry on sections containing metallic implants. *Journal of Biomedical Materials Research*, 32(2):243–248, 1996.

[50] F. Takeshita, H. Takata, Y. Ayukawa, and T. Suetsugu. Histomorphometric analysis of the response of rat tibiae to shape memory alloy (nitinol). *Biomaterials*, 18(1):21–25, 1997.

[51] X. Wen, N. Zhang, X. Li, and Z. Cao. Electrochemical and histomorphometric evaluation of the tinicu shape memory alloy. *Bio-Medical Materials and Engineering*, 7(1):1–11, 1997.

[52] S. Idelshohn, J. Peña, D. Lacroix, J. A. Planell, F. J. Gil, and A. Arcas. Continuous mandibular distraction osteogenesis using superelastic shape memory alloy (sma). *Journal of Materials Science: Materials in Medicine*, 15(4):541–546, 2004.

[53] C. Y. Li, X. J. Yang, L. Y. Zhang, M. F. Chen, and Z. D. Cui. In vivo histological evaluation of bioactive niti alloy after two years implantation. *Materials Science and Engineering: C*, 27(1): 122–126, 2007.

[54] X. Liu, S. Wu, K. W. K. Yeung, Y. L. Chan, T. Hu, Z. Xu, X. Liu, J. C. Y. Chung, K. M. C. Cheung, and P. K. Chu. Relationship between osseointegration and superelastic biomechanics in porous niti scaffolds. *Biomaterials*, 32(2):330–338, 2011.

[55] G. F. von Salis-Soglio. Memory-spondylodesis in the lumbar spine - results after 76 operations. *Z Orthop Unfall*, 127(2):191–196, 1989.

[56] C. Y. Qiu. Shape memory alloy spiral for urethrostenosis caused by benign prostatic hyperplasia. *Zhonghua wai ke za zhi*, 31(5):272–274, 1993.

[57] R. Tang, K. R. Dai, and Y. Q. Chen. Application of a niti staple in the metatarsal osteotomy. *Bio-Medical Materials and Engineering*, 6(4):307–312, 1996.

[58] A. Itro, V. Garau, G. P. Tartaro, and G. Colella. Experience with a rigid fixation device in maxillofacial surgery using shape-memory clips. *Minerva stomatologica*, 46(7–8):381–389, 1997.

[59] H. R. Kim, W. Y. Lee, K. U. Jung, H.-R. Yun, Y. B. Cho, S. H. Yun, H. C. Kim, and H.-K. Chun. Early surgical outcomes of niti endoluminal compression anastomotic clip (niti cac 30) use in patients with gastrointestinal malignancy. *Journal of Laparoendoscopic Advanced Surgical Techniques*, 22(5):472–478, 2012.

[60] M. Sumita and T. Hanawa. Failure processes in biometallic materials. *Reference Module in Materials Science and Materials Engineering: Comprehensive Structural Integrity*, 9:131—167, 2003.

[61] J. S. Fernandes and F. Montemor. Corrosão: Prevenção e protecção. In M. C. Gonçalves and F. Margarido, editors, *Ciência e Engenharia de Materiais de Construção*, chapter 15, pages 773–812. IST Press, 2012.

[62] G. Koch, J. Varney, N. Thompson, O. Moghissi, M. Gould, and J. Payer. International measures of prevention, application, and economics of corrosion technologies study. Technical report, NACE International, 2016.

[63] http://www.magazine8.com/top-10-quick-tricks-on-how-to-get-rid-of-rust-on-a-car/. Last access on: 28-08-2016.

[64] https://commons.wikimedia.org/wiki/File:Nandu_River_Iron_Bridge_corrosion_-_03.jpg. Last access on: 28-08-2016.

[65] http://www.exbtengineers.com/phone-line-dead/. Last access on: 28-08-2016.

[66] D. A. Jones. *Principles and Prevention of Corrosion*. Prentice Hall, New York, 2^{nd} edition, 1996.

[67] http://www.corrosion-club.com/uniform.htm, . Last access on: 28-08-2016.

[68] Nace international - uniform corrosion. https://www.nace.org/Corrosion-Central/Corrosion-101/Uniform-Corrosion/. Last access on: 28-08-2016.

[69] Corrosion of metals. http://xapps.xyleminc.com/Crest.Grindex/help/grindex/contents/Metals.htm. Last access on: 28-08-2016.

[70] http://www.corrosion-club.com/crevice.htm, . Last access on: 29-08-2016.

[71] http://dynamicmachinedesign.com/wp/tag/corrosion/. Last access on: 29-08-2016.

[72] http://www.nitty-gritty.it/pitting-corrosion/?lang=en, . Last access on: 29-08-2016.

[73] http://www.corrosion-club.com/intergr.htm, . Last access on: 29-08-2016.

[74] Astm a262. http://www.g2mtlabs.com/corrosion/astm-a262-testing/. Last access on: 29-08-2016.

[75] Failure analysis case studies. http://www.berkeleyrc.com/FAcasestudies.html. Last access on: 29-08-2016.

[76] http://www.nitty-gritty.it/corrosion-erosion/?lang=en, . Last access on: 29-08-2016.

[77] J. Fan, J. Mazur, N. Melicharek, and M. Schmittdiel. *Erosion, cavitation and fretting corrosion*.

[78] Stress corrosion cracking and corrosion fatigue. http://www.christoforidis.gr/en/stress_corrosion_cracking_corrosion_fatigue.php. Last access on: 29-08-2016.

[79] Analysis of the failure of a synthesis gas rotor coupling and turbine shaft. http://www.pkn.co.za/pap-VZVWR.html. Last access on: 29-08-2016.

[80] https://en.wikipedia.org/wiki/Hydrogen_embrittlement, . Last access on: 30-08-2016.

[81] W. J. Buehler and F. E. Wang. A summary of recent research on the nitinol alloys and their potential application in ocean engineering. *Ocean Engineering*, 1(1):105–120, 1968.

[82] K. M. Speck and A. C. Fraker. Anodic polarization behavior of ti-ni and ti-6a 1-4 v in simulated physiological solutions. *Journal of Dental Research*, 59(10):1590–1595, 1980.

[83] J. W. Edie, G. F. Andreasen, and M. P. Zaytoun. Surface corrosion of nitinol and stainless steel under clinical conditions. *Angle Orthodontist*, 51(4):319–324, 1981.

[84] N. K. Sarkar, W. Redmond, B. Schwaninger, and A. J. Goldberg. The chloride corrosion behaviour of four orthodontic wires. *Journal of Oral Rehabilitation*, 10(2):121—-128, 1983.

[85] R. D. Barrett, S. E. Bishara, D. Ortho, and J. K. Quinn. Biodegradation of orthodontic appliances. part i. biodegradation of nickel and chromium in vitro. *American Journal of Orthodontics and Dentofacial Orthopedics*, 103(1):8–14, 1993.

[86] A. H. Cragg, S. C. D. Jong, W. H. Barnhart, S. K. Landas, and T. P. Smith. Nitinol intravascular stent: results of preclinical evaluation. *Radiology*, 189(3):775–778, 1993.

[87] G. Rondelli. Corrosion resistance tests on niti shape memory alloy. *Biomaterials*, 17:2003–2008, 1996.

[88] D. J. Wever, A. G. Veldhuizen, J. de Vries, H. J. Busscher, D. R. A. Uges, and J. R. van Horn. Electrochemical and surface characterization of a nickel-titanium alloy. *Biomaterials*, 19(7–9): 761–769, 1998.

[89] J. Izquierdo, M. B. González-Marrero, M. Bozorg, B. M. Fernández-Pérez, H. C. Vasconcelos, J. J. Santana, and R. M. Souto. Multiscale electrochemical analysis of the corrosion of titanium and nitinol for implant applications. *Electrochimica Acta*, 203(10):366—-378, 2016.

[90] S. A. Shabalovskaya, G. C. Rondelli, A. L. Undisz, J. W. Anderegg, T. D. Burleigh, and M. E. Rettenmayr. The electrochemical characteristics of native nitinol surfaces. *Biomaterials*, 30(22): 3662—3671, 2009.

[91] L. L. Stepan, D. S. Levi, and G. P. Carman. A thin film nitinol heart valve. *Journal of Biomechanical Engineering*, 127(6):915–918, 2005.

[92] L. B. Pértile, P. M. S. Silva, V. B. Peccin, R. Peres, P. G. Silveira, C. Giacomelli, F. C. Giacomelli, M. C. Fredel, and A. Spinelli. In vivo human electrochemical properties of a niti-based alloy (nitinol) used for minimally invasive implants. *Journal of Biomedical Materials Research*, 89(4):1072–1078, 2008.

[93] N. Figueira, T. M. Silva, M. J. Carmezima, and J. C. S. Fernandes. Corrosion behaviour of niti alloy. *Electrochimica Acta*, 54(3):921–926, 2009.

[94] E. J. Kassab and J. P. Gomes. Assessment of nickel titanium and beta titanium corrosion resistance behavior in fluoride and chloride environments. *Angle Orthodontist*, 83(5):864–869, 2013.

[95] M. Mirjalili, M. Momeni, N. Ebrahimi, and M. H. Moayed. Comparative study on corrosion behaviour of nitinol and stainless steel orthodontic wires in simulated saliva solution in presence of fluoride ions. *Materials Science and Engineering: C*, 33(4):2084—2093, 2013.

[96] L. M. Muresan. Corrosion protective coatings for ti and ti alloys used for biomedical implants. In A. Tiwari, L. Hihara, and J. Rawlins, editors, *Intelligent Coatings for Corrosion Control*, chapter 17, pages 585–602. 2015.

[97] A. W. Hassel. Surface treatment of niti for medical applications. *Minim Invasive Ther Allied Technol*, 13(4):240–247, 2004.

[98] D. L. L. Madamba. The effect of surface treatment on nickel leaching from nitinol. Master's theses, San Jose State University, 2013. Paper 4287.

[99] I. Milošev and B. Kapun. The corrosion resistance of nitinol alloy in simulated physiological solutions - part 1: The effect of surface preparation. *Materials Science and Engineering C*, 32(5): 1087–1096, 2012.

[100] W. Miao, X. Mi, G. Xu, and H. Li. Effect of surface preparation on corrosion properties and nickel release of a niti alloy. *Rare Metals*, 25(6):243–245, 2006.

[101] M. Chembath, J. N. Balaraju, and M. Sujata. Effect of anodization and annealing on corrosion and biocompatibility of niti alloy. *Surface & Coatings Technology*, 302:302–309, 2016.

[102] S. Cui, J. Han, Y. Du, and W. Li. Corrosion resistance and wear resistance of plasma electrolytic oxidation coatings on metal matrix composites. *Surface & Coatings Technology*, 201(9–11):5306–5309, 2007.

[103] J. M. M. Vieira. Tratamentos superficiais da liga de niti para optimização da biocompatibilidade e resistência à corrosão. Master's thesis, Instituto Superior Técnico, 2013.

[104] S. A. Bernard, V. K. Balla, N. M. Davies, S. Bos, and A. Bandyopadhyay. Bone cell–materials interactions and ni ion release of anodized equiatomic niti alloy. *Acta Biomaterialia*, 7(4):1902–1912, 2011.

[105] N. Bayat, S. Sanjabi, and Z. H. Barber. Improvement of corrosion resistance of niti sputtered thin films by anodization. *Applied Surface Science*, 257(20):8493–8499, 2011.

[106] S. V. Gnedenkov, Y. P. Sharkeev, S. L. Sinebryukhov, V. S. Egorkin, O. A. Khrisanfova, E. V. Legostaeva, A. G. Zavidnaya, A. V. Puz', I. A. Khlusov, and D. P. Opra. Anticorrosion coatings for ti and niti implants. In *Materials Technology*. 2016.

[107] H. Wang, F. Liu, X. Xiong, S. Ke, X. Zenga, and P. Lin. Structure, corrosion resistance and in vitro bioactivity of ca and p containing tio_2 coating fabricated on niti alloy by plasma electrolytic oxidation. *Applied Surface Science*, 356:1234–1243, 2015.

[108] D. Vojtech, M. Voderová, J. Fojt, P. Novák, and T. Kubásek. Surface structure and corrosion resistance of short-time heat-treated niti shape memory alloy. *Applied Surface Science*, 257(5): 1573–1582, 2010.

[109] Y. Yu, T. Sun, and Y. Wang. Bioactive titanium oxide coatings fabricated on niti sma via thermal treatment for medical applications. In *8th International Conference on Materials for Advanced Technologies*, volume 141, pages 115–120. MRS Singapore – ICMAT Symposia Proceedings, 2016.

[110] D. Vojtech, J. Kubásek, M. Voderová, P. Sedá, and A. Michalcová. Study of mechanical, fatigue and corrosion properties of the superelastic ni-ti alloys. *Metal*, pages 1–7, 2011.

[111] M. R. Etminanfar, J. Khalil-Allafi, A. Montaseri, and R. Vatankhah-Barenji. Endothelialization and the bioactivity of ca$-$p coatings of different ca$/$p stoichiometry electrodeposited on the nitinol superelastic alloy. *Materials Science and Engineering C*, 62:28–35, 2016.

[112] J. X. Zhang, R. F. Guan, and X. P. Zhang. Synthesis and characterization of sol–gel hydroxyapatite coatings deposited on porous niti alloys. *Journal of Alloys and Compounds*, 519(13):4643–4648, 2011.

[113] D. P. Aun, I. F. da Cunha Peixoto, M. Houmard, and V. T. L. Buono. Enhancement of niti superelastic endodontic instruments by tio_2 coating. *Materials Science and Engineering C*, 68:675–680, 2016.

[114] T. Sun, N. Xue, C. Liu, C. Wang, and J. He. Bioactive (si, o, n)/(ti, o, n)/ti composite coating on niti shape memory alloy for enhanced wear and corrosion performance. *Applied Surface Science*, 356:599–609, 2015.

[115] A. Shanaghi, P. K. Chu, R. Xu, and T. Hua. Structure and properties of tic/ti coatings fabricated on niti by plasma immersion ion implantation and deposition. *Vacuum*, 89:238–243, 2013.

[116] T. Sun, L.-P. Wang, M. Wang, H.-W. Tong, and W. W. Lu. Characteristics and *in vitro* biological assessment of (ti, o, n)/ti composite coating formed on niti shape memory alloy. *Thin Solid Films*, 519(15):4623–4628, 2011.

[117] E. Bazochaharbakhsh. Surface nitriding and oxidation of nitinol. Master's theses, San Jose State University, 2011. Paper 4037.

[118] R. Ion, C. Luculescu, A. Cimpean, P. Marx, D.-M. Gordin, and T. Gloriant. Nitride coating enhances endothelialization on biomedical niti shape memory alloy. *Materials Science Engineering C*, 62: 686–691, 2016.

[119] Coronary stenting. http://www.wkhs.com/Heart/Services/Cardiovascular_Procedures/Coronary_Stent.aspx. Last access on: 18-09-2016.

[120] F. Auricchio, E. Boatti, and M. Conti. Sma biomedical applications. In L. Lecce and A. Concilio, editors, *Shape Memory Alloy Engineering: for Aerospace, Structure and Biomedical Applications*, chapter 11, pages 307–341. Elsevier Ltd., 2015.

[121] A. Matsuzaki, T. Morita, A. Tokue, and Y. Kobayashi. Clinical study of intraurethral stent (memokath®) for prostatic hyperplasia - study of the changes in uroflowmetry and international prostate symptom score in the early phase after insertion of the stent. *Nishinihon Journal of Urology*, 66(10):637–643, 2004.

[122] D. Yachia, Z. Markovic, B. Markovic, and V. Stojanovic. Endourethral prostheses for urethral stricture. *Acta Chir Iugosl.*, 54(3):105–114, 2007.

[123] J.-S. Luo, P.-C. Cui, P.-F. Gao, H. Nan, Z. Liu, and Y.-Z. Sun. Reconstruction of tracheal wall defect with a mesh patch of nickel-titanium shape-memory alloy. *Annals of Otology, Rhinology Laryngology*, 120(3):198–203, 2011.

[124] http://flourishmedical.en.made-in-china.com/product/CodxSAZUENRE/China-Dental-Orthodontic-Super-Elastic-Niti-Arch-Wires-Dental-Instruments.html. Last access on: 18-09-2016.

[125] http://pic.pimg.tw/lytornado/1384574667-1986169935.jpg. Last access on: 18-09-2016.

[126] Y. Wang, G. Zheng, X. Zhang, Y. Zhang, S. Xiao, and Z. Wang. Temporary use of shape memory spinal rod in the treatment of scoliosis. *European Spine Journal*, 20(1):118–122, 2011.

[127] H. Z. Morawiec, Z. H. Lekston, K. F. Kobus, M. C. Wegrzyn, and J. T. Drugacz. Superelasticity of niti ring-shaped springs induced by aging for cranioplasty applications. *Journal of Materials Engineering and Performance*, 18(5):818–823, 2009.

[128] M. Niinomi. Fatigue characteristics of metallic biomaterials. *International Journal of Fatigue*, 29 (6):992–1000, 2007.

[129] T. Habijan, T. Glogowski, S. Kühn, M. Pohl, J. Wittsiepe, C. Greulich, G. Eggeler, T. A. Schildhauer, and M. Köller. Can human mesenchymal stem cells survive on a niti implant material subjected to cyclic loading? *Acta Biomaterialia*, 7(6):2733–2739, 2011.

[130] A. Yoshida, K. Yokoyama, T. Inaba, K. Mutoh, and J. Sakai. Fracture and corrosion behaviors of ni-ti superelastic alloy under sustained tensile loading in neutral fluoride solution containing hydrogen peroxide. *Journal of Alloys and Compounds*, 544:24–29, 2012.

[131] E. Pedullà, N. M. Grande, G. Plotino, F. Palermo, G. Gambarini, and E. Rapisarda. Cyclic fatigue resistance of two reciprocating nickel–titanium instruments after immersion in sodium hypochlorite. *International Endodontic Journal*, 46(2):155–159, 2012.

[132] A. U. Dragoş, S. Stanciu, R. Cimpoeşu, I. Ionita, M. Raţoi, T. Constantin, I. Cimpoeşu, and M. Agop. The corrosion resistance of niti-active element before and after thermo-mechanical solicitation. *Applied Mechanics and Materials*, 371:353–357, 2013.

[133] T. Kosec, P. Mocnik, and A. Legat. The tribocorrosion behaviour of niti alloy. *Applied Surface Science*, 288:727–735, 2014.

[134] J. Racek, P. Šittner, L. Heller, J. Pilch, P. Sedlák, and L. Kadeřávek. Electrochemistry of niti wires/springs subjected to static/cyclic loadings. In *International Conference on Martensitic Transformations, ICOMAT-2014*, volume 2, pages S965–S969, 2015.

[135] http://srizam-expro.blogspot.pt/2011/03/how-to-explain-potentiodynamic.html. Last access on: 10-10-2016.

[136] J. P. E. Caldeira. Estudo da resistência à corrosão de ligas de magnésio para a indústria automóvel. Master's thesis, Instituto Superior de Engenharia de Lisboa, 2011.

[137] *Basics of Electrochemical Impedance Spectroscopy*. Gamry Instruments. Application Note.

[138] N. C. A. Figueira. Caracterização do comportamento face à corrosão da liga niti - qualidade em aplicações biomédicas. Master's thesis, Instituto Superior Técnico, 2008.

[139] J. C. S. Fernandes. Espectroscopia de impedância electroquímica, 2007.

[140] R. Haasch. Xray photoelectron spectroscopy (xps) and auger electron spectroscopy (aes). In 6^{th} *Advanced Materials Characterization Workshop*. University of Illinois, June 2012.

[141] Chapter 2. x-ray photoelectron and auger electron spectroscopy. https://www.researchgate.net/file.PostFileLoader.html?id=5134dbf8e5438f9c14000010assetKey=AS%3A271833427841026%401441821548006.

[142] M. F. Montemor. *Espectroscopia de Electrões Auger e Espectroscopia de Fotoelectrões X*. Instituto Superior Técnico, July 2002.

[143] V. V. Andreeva. Behavior and nature of thin oxide films on some metals in gaseous media and in electrolyte solutions. *Corrosion*, 20(2):35t–46t, 1964.

[144] A. Michiardi, C. Aparicio, J. A. Planell, and F. J. Gil. Electrochemical behaviour of oxidized niti shape memory alloys for biomedical applications. *Surface and Coatings Technology*, 201(14): 6484–6488, 2007.

[145] F. Villermaux, M. Tabrizian, L. Yahia, M. Meunier, and D. L. Piron. Excimer laser treatment of niti shape memory alloy biomaterials. *Applied Surface Science*, 109–110:62–66, 1997.

[146] B. G. Pound. Susceptibility of nitinol to localized corrosion. *Journal of Biomedical Materials Research Part A*, 77(1):185–191, 2006.

[147] C. Liang and Z. Mou. Effects of different simulated fluids on anticorrosion biometallic materials. *Transactions of Nonferrous Metals Society of China*, 11(4):579–582, 2001.

[148] S. Liu, B. Wang, and P. Zhang. Effect of glucose concentration on electrochemical corrosion behavior of pure titanium ta2 in hanks' simulated body fluid. *Materials*, 9(11):874–884, 2016.

[149] L. Tan, R. A. Dodd, and W. Crone. Corrosion and wear-corrosion behaviour of niti modified by plasma source ion implantation. *Biomaterials*, 24:3931–3939, 2003.

[150] J. Mieluch. Impedance methods in electrochemical investigations. *Corrosion Protect*, 3:78, 1990.

[151] B. E. Conway. *Electrochemical Data*. Elsevier, 1952.

[152] Ellingham diagrams. http://web.mit.edu/2.813/www/readings/Ellingham_diagrams.pdf. Last access on: 19-11-2016.